# SYNTHESIS OF SEMICONDUCTOR QUANTUM DOTS ON POLYMER MATRIX AND THEIR APPLICATIONS IN ELECTRONICS, PHOTONICS AND NONLINEAR OPTICS

*A Thesis Submitted to*

**TEZPUR UNIVERSITY**

In partial fulfillment of the requirements

for the Degree of



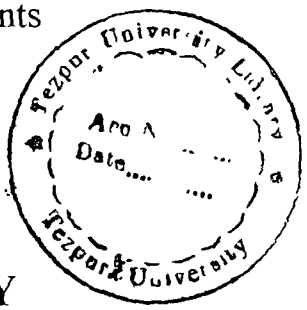


**DOCTOR OF PHILOSOPHY**

*by*

**SIDDHARTHA SANKAR NATH**

Department of Physics

School of Science and Technology

Tezpur University, Napaam

Tezpur-784 028, Assam, India

July , 2003.

## DECLARATION

I hereby declare that the thesis entitled **"Synthesis Of Semiconductor *Quantum Dots On Polymer Matrix And Their Applications In Electronics,* Photonics and Nonlinear Optics"** being submitted to Tezpur University, Tezpur, Assam in partial fulfillment of the requirements for the award of the Degree of Doctor of Philosophy, has not formed the basis for the award of any degree, diploma, associateship, fellowship or any other similar title or recognition.

Siddhartha Sankar Nath

July ,16, 2003.

***( Siddhartha Sankar Nath )***

Department of Physics
Tezpur University
Tezpur-784 028 (Assam).

# TEZPUR UNIVERSITY

(A Central University established by an Act of Parliament)
NAPAAM, TEZPUR - 784 028
DISTRICT : SONITPUR :: ASSAM :: INDIA

Ph: 03712 - 267004
03712 - 267005
Fax : 03712 - 267006
03712 - 267005
e-mail :adm@agnigarh.tezu.ernet.in


## CERTIFICATE

This is to certify that the thesis entitled **"Synthesis Of Semiconductor Quantum Dots On Polymer Matrix And Their Applications In Electronics, Photonics and Nonlinear Optics"** being submitted by **Siddhartha Sankar Nath** to Tezpur University, Tezpur, Assam in partial fulfillment of the requirements for the award of the degree of Doctor of Philosophy, is a record of original bonafide research work carried out by him. He has worked under our joint guidance and supervision and has fulfilled the requirements for the submission of this thesis. The results contained in the thesis have not been submitted in part or full to any other university or institute for award of any degree or diploma.

***( Amarjyoti Choudhury )***

Professor,
Department of Physics,
University of Florence
On leave from:
Tezpur University
Tezpur-784 028 (Assam)

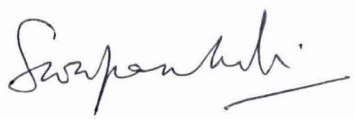

***( Swapan Kr. Dolui )***

Professor,
Department of Chem.Science
Tezpur University
Tezpur 784028 (Assam)

## *ACKNOWLEDGEMENT*

*I express my deep sense of gratitude to* ***Prof. A. Choudhury*** *who introduced me to the area of quantum dot nano particles. I received his dynamic guidance, meticulous supervision and moral support throughout my research work. Without his valuable suggestions, lively discussions and constant encouragement, the work could not have taken the present shape.*

*It is a fortune to express my deep sense of gratitude to* ***Prof. S. K. Dolui*** *for his keen interest and inspiring supervision for synthesizing and characterizing the samples. Without his constructive comments, immense help and assistance during my research, the present work would not have been materialized.*

*I extend my sincere and hearty gratitude to Prof. N. C. Mishra, NSC, New Delhi for his sincere involvement and stimulating discussions to carry out swift heavy ion irradiation on our samples.*

*I would like to take this opportunity to thank Indian Space Research Organization (ISRO) for assistance and associating me with the "Quantum dot project".*

*I am highly grateful to Prof. G. K. D. Mazumdar, Dr. S. .Karmakar, S. Bordoloi and Mr. D. Das, Dr. K .C. Sarma and Dr. P. K. Boruah USIC, Gauhati University for extending their valuable suggestions and sincere help to carry out XRD studies.*

*I am highly thankful to Dr. M. Myrboh, RSIC, NEHU for his cooperation for TEM study.*

*I acknowledge my thanks to Dr. K. V. Reddy, CIL , Hyderabad University for his kind help and cooperation to carry out PL experiment.*

*My special thanks go to Mr. D. Mohanta, Dr.G. A. Ahmed, Mr. A. K. Bordoloi , Dr. K. Boruah and Miss S. Chowdhury, Tezpur University, for their sincere assistance and cooperation in the crucial moments of my research. Also, I acknowledge my regards to Dr. A. Kumar, Dr. J. K. Sarma, Dr. N. Das, and Dr. N S. Bhattacharyya Tezpur University for their valuable suggestions during my research.*

*I like to extend my hearty thanks to my research friends at this university, namely, Juti, Diganta, Abu, Nava, Illias, Nandini, Abhijit, Gwjwn, Deep and Anjan for their cooperation and help during my research.*

*I like to thank Mr. A. Pathak and H. Pathak, Tezpur University for their constant help to prepare my thesis.*

*I am indebted to my parents, elder brother, sister in law and my loving niece for their constant inspiration, moral support, valuable suggestions, love and blessings.*

Siddhartha Sankar Nath

*(SIDDHARTHA SANKAR NATH)*

## *PREFACE*

*This thesis contains new and original investigations in the area of semiconductor quantum dots. Ideally quantum dots are quasizero structures. In practice, they are in nm range. Due to size quantization, some new phenomena like enhancement in band gap, creation of surface states, etc occur in the specimens. These properties make them very attractive candidates for developing nano electronic, optoelectronic and optic devices. This work is a result of my present investigations of related preparation of semiconductor quantum dots on polymer matrix, study of their sizes, optical absorption, and luminescence studies of the prepared samples from the point of view of possible applications. The modifications in the sample properties of the samples after Swift Heavy Ion (SHI) irradiation are also reported*

*The thesis is broadly divided into six chapters, each of which are again split into sub-sections. The first chapter discusses properties, advantages, and possible applications of semiconductor quantum dots. It also introduces my investigation in the overall perspective of the contemporary research in quantum dots. The second chapter contains the details synthesis procedures of quantum dots by chemical route and quenching method. The third chapter details characterizations of the samples by X-ray diffraction (XRD) study. Transmission Electron Microscopy (TEM), Optical absorption absorption spectroscopy and photoluminescence studies.While XRD AND TEM studies are used to mainly study the sample size, optical spectroscopy and photoluminescence studies are mainly used for revealing*

*the different energy states and the electro transition speed among these level. In the fourth chapter, ion beam irradiated samples are characterized by the tests already mentioned in chapter3. These studies show that in the ion irradiated samples better optical sensitivity and higher emission efficiency are obtained in comparison to that of unirradiated samples. In fifth chapter the applications of quantum dots are recorded. These are its possible applications as electronic, photonic switch and optic switch. We have chosen to confine our studies to the application of quantum dots in electronic, photonic and optical switching out of its large potential in the entire area of electronics, photonics and nonlinear optics. In the last chapter (i.e. sixth chapter), some modification in synthesis and future direction of research in this area are highlighted. Lastly, the photographs and specifications of instruments used are displayed in the appendix.*

# CONTENTS

# CHAPTER 1

# INTRODUCTION

# CHAPTER 1

# Introduction

Modern research has made it possible to design and fabricate semiconductor nano particles, especially those belonging to II-VI, III-V and IV-V group of the periodic table. These semiconductors exhibit considerable quantum size effects leading to size dependent electronic, optoelectronic and nonlinear optical properties[1-7]. The fact that the band gap of any of these materials varies with size, gives a great potential for optoelectronic and optical applications. The dramatic change, as one goes from bulk to nanometer size, is principally due to redistribution of the electronic states and changes in the corresponding wave function.

## 1.1 Classifications of nano particles

Depending upon the dimensional confinement of particle size and electronic motions, nano structures can be classified into three categories[8]. These are

**I. Quantum well**

If the thickness of any structure / particle becomes comparable to de-Broglie's wavelength of electron at Fermi energy and the electronic motion is restricted along the thickness only, the structure is called quantum well.

**II. Quantum wire**

If the thickness as well as width of any structure are comparable to de-Broglie's wavelength of electron at Fermi energy, and the electronic motion is restricted along both, thickness and width, the structure is called quantum wire.

**III. Quantum dot.**

If all the three dimensions, that is thickness, width and length of any structure are comparable to de-Broglie's wavelength of electron at Fermi energy, and the electronic motion is restricted in all the three dimensions, the structure is called quantum dot. It is ideally a quasi zero structure. Practically, its dimensions range from a few nm to few hundred nm that are circular, elliptical or rectangular in shape. Physically, semiconductor quantum dots are three dimensionally confined systems embedded in polymer host. The polymer host provides the mechanism for three dimensional confinement.

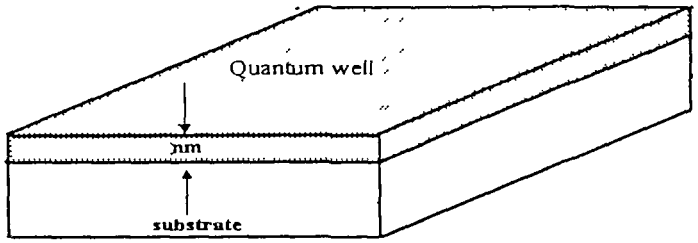


Fig.1.1 : Schematic diagram of quantum well

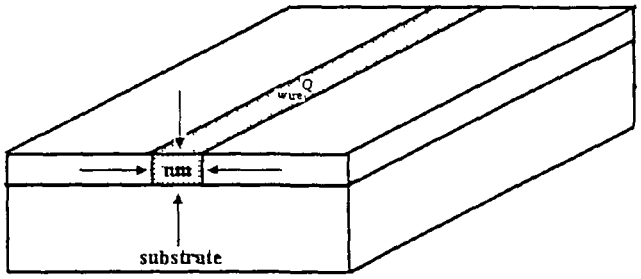


Fig.1.2 : Schematic diagram of quantum wire

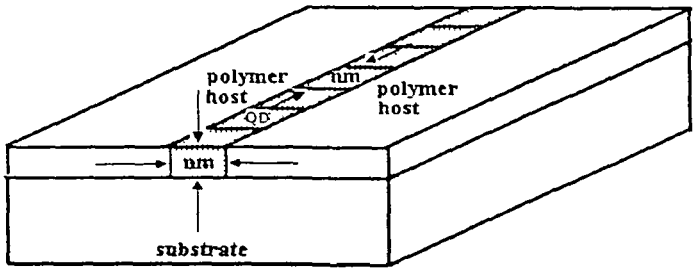


Fig.1.3: Schematic diagram of quantum dot array

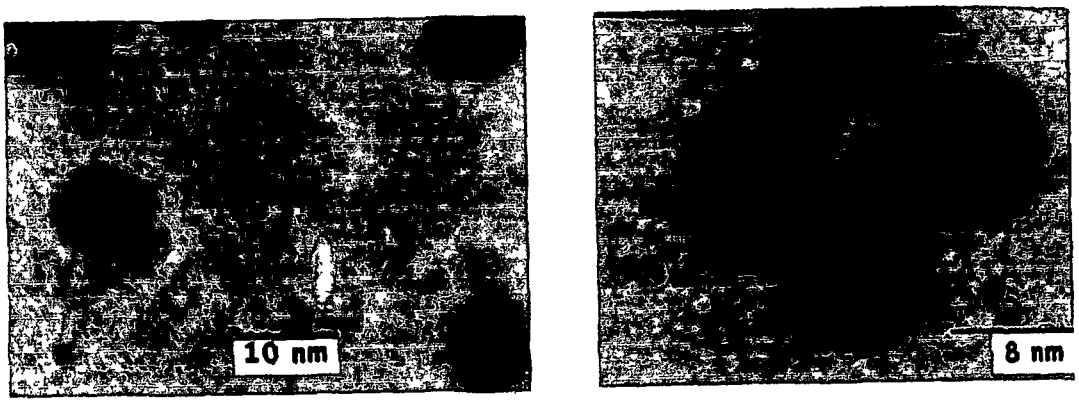


**Fig. 1.4: TEM images of quantum dot assembly**

## 1.2 Properties of quantum dots

Quantum dots possess some unique properties, by which they differ from bulk materials. These are

### I. Enhancement in band gap

As a consequence of quantum confinement, the continuum of states in conduction and valence band are split into discrete states with energy spacing relative to the band edge, which is approximately inversely proportional to the square of the particle radius, resulting in widening the band gap in comparison with the bulk[8,9].

### II. Blue shift

As the band gap of quantum dot enhances, the strong absorption of optical pulse occurs in UV region that is, absorption edge shifts towards UV. For that reason, it is said that quantum dots possess blue shift in optical absorption spectra[10-14].

### III. Large surface to volume ( S/ V ) ratio

Another important property associated with quantum dots is the existence of large surface to volume ratio (S/V) which results in producing some discrete electronic states within the band gap of the specimen. These are called surface states or more commonly called 'Trap'.

### IV. Intense photoluminescence

Due to the occurrence of surface states, unlike in bulk specimen, in quantum dots, the excited electrons are captured by the surface states, either before or after the direct relative recombination which ultimately enhances the luminescence intensity of the specimen[15]. Some crystal defects may also be artificially created in quantum dot that behave as trap. The trapping as well as de trapping rate of electrons in the traps is very fast. These properties are utilized to develop quantum dot optic switch.

### V. Change in optoelectronic property

Unlike in bulk material, electronic transition between traps and valence band as well as traps and conduction band is faster due to fast trapping and de trapping of charge carriers by traps[11,16] than band edge transition. This property of quantum dot makes it very efficient for fast photonic switch.

## 1.3 Technological importance of quantum dots

The road map of so called Semiconductors Industries Association (SIA) For Silicon Process Technology has now been established. According to it, the minimum design rule, which was 0.35 μm in 1995 will be multiplied by 0.7 every 3 years. In 2010 it will be possible to create 64 GB DRAM with average area of 'FET' being 1.1μm. But this conventional technology has some serious constraints[8] which are completely absent in semiconductor quantum dots as discussed below:

I. In conventional devices, as the gate length shrinks to 0.1μm or less, some of physical effects like (a) Hot electron effects (b) Oxide tunneling (c) Silicon Tunneling (d) Drain induced barrier lowering etc. comprise to make successful 'CMOS' operation difficult.

   In quantum dot devices, the above said physical effects are absent

II. In silicon technology, when the device size shrinks, the capacitances of their interconnections connections become increasingly important. If very small conductors are used, the capacitances of their inter connections becomes the limiting factor in circuit speed.

   But in quantum dots, the transition speed of the charge carriers between two different energy states define the operation speed[16] and there is no affect of capacitance.

III. In conventional devices, power must be supplied to each component through different power connections. Moreover, the various components themselves are connected to each other by various interconnections. This causes loss of power in these connections as well as in the individual components of the devices.

Quantum dot (or its assembly) itself is a complete device, that can perform several functions depending on various input conditions only. For example, the same quantum dot can act as optic as well as photonic device if the input is optical signal. On the other hand, if the input is electrical signal it can function as single electron transistor. This proves that need for inter connections does not occur.

IV. In silicon technology, power dissipation becomes a great problem as the size reduces. For example, to work at 10 $GH_z$, it requires power dissipation over 3 $kW / cm^2$ .

But quantum dot and its assembly need very less power for its successful operation and so the power dissipation problem does not occur.

## 1.4 Overview of recent research in the area of nano particle

For the last few years, a great deal of interest has been shown by many research workers to prepare semiconductor nanoparticles and to study their optoelectronic and optical properties. They[13,17] have synthesized the samples by various techniques like MBE, r f sputtering, chemical route etc. Further, They

have reported Optical absorption spectroscopy and phtoluminescence study as two powerful tools[13,18,19] to reveal the existence of different energy states and to explore their related phenomena to develop quantum dot electronic and optoelectronic devices with ultra fast switching speed.

Passler et al.[17] prepared the films of ZnS, ZnSe, and ZnTe nanoparticles on GaAs substrate by MBE and studied their temperature dependent optical spectroscopy while Benerjee et al.[18] studied the room temperature optical behaviour of ZnSe quantum dots prepared by d.c magnetron sputtering. Mahamuni et al.[13] reported the synthesis of ZnO nanostructure by chemical route and studied its photoluminescence behaviour that revealed its ultra fast switching phenomena. Zhang et al.[20] studied the X-ray absorption of dendrimer stabilized CdS quantum dots. Chen et al.[11] has detected the surface states of ZnS nanoparticle by UV/VIS absorption spectroscopy and luminescence study. Also, they have reported the ultra fast trapping and detrapping of electrons by these surface states. Boroditsky et al.[19] exclusively carried out the photoluminescence studies on III-V semiconductor nanostructures to develop ultra small light emitting diodes. Coe et al[6] carried out electroluminescence study of CdSe nanoparticle to develop highly efficient quantum dot LEDS.

## 1.5 Improvement in sample characteristics by doping

Bhargava et al.[9], reported that quantum dot shows a great deal of improvement in its luminescence property when doped with impurity like Mn, Cu

etc. The similar works have also been reported somewhere else[1]. These impurities produce artificial energy states (impurity levels) that trap and detrap the charge carriers at very fast rate and hence the device operates as faster switch than the undoped ones. Bol et al.[22] also studied the luminescence process of PbS doped ZnS nanoparticles.

## 1.6 Present work

In the present investigation, an attempt has been made to synthesize II-VI semi conductor quantum dots and apply them in the area of electronics, photonics and nonlinear optics that are very new and hot area of nanoparticle research. For sample preparation, we have adopted chemical route and quenching method due to manifold advantages (like its simplicity, less cost, large scale production etc.) over epitaxial growth or sputtering method. Also, We have irradiated the prepared specimens by high energy ion beam to find whether there is any improvements in sample properties. In fact, We have been successful to show that tremendous improvement in luminescence property of quantum dots is achieved after ion irradiaton. To be specific, the prepared quantum dots have successfully been operated as electronic switch. These specimens act as a photonic switch that detects light and produces the electrical output. The quantum dot devices have also work as optic switch that converts optical signal of one wavelength to another. In all the cases the response speed is very high and in the range of $10^{-9}$sec. to or more than $10^{-14}$sec.

Though some earlier reports[11,13,19,22] are available on trapping and detrapping of charge carriers in quantum dots, but no worker has implemented the same for electronic, photonic and optic switching where we applied the specimens for switching. These are our original and new findings in the area of quantum dots

We have synthesized three undoped and one manganese doped semiconductor quantum dots. These are:

I. Cadmium Sulphide (CdS)

II. Zinc Sulphide (ZnS)

III. Zinc Oxide (ZnO) and

IV. Zinc Sulphide doped with manganese ( ZnS:Mn )

## 1.7 Reasons for selecting II-VI semiconducting materials

The reasons for fabricating the quantum dots of the materials belonging II-VI group of periodic tables are

1. II-VI semiconductor materials have wide band gap and become wider when quantum confinement is introduced. That is why, it is easy to work with the device in the optical range from UV to visible region[23].
2. These semiconductors possess good photosensitivity. So, it is possible to develop efficient optic and photonic devices with these materials.

## 1.8 Thesis outline

In this thesis, the whole research work has been arranged in the following way

**Chapter 2:** In this chapter the details synthesis technique of different quantum dots on different matrices have been discussed.

**Chapter 3:** This chapter contains the details characterizations of quantum dot samples by XRD, TEM, optical spectroscopy and photoluminescence study.

**Chapter 4:** In this chapter, the above mentioned characterizations are carried out, on 100 MeV Cl ion beam irradiated samples.

**Chapter 5:** In this chapter, two important applications of quantum dots have been discussed. These are (a) quantum dot as electronic and photonic switch. (b) quantum dot as optic switch. We have chosen to confine our studies to the application of quantum dots in electronic, photonic and optic switching out of its large potential in the entire area of electronics, photonics and nonlinear optics.

**Chapter 6:** It contains thesis conclusion, some possible modifications of synthesis procedures along with future direction of the work.

**Appendix :** Photographs and specifications of instruments used.

## References


1. Suyve. J. F, Wuister. S. F, Kelly. J. J and Meijerink. A; *Nano. Lett.* Vol. 1, No. 8, pp 428, 2001.
2. Takahashi Naoyuki, Kaiya Kazuhiko, Nakamura Takato, Momose Yoshimi and Yamamoto Hajime; *Jpn. J. Appl. Phys.* Vol. 38, part 2, No. 4B, pp L 454, 1999.
3. Sharma K. K.and Maimeddian, : *Laser Horizon*, ( Journal of Defense Science Centre ), Vol. 2, 1998.
4. Wang. Y and Herron. N; *J. Phys. Chem.* Vol. 95, pp 525, 1991.
5. Brus. L. E; *J. Chem. Phys.* Vol. 79, pp 5556, 1983.
6. Coe Seth, Woe Wing–Keung, Bawendi Moungi and Bulovic Vladimir; *Letter To Nature* , Vol. 420, pp 800, 2002.
7. Salata. O. V, Dobson. P. J, Hull. P.J, Hutchison. J. L; *Thin Solid Films*, Vol. 251, pp 1, 1994.
8. K.K.Sharma and Mainuddian; *Laser Horizon* , ( Journal of Defence Science Centre ). Vol. 2, No. 2, pp 26,1998
9. Bhargava. R. N, Gallagher. D, Hong X, Nurmikko. A; *Phy. Rev. Lett.* Vol. 72, pp 416, 1994.
10. Brus. L. E; IEEE J. *Quantum Elect.* QE 22, pp 1909, 1986.
11. Chen. Wei, Wang. Zhanguo, Lin Jhaojun and Lin Lanying; *J. Appl. Phys.* Vol. 82, No. 6, 1997.

12 Murti Y V G S, Nandakumar P, Vijayan C, *Phys Edn*, pp 229 (Oct -Dec) 1999

13 Mahamuni S, Bendre B S, Leppert V J, Smith C A, Cooke D, Risbud S H and Lee H W H, *Nano Struct Mater* Vol 7, No 6, pp 659, 1996

14 Gimzewski James, *Phys World,* pp 29, ( March) 1999

15 Kouwenhoven Leo, Marcus Charles, *Phys World*, pp 35, (June) 1998

16 Behera S N, Sahu S N, Nanda K K, *Ind J Phys* 74 A (2), pp 81, 2000

17 Passler R, Griebl E, Riepl H, Lautner G, Bauer S, Preis H, Gebhardt W, Buda B, As D J, Schikora D, Lischka K, Papagelis K, and Ves S, *J Appl Phys* Vol 86, No 8, pp 4403, 1999

18 Benerjee S, Pal R, Maity A B,Chaudhuri S and Pal A K, *Nano Struct Mater* Vol 8, No 3, pp 301, 1997

19 Boroditsky M, Gontijo I, Jackson M, Vrijen R, Yablonovitch E, Krauss T, Cheng- Chuan-Cheng, Scherer A, Bhat R, Krames M, *J Appl Phys* Vol 87, No 7, pp 3497, 2001

20 Zhang P, Naftel J, Sham T K , *J Appl Phys* Vol 90, No 6 pp 2755, 2001

21 Tanaka M, Masumoto Y , *Chem Phys Lett* Vol 324, pp 249, 2000

22 Bol A, Meijerink A, *Phys Chem Chem Phys* 3, pp 2105, 2001

23 Nanda J, Sarma D D, *J Appl Phys* , Vol 90, No 5, 2001

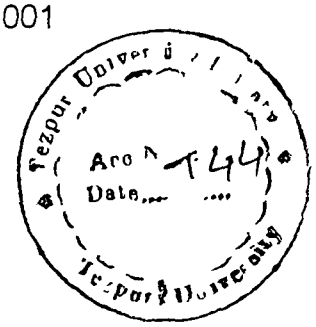

**********

# CHAPTER 2

# SYNTHESIS OF QUANTUM DOTS

# CHAPTER 2

## Synthesis of Quantum Dots

During Late 1970s and early 1980 revolutionary advancements were made in semiconductor technology that gives birth to sophisticated technique to prepare ultra small particles like quantum dot nano particles. Synthesis technique of these quantum dots is of great importance as the size, shape and hence their properties importantly depend on preparation method. There are many popular routes to synthesize semiconductor quantum dot. These are

I. Molecular beam epitaxy (MBE).

II. Vapor phase epitaxy.

III. Magnetron sputtering.

IV. Radio frequency sputtering.

V. Optical ablation.

VI. Chemical method.

In this chapter, we report quantum dot preparation by chemical route and quenching method that are easy, simple, cheap and suitable for large scale production. In chemical route, the polymer matrix controls the particle size while in quenching method, the particle growth is controlled by polymer matrix as well as sintering temperature. These indicate my contribution to quantum dot synthesis.

## 2.1 Overview of nanoparticle preparation techniques, adopted by other workers

Zhang et al.[1] synthesized InAs quantum dots on GaAs substrate using RIBBER 32 MBE technique. Benerjee et al.[2] prepared ZnSe nanoparticles with d.c magnetron sputtering. Ueda et al.[3] used r f sputtering to obtain CdO nanostructure. Patrone et al.[4] fabricated Si nanoclusters by laser ablation. Similarly, Marfaing[5] used optical source to control the growth of ZnSe crystal Recently, chemical method[6] for quantum dot preparation has been popularly adopted by many workers as mentioned below

Murty et al.[7] synthesized CdS quantum dot using polymer perfluroethylene sulfonic acid. Chen et al.[8] prepared ZnS quantum dots where the particle size is varied by changing the reaction temperature. Qadri et al.[9] synthesized ZnS quantum dots by using some lipids and surfactants that control the particle size Similarly Nanda et al.[10] prepared ZnS nanocrystal with 1-thyglycolas caping agent. Using poly vinyl pyrolidane as caping agent Mahamuni et al.[11] obtained ZnO quantum dots.

## 2.2 Quantum dot synthesis technique adopted in the present work

The methods other than chemical route, mentioned above to prepare quantum dots, are complex, costly and need sophisticated instrumentation. In the present work, an attempt has been made to prepare II-VI semiconductor quantum dots using two routes that are simple, cheap and suitable for large scale production. Considering these factors, we have adopted the following two methods[12-18].

1. Chemical method.
2. Quenching method.

### 2.2.1 Chemical method

In chemical route, polymer matrices play the central role in controlling the particle size. Physically, the matrices provide some gaps in the polymer chain. These gaps are of nm range. During chemical reaction to produce semi conductor nano material, the matrix is mixed with the reactants and then stirred As soon as the nano structure is produced, it immediately enters into the gap provided by the polymer matrix. Once the particle enters the gap, it can neither come out nor can enhance in size. During sample preparation the particle size can be varied by controlling

a. Temperature of the reaction.

b. Stirring rate of the reactants and matrix.

c. The amount of reactants as well as matrix.

### 2.2.2 Quenching method

In quenching method, the bulk powder of the specimen is sintered in furnace at very high temperature for a long time and then it is immediately put into polymer matrix, kept at ice cold condition followed by its moderate stirring. Sudden cooling of very hot (about $800^0$C) semiconductor material, causes its fragmentation, and produce quantum dot nano particles. These nano particles enter into the gaps of matrix and produce stable quantum dots.

In quenching method, size of quantum dot can be controlled by varying

a. Sintering temperature.

b. Sintering period and

c. Temperature of matrix during quenching.

## 2.3 Physical properties of matrices used in the present work

We have selected two polymer matrices as

a. Polyvinyl Alcohol (PVA)

b. Carboxylated Styrene Butadane Rubber (SBR) latex.

Table 2.1 lists the properties while fig 2.1 displays the polymeric structures of PVA and SBR latex respectively.

| Physical properties | PVA | SBR latex |
|---|---|---|
| Glass transition temperature (K) | 343 | 211 |
| Melting temperature (K) | 413 | 273 |
| Refractive index | 1.55 | 1 53 |
| Specific gravity | 1.30 | 0.93 |
| Specific heat (J/gm-K) | 1.66 | 1.89 |
| Thermal conductivity ($W\ m^{-1}K^{-1}$) | 2.0 | 1 34 |
| Dielectric constant | 2.0 | 3 1 |

**Table 2.1 : Physical properties of PVA and SBR latex**

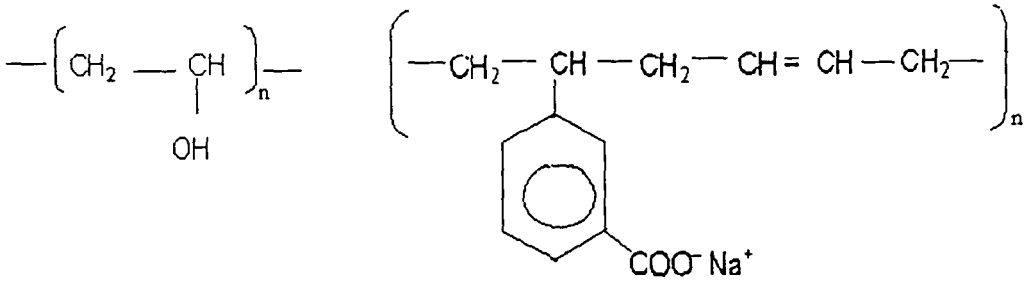


a b

**Fig 2.1: Structures of polymers. a: PVA b: SBR latex**

## 2.4 Quantum dot synthesis by chemical method

### 2.4.1 CdS quantum dots on different matrices

**a. Synthesis of CdS quantum dots on PVA matrix**

5 grams PVA are dissolved into 100 ml double distilled (D/D) water. The mixture is taken in a three necked flask fitted with thermometer pocket and $N_2$ inlet. The solution is stirred in a magnetic stirrer at a stirring rate of 200 rpm in the constant temperature of $70^0$ C for 3 hours. Thus, a transparent water solution of PVA has been prepared. The solution is degassed by boiling $N_2$ for 3 to 4 hours. Similarly, $CdCl_2$ solution is made by dissolving 5 gms of $CdCl_2$ in 100 ml D/D water. Next PVA solution and $CdCl_2$ solution are mixed in the volume ratio of 2 :1 and few drops of $HNO_3$ is added to the mixture and stirred at the rate of 250 rpm at a constant temperature of $55^0$C while 2Wt % aqueous solution of $Na_2S$ is put into it by dropping funnel slowly unless the whole solution turns into yellow colour. The solution is kept in dark chamber at room temperature for 12 hours for its stabilization followed by its casting over glass substrate and drying in oven at $50^0$ C. This film contains CdS quantum dot[6] embedded in PVA matrix.

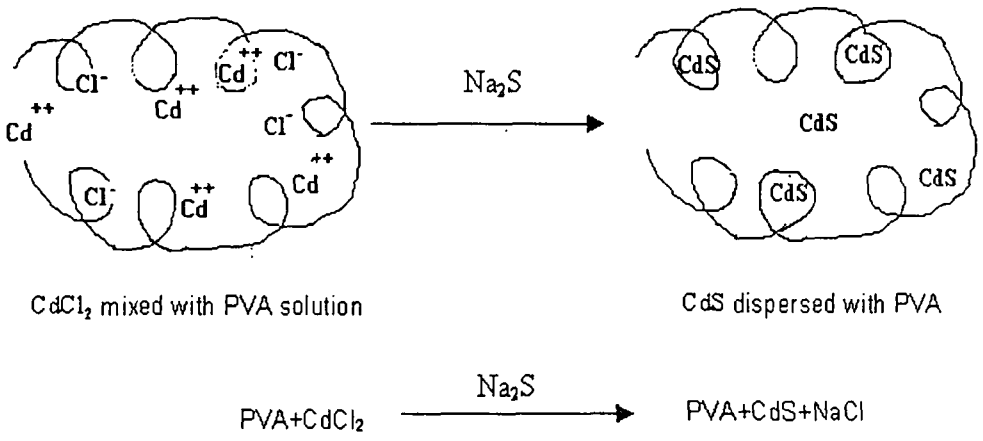


**Fig.2.2: Schematics of CdS quantum dot formation in PVA**

### b. Synthesis of CdS quantum dots on SBR Latex

One coat of SBR latex is drawn over glass substrate and then dried slowly to avoid spilling. The coated glass substrate is dipped into $CdCl_2$ solution mixed with few drops of $HNO_3$ for one hour and then taken out followed by ammonia passivation for half an hour. Finally the glass substrate is dipped into freshly prepared 2wt% $Na_2S$ D/D water solution, until it appears fully yellow. The yellow thin film contains the semiconductor CdS quantum dots embedded in SBR latex.

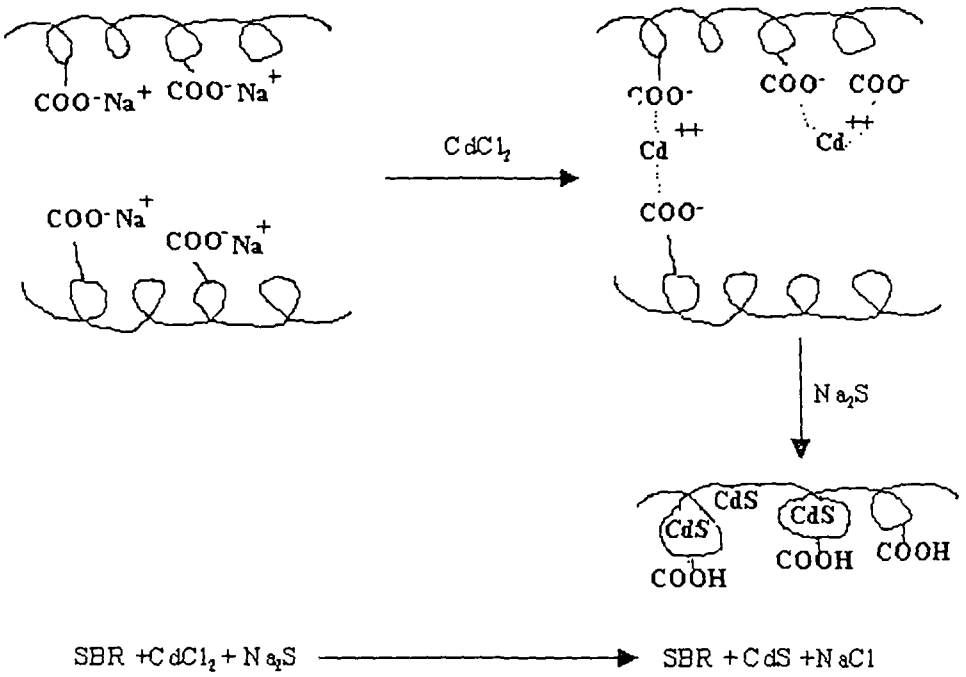


**Fig 2.3: Schematics of CdS quantum dot formation in SBR latex matrix.**

### 2.4.2 Synthesis of ZnS quantum dots on PVA matrix

5wt% D/D water solution of PVA is prepared and treated in the similar way as in case of CdS quantum dots. Next 1.36wt% aqueous solution of $ZnCl_2$ and 0.75wt% solution of $Na_2S$ are prepared so that the molecular weight ratio of $ZnCl_2$ and $Na_2S$ becomes 1:1. With this, few drops of $HNO_3$ is added. The solutions of PVA and $ZnCl_2$ are mixed in the ratio of 2:1 and then stirred at 250 rpm at $60^0$C while with dropping funnel, $Na_2S$ solution is put into it, until the whole solution appears completely milky. The prepared solution is kept in dark chamber at room temperature for 12 hours for stabilization. Finally, the solution is

cast over glass substrate and then dried in oven at $40^0$C. The film over substrate contains the quantum dots of ZnS specimens embedded in PVA matrix.

### 2.4.3 Synthesis of manganese doped ZnS ( ZnS:Mn ) quantum dots on PVA Matrix

5 wt % and 2wt% aqueous solutions of PVA and $Na_2S$ respectively are mixed by dissolving 5 gms of zinc amonium sulphate and 1 gm $MnCl_2$, and a few drops of $HNO_3$. The mixed solution is then stirred at 200 rpm in a temperature environment of $65^0$C for four hours until it appears milky. Next, the solution is kept in dark chamber at room temperature for 12 hours and Finally, it is cast over glass substrate and then dried in oven at 55 $^0$C.The deposited film contains the quantum dots[12-15] of ZnS:Mn.

## 2.5 Synthesis of ZnO quantum dots by quenching method

ZnO quantum dots are prepared by quenching method on PVA matrix. The procedure[16-18] is as follows

2 gms of bulk ZnO powder is kept in the furnace for sintering at $800^0$C for 5 hours. After sintering, the sample is taken out of the furnace very carefully and immediately put into 6wt% ice cold aqueous solution of PVA followed by its moderate stirring in room temperature for half an hour. After stabilizing the solution (by keeping it in dark chamber for 5 hours) it is cast over glass substrate and then dried in oven at $40^0$ C to prepare film of ZnO quantum dots.

## 2.6 Advantages and disadvantages of PVA matrix

### a. Advantages of PVA matrix

I. PVA is easily soluble in water at room temperature.

II. It provides uniform gaps that are very close to each other and distributed in the form of array. So the quantum dots embedded in PVA matrix are of uniform size and arranged in the fashion of array.

III. It is not corrosive in nature. So the samples on the matrix can be easily used for electronic and optoelectronic studies.

IV. On PVA matrix, the particle size can be easily controlled by changing the reaction time or temperature.

V. The samples can be obtained in both liquid and solid form.

### b. Disadvantages of PVA matrix

I. Quantum dot preparation on PVA matrix takes long time.

II. Quantum dots are very closely distributed in PVA matrix and so the property of individual sample is difficult to study.

## 2.7 Advantages and disadvantages of SBR latex matrix

### a. Advantages of SBR matrix

I. Quantum dot preparation with SBR latex matrix is possible in a short period of time.

II. It provides uniform gaps while the distances between any two gaps are large in compare to sample dimensions. So, the quantum dots embedded in SBR latex are of uniform size with large interparticle distances. That is why, properties of individual quantum dot can be studied.

III. Like PVA, SBR latex is also not corrosive. That is why; the samples on the matrix can be used in optoelectronic and electronic circuits.

### b. Disadvantages of SBR latex

I. Unlike PVA, the gaps of SBR latex and hence the size of particle embedded in it cannot be controlled easily.

II. Samples embedded in this matrix are distributed randomly.

## 2.8. Advantages and disadvantages of chemical method

### a. Advantages of Chemical method

I. In chemical route, just by fixing stirring rate and reaction temperature as well as the amount of reactants along with matrix, optimum nano size of particle can be obtained.

II. Sophisticated instrumentation is not needed.

III. This method is very cheap and simple.

IV. This route is suitable for large scale production of sample.

**b. Disadvantages of chemical method**

I. To obtain very good quantum dot, chemical reaction should take place in dark and vacuum chamber.

II. The reaction temperature and stirring rate should be continuously monitored, because slight variations in these parameters cause much variation in particle size.

III. In chemical method, quantum dots are embedded in matrix. So, it is very difficult to obtain freestanding samples.

## 2.9. Advantages and disadvantages of quenching methods

**a. Advantages of quenching method**

I. It is very simple method

II. The nano particles are obtained due to fragmentation of pure bulk powder. That is why, by quenching method, ultra pure quantum dots can be obtained, which is not possible in chemical route.

III. Like chemical method this route is also suitable for large scale production of samples

**b. Disadvantages of quenching method**

I. It is costlier than chemical method.

II. In ice cold condition, matrix solution becomes very condensed.

III. Care should be taken while taking out the sample from the furnace, because furnace temperature is very high (e g. $900^0$C).

IV. Time required in quenching method is more than chemical Route.

## References


1. Zhang. Y. C, Huang. C. J, Liu. F. Q, Xu. B, Wu. J, Chen. Y. H, Ding. D, Jiang. W. H, Ye. X. L and Wang. Z. G; *J. Appl. Phys.* Vol. 90, No. 4, pp 1973, 2001.
2. Benerjee. S, Pa.l R, Maity. A. B, Chaudhuri. S and Pal. A. K; *Nano. Struct. Mater.* Vol. 8, No 3, pp 301, 1997.
3. Ueda Naoyuki, Maeda Hiroo, Hosono Hideo and Hiroshi Kawazoe; *J. Appl. Phys.* Vol. 84, No.11, pp 6174, 1998.
4. Patrone. L, Nelson. D and Safarov. I, Sentis. M, Marine. W and Giorgio S; *J. Appl. Phys.* Vol. 87,No.8, pp 3829, 2000.
5. Marfaing. Y ; *Semicond Sci. Technol.* (6), pp A 60, I991.
6. Mohanta. D, Dolui. S. K and Choudhury. A ; *Ind. J. Phys.* 75 (A), pp 53, 2001.
7. Murti. Y. V. G. S, Nandakumar. P, Vijayan. C ; *Phys. Edn.* Pp 229, 1999.
8 Chen Wei, Wang Zhanguo, Lin Zhaojun and Lin Lanying; *J. Appl. Phys.* Vol. 82, No 6, pp111, 1997.
9. Qadri. S. B and Skelton. E. F; *J. Appl. Phys.* Vol. 89, No. 1, pp 115, 2001.
10. Nanda J, Sarma D. D ; *J. Appl. Phys.* Vol. 90, No. 5, pp 2504, 2001.
11. Mahamuni. S, Bendre. B. S, Leppert. V .J, Smith. C. A, Cooke. D, Risbud. S. H and Lee. H .W. H; *Nano. Struct. Mater.* Vol. 7, No. 6, pp 659, 1996.

12 Nath S S, Mohanta D, Chowdhury S, Bordoloi A, Dolui S K and Choudhury A, National Conference on laser and spectroscopy, November, 2001, Dibrugarh, Assam, India, 2001

13 Mohanta D, Nath S S, Mishara N C and Choudhury A , *Bull Mater Sci* Vol 26, No 3, 2003

14 Nath S S, Chowdhury S, Mohanta D, Bordoloi A, Dolui S K and Choudhury A, *Asian J Phys* (communicated)

15 Nath S S, Mohanta D, Chowdhury S, Bordoloi A, Dolui S K and Choudhury A, *J Appl Phys* (communicated )

16 Nath S S, Mohanta D, Chowdhury S, Bordoloi A, Dolui S K and Choudhury A , *Proceedings of the 4th Annual Technical Session*, Assam Science Society, Dibrugarh, Assam, India, February, pp 128,2002

17 Mohanta D, Nath S S, Bordoloi A, Choudhury A, Dolui S K and Mishra N C, *J Appl Phys* Vol 92, No 12, pp 1, December, 2002

18 Nath S S, Mohanta D, Chowdhury S, Bordoloi A, Dolui S K and Choudhury A , *Ind J Pure and Appl Phys* (communicated)

**********

# CHAPTER 3

# Characterization

# CHAPTER 3

## Characterization

Quantum dots of II-VI semiconductor material show very interesting electronic, optoelectronic, and optical properties[1-5] These properties[6-9] become more attractive when the sizes reduce to a very small value within 100 nm or less To explore these properties of our prepared semiconductor quantum dots, the samples have been subjected to the following tests

1 X-ray diffraction study (XRD)

2 Transmission Electron Microscopy (TEM)

3 Optical Absorption Spectroscopy (OAS)

4 Photoluminescence (PL) study

In this chapter, we report sample characterization by the above mentioned tests The different sample sizes have been estimated by XRD and TEM studies The band gap enhancement, that is blue shift which occurs due to size quantization of the specimens, have been explored by optical absorption spectroscopy while the optical emission phenomena of quantum dots are revealed by photoluminescence spectroscopy These form the outlines of my contribution to spectroscopic studies of quantum dots

Next consecutive sections explain the theoretical details of each of the test, mentioned above

## 3.1 X-ray diffraction study (XRD)

X-ray diffraction study is an important tool for finding different crystal parameters like size, d-spacing, diffraction planes, structure, phase, and lattice constants. The intensities and the angles of diffracted X-ray beams are related to atomic arrangement of the crystal.

In this study, X-ray diffractometer detects the X-ray, diffracted by crystal and gives the diffractogram, which is a plot between intensity and diffraction angle. Intensity is given in terms of counts and the angle is in degrees. Fig 3.1 shows a pattern of such X-ray diffractogram.

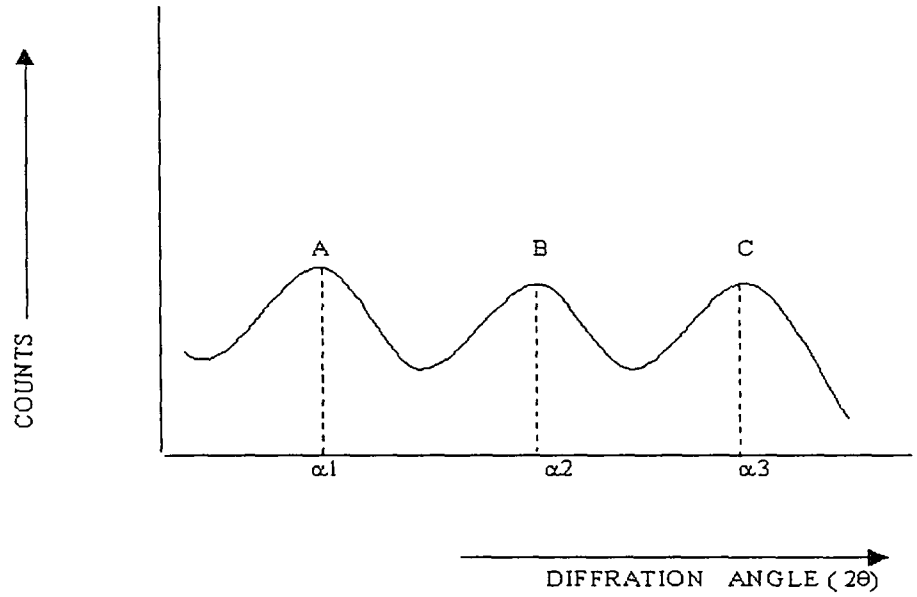


**Fig 3.1: XRD pattern**

Next we explain how X-ray diffractogram is used in finding various crystal parameters of quantum dots, prepared in our laboratory.

### 3.1.1 Sample identification

To identify any specimen, the diffraction angles produced by a particular sample are compared with the standard diffraction angles of the same material. A good match between experimental and standard values of diffraction angles is required to identify the specimen.

### 3.1.2 Size (diameter) Estimations

X-ray diffractogram is extensively used to calculate particle size using Debye-Scherrer equation[10] which gives reasonably accurate particle diameter (size) 'D'. The equation is written as

$$D = \frac{0.9\lambda}{W\cos\theta} \quad \text{.....(1)}$$

Where λ is the wavelength of X-ray used, W is the full width at half maximum (FWHM), θ is the diffraction angle or glancing angle in radians. The different parameters used in equation (1) can be obtained from X-ray diffractogram, in the following way

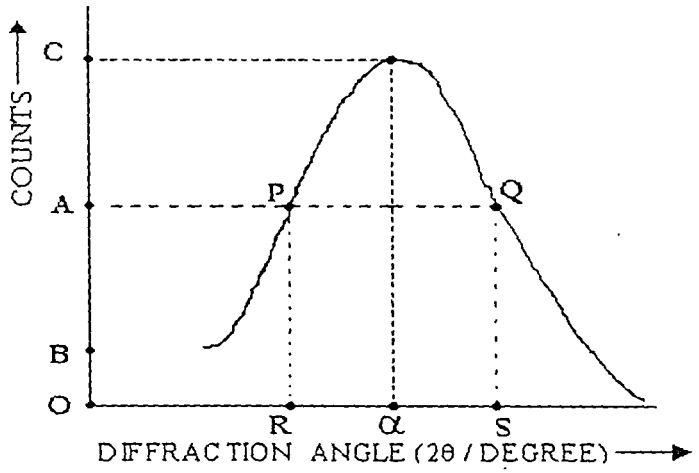


Fig 3.2 Single XRD peak

### I. Full Width at Half Maximum (FWHM )

In the example shown in figure 3.2, the maximum height of the XRD peak is BC and OB is the noise. Half of the maximum height is either AB or AC. That is, the middle point of the peak is A. Two more points P and Q are taken on the plot collinear to point A. Two perpendiculars from points P and Q are drawn on the abscissa, which is cut by the perpendicular lines at point R and S. The segment RS is the full width at half maximum (FWHM) in degrees. Finally, this is converted into radians, which is the actual required FWHM (W).

### II. Diffraction angle or glancing angle ($\theta$) and X-ray wavelength

In the diffractogram, the angle axis is calibrated in terms of "$2\theta$ / degree". From this, glancing angle "$\theta$" can be obtained. The X-ray wavelength "$\lambda$" used in the X-ray diffractometer is 0.1541 nm.

In practice, the experimental data obtained from XRD study of any specific specimen may slightly differ from the standard values due to the following reasons.

1. Calibration error
2. Instrumental error
3. Sudden power fluctuation during experiment
4. External noises.

### 3.1.3. Estimation of "d" spacing between two parallel planes

By knowing the value of glancing angle θ and the X-ray wavelength λ, one can find out 'd' spacing between two parallel planes of atoms in crystals, using Bragg's equation which is written as

$$2d\,Sin\theta = n\,\lambda$$

$$d = \frac{n\lambda}{2Sin\theta} \quad \ldots\ldots\ldots\ldots\ldots\ldots\ldots\ldots(2)$$

After knowing the value of 'd', following crystal parameters may be found by using computer software

I. Lattice constants a, b, and c

II. Structure and phase of a crystal

III. Position and arrangements of atoms in a crystal lattice

Due to non-availability of this software, the above mentioned parameters can not be revealed in the present investigation.

## 3.2 Transmission Electron Microscopy

Transmission Electron Microscope (TEM) has opened a new door to nanoparticle research by providing pictorial view of them with very high magnification of 8 lacks or more. This study, gives the information about size, shape and surface morphology of any specimen. Some sophisticated microscopes give the size distribution of nano particles in the host matrix also

## 3.3 Optical absorption spectroscopy

Optical absorption spectroscopy is an important way to explore the different energy states in semiconductor material. This study[1,11-13] is based on the fact that, if two possible energy states $E_1$ and $E_2$ exist in a system as shown in fig 3.3, then

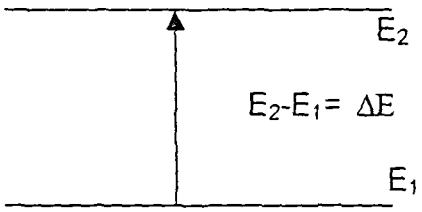


**Fig. 3.3: Electronic excitation between two energy states**

electronic transition from level $E_1$ to $E_2$ can takes place when appropriate energy $E_2 - E_1 = \Delta E$ is absorbed and the frequency of radiation has the simple form of

$$\nu = \frac{\Delta E}{h} Hz$$

or, $\Delta E = h\nu$ *joules*.

That is, absorption wavelength or edge can be written as

$$\lambda_a = \frac{hc}{\Delta E} \qquad (3)$$

where '$\lambda_a$' is the absorption edge, 'h' is the Planck's constant and 'c' is the velocity of light. Next, we discuss the procedure to characterize quantum dots with the help of optical spectroscopy.

### 3.3.1 Information about band gap

It is mentioned in chapter 1 that reduction in particle size that is, size quantization, results in band gap enhancement. For example, If $E_{gb}$ is the band gap of bulk specimen, and $E_{gn}$ is that of quantum dot, then

$$E_{gn} > E_{gb}$$

If $h\nu_n$ and $h\nu_b$ are the required energy to excite the electrons from valence band to conduction band in quantum dot and bulk samples respectively,

then $$h\nu_n > h\nu_b$$

$$\text{or, } \nu_n > \nu_b$$

$$\text{or, } \lambda_{an} < \lambda_{ab} \quad \ldots\ldots\ldots\ldots\ldots\ldots \quad (4)$$

Where, $\lambda_{an}$ and $\lambda_{ab}$ are the absorption edges of quantum dot and bulk samples respectively. Relation (4) clearly infers that optical absorption edge in quantum dot is blue shifted. For estimating particle size from blue shift, a theoretical model[13] has been proposed, known as hyperbolic band model that is written as

$$R = \sqrt{\frac{2\pi^2 h^2 E_{gb}}{m^*(E_{gn}^2 - E_{gb}^2)}} \quad \ldots\ldots\ldots\ldots\ldots\ldots (5)$$

Where, R is the quantum dot radius, $E_{gb}$ is the bulk band gap, $E_{gn}$ is the quantum dot band gap, h is planck's constant, m* is the effective mass of the specimen. The value of m* is expressed in terms of electronic mass $m_e$. The bulk band gaps at room temperature and the effective masses[11] of three semiconductors CdS, ZnS, ZnO are listed in the table 3.1.

| Name of the samples | Bulk Band gap | Effective mass ($m^*$) | Values of effective mass |
|---|---|---|---|
| CdS | 2.42 eV | 0.2 $m_e$ | 1.82 x $10^{-31}$ Kg |
| ZnS | 3.54 eV | 0.4 $m_e$ | 3.64 x $10^{-31}$ Kg |
| ZnO | 3.20 eV | 0.27 $m_e$ | 29.15 x $10^{-31}$ Kg |

**Table 3.1: Bulk band gap and effective masses of II-VI semiconductor**

$m_e$ is the mass of electron ( 9 x $10^{-31}$ Kg )

This model provides reasonably accurate quantum dot size (diameter 2R) Accuracy of this model is more when the particle geometry is spherical in shape[13].

### 3.3.2 Information about the crystal defects and surface states

Optical spectroscopy is a very efficient technique to reveal the existence of crystal defects and surface states etc. in semiconductor specimen provided they are present in large numbers[11-14]. In that case, an absorption weaker than the band edge absorption occurs in the longer wavelength region in the spectrum as shown in the example in fig. 3.4. The energy corresponding to this absorption is much less than band gap. In undoped and unirradiated quantum dots, due to presence of very few crystal defects, they are hardly detected by this technique. After doping or ion irradiation, number of defects increases and they are well detected by optical spectroscopy.

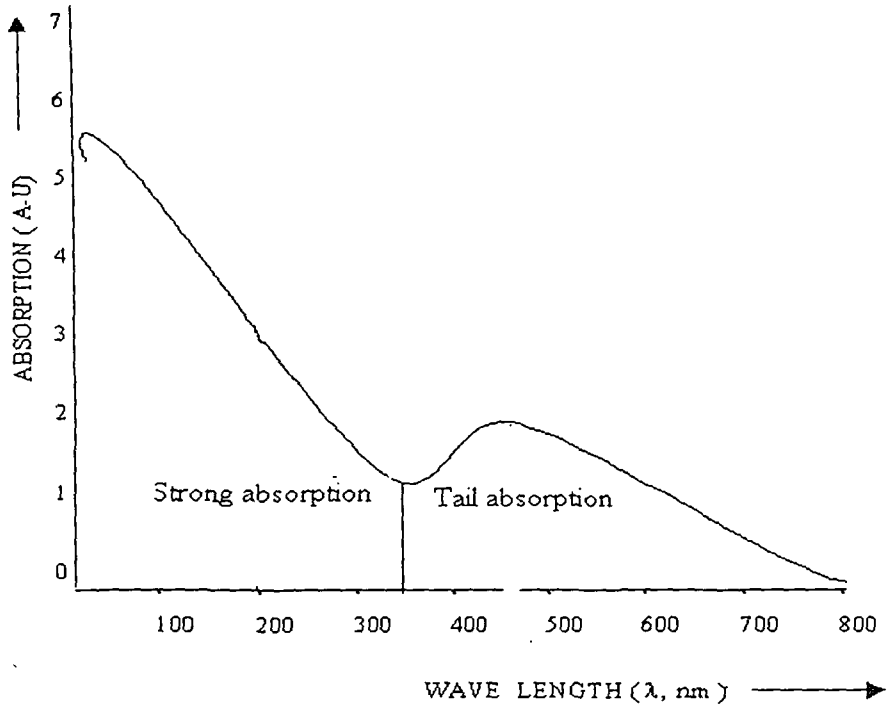


**Fig. 3.4: General pattern of UV / Visible absorption spectra of quantum dots**

## 3.4 Photoluminescence (PL) study

Photoluminescence is the phenomenon, when an optical sensitive material is excited by photons of proper frequency, it emits energy in the form of light during excitation or within $10^{-8}$ seconds after the excitation source is removed. Sometimes emission occurs after a considerable time of removing the source. This process[1,12] is based on the principles explained below.

Excitations of electrons are associated with absorption of optical signal (photons) that may be infrared, visible, ultraviolet or X-ray radiations depending upon the frequency required to excite the specimen.

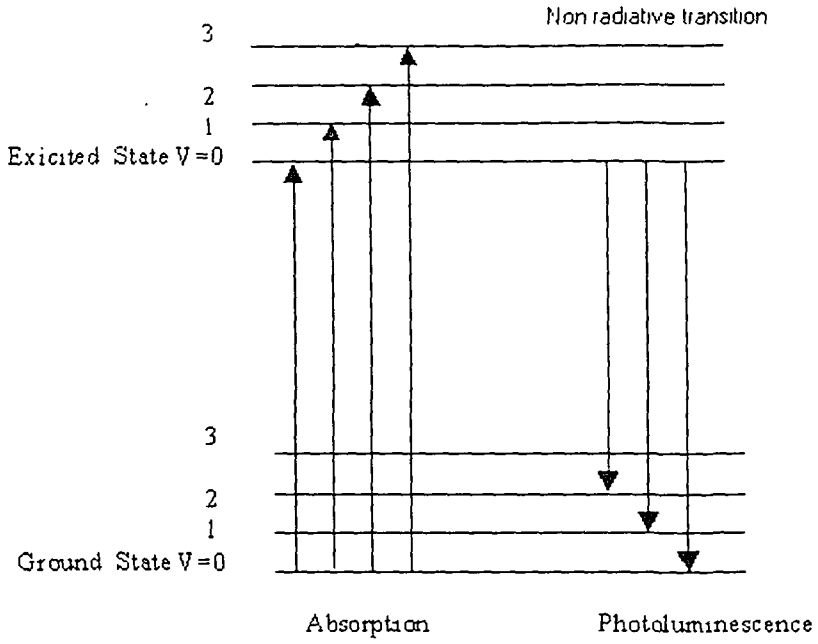


**Fig. 3.5: Energy levels of pure crystal**

Figure 3.5 illustrates photoluminescence process in ideal pure specimen At ground state, the atoms absorb light and jumps to conduction band. Some of the absorbed energy is lost due to molecular vibration and friction. Though the photosensitive material like CdS, ZnS and ZnO luminescence in pure form, but the luminescence quantum efficiency of these materials increases remarkably, when doped with some impurity[1,12] atoms like Mn.

### 3.4.1 Excitation and emission in doped crystals

The presence of doped atoms produces some localized energy levels in the forbidden energy gap of the solid[1,12]. These levels may be classified into two categories.

I. Levels that belong to impurity atoms themselves.

II. Levels that belong to host atoms which are under the perturbing influence of the activator atoms or belonging to lattice defects. (e.g. Vacancies).

For a general semiconductor specimen, in figure 3.6 let G and A be two levels corresponding to one of the two categories (I) and (II). In the ground state, level G is occupied by electron and A is empty while in the excited state the reverse is true. The excitation from G to A may be achieved at least through three processes[11]

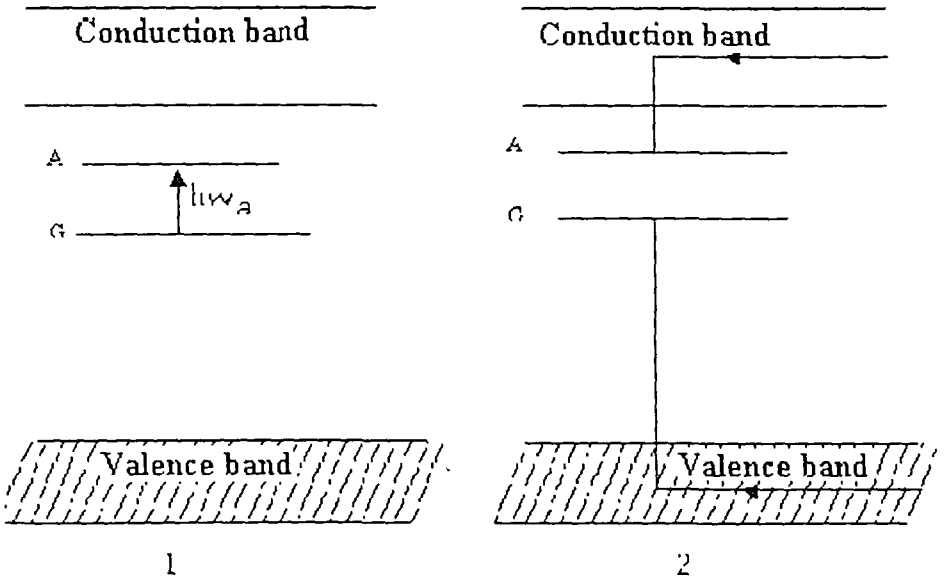


Fig. 3.6: Energy band picture of luminescence center: G is ground state and A is excited state. In (1) Excitation takes place by direct absorption of energy where in fig (2) capture of a hole at G and electron at A achieves excitation.

I. An incident photon of proper frequency may be absorbed directly by the electron[1] in the level G where upon it arises in A as in figure 3.6.

II. Excitons[12], which are stable bound electron hole pair, may reach luminescent centers such as AG, whereupon it gives off its energy to the center resulting in excitation of electron. Exciton may be produced in any part of the crystal and its diffusional motion carries it to the center like AG.

III. Electron hole pairs[12] may be created in the crystal by bombardment with photons and subsequently the level G may capture a hole from the valence band and A may trap an electron from conduction band. This type of excitation is illustrated in figure 3.6(b).

Again, in the emission phenomena, the return of electron from excited state A to ground state G is not a simple process accompanied by emission of photon of frequency equal to the absorption frequency. As shown in figure 3.7 level G is presented as a function of configurational coordinate q. Each value of q corresponds to a particular configuration of the nucleus in the vicinity of luminous centers. In figure 3.7(a), transition GA and A´G´ are allowed by Frank-Condon principle. Thus, transition is vertical and starts from the minima of respective curves. It is clear that during the optical excitations from G to A, nuclei remain exactly in the same configuration that is time average q remains the same but after the absorption act, they undergo slight rearrangement because, after absorption, the nuclei do not occupy the equilibrium position and the system

moves gradually to acquire it. The emission of photon therefore occurs according to Stoke's law at a new value of the configurational coordinate such that $h\omega_c < h\omega_a$ or $\omega_c < \omega_a$ and the system that arises at G′ finally returns to G.The extra energy E , $E_A - E_A'$ and $E_G - E_G'$ are dissipated in the generation of lattice phonons.

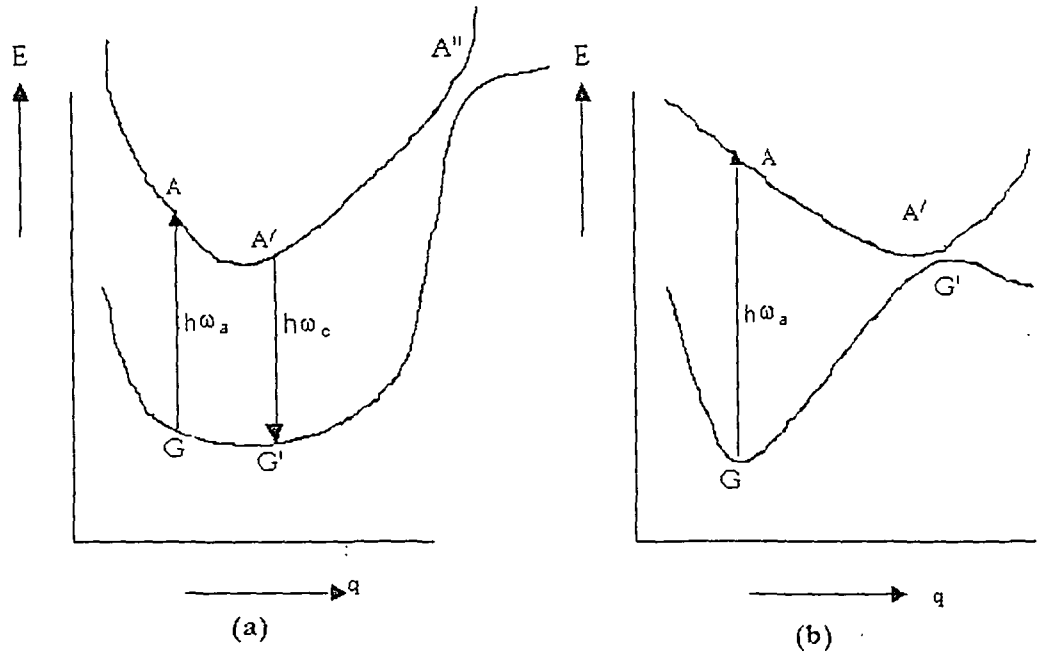


**Fig. 3.7: Energy of ground state and excited state (a) as a function of the configurational co-ordinate q. The situation (a) gives luminescence and (b) corresponds to dissipation of excitation energy in the form of heat.**

The above model explicitly assumes that the transition of an excited center to the ground state is accompanied by the emission of photons. The model holds for luminescent materials and discussion is applicable to them only. In non-luminescent material, on the other hand, the transition occurs without emission of photons and the absorbed energy is essentially transformed into heat. In this case, the transition is said to be nonradiative. It may be noted that

the system moves from A to A′ after absorption of optical energy and then crosses the narrow gap to point G′, associated with ground state emission of low frequency photon as shown in Figure 3.7(b).

### 3.4.2 Luminescence in II – VI semiconductor quantum dots

Photoluminescence is very useful technique to reveal different energy states like surface states and crystal defects (in general these are called traps) in semiconductor quantum dots[12-15]. The absence of band edge emission has been attributed to be quenched by trap related emission. This is because as the particle size becomes smaller, the surface state and various crystal defects increase, reducing the band to band emission[12,14]. The reasons are explained below.

I. In small particle, the trapping and detrapping of electrons in the traps is an extremely fast process, occurring in $10^{-13}$ to $10^{-14}$ seconds range[14]. Spontaneous band edge emission has no chance of competing with it.

II. The trap absorption edge is extended to band to band emission of specimen. Thus, the band edge emission overlaps with trap absorption. The energy transfer from interband states, to the trap centers may occur easily via reabsorption. That is why, most nanoparticles exhibit the trap luminescence though excited by band to band absorption.

Next, we discuss the characterizations of our quantum dot samples.

## 3.5 Cadmium Sulphide

| | | |
|---|---|---|
| Chemical formula | : | CdS |
| Name of matrix used | : | SBR latex / Poly Vinyl Alcohol (PVA) |
| Sample code used | : | $S_1$ |
| Method of preparation | : | Chemical route. |

### 3.5.1 X-ray diffraction study

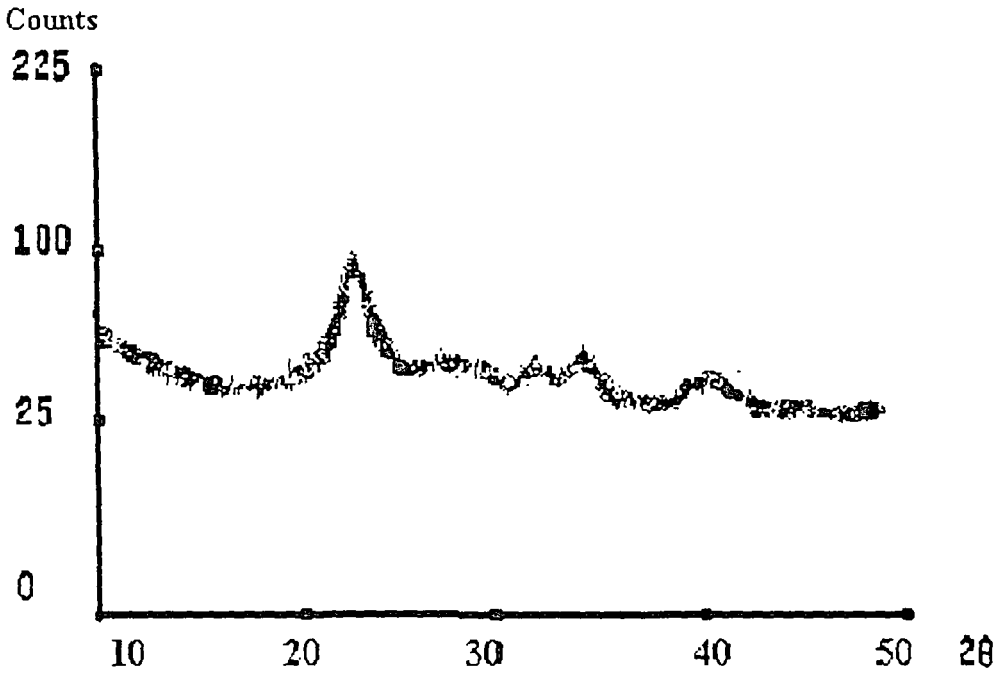


Fig 3.8: X-ray diffractogram of CdS

Fig 3.8 displays the X-ray diffractogram and Table 3.2 shows the experimentally obtained X-ray diffraction angles and the standard diffraction angles of CdS specimen while table 3.3 gives the average size, diffraction planes etc.

| Experimental diffraction angle (2θ in degrees) | Standard diffraction angle (2θ in degrees) |
|---|---|
| 25 | 24.8 |
| 30.66 | 29 |
| 31.40 | 30.8 |

**Table 3.2: Experimental and standard diffraction angles of CdS specimen**

| Diffraction angle (degrees) | FWHM (radians) | d spacing (nm) | Diffraction planes | Size (in nm) | Average size (nm) |
|---|---|---|---|---|---|
| 25 | 0.020 | 0.36 | 100 | 6.8 | 8.41 |
| 30.66 | 0.016 | 0.29 | 010 | 8.9 | |
| 31.40 | 0.014 | 0.28 | 001 | 10.1 | |

**Table 3.3: Various XRD data of CdS quantum dot**

### 3.5.2 Transmission Electron Microscopy

TEM images of CdS quantum dots are displayed in fig 3.9 and the corresponding size and shape are produced in table 3.4

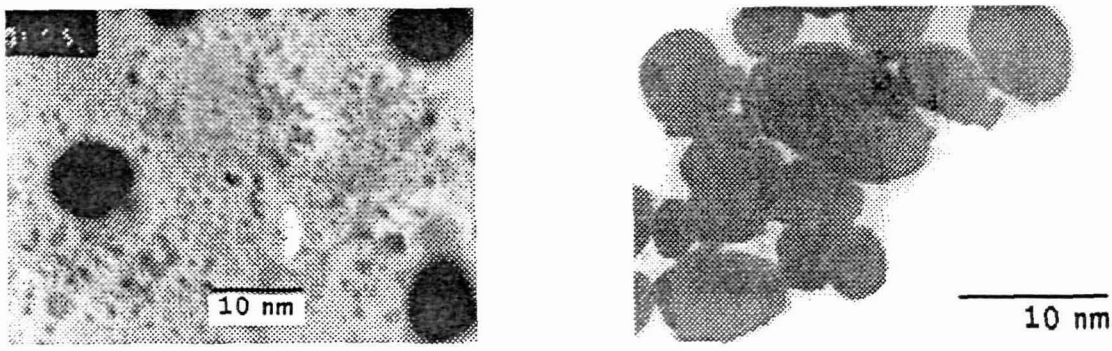


CdS/SBR CdS/PVA

Fig 3.9: TEM image of CdS

| Particle size | Particle shape |
|---|---|
| 8.8 nm | Spherical |

Table 3.4: Various data obtained form TEM study of CdS sample

### 3.5.3 Optical absorption spectroscopy

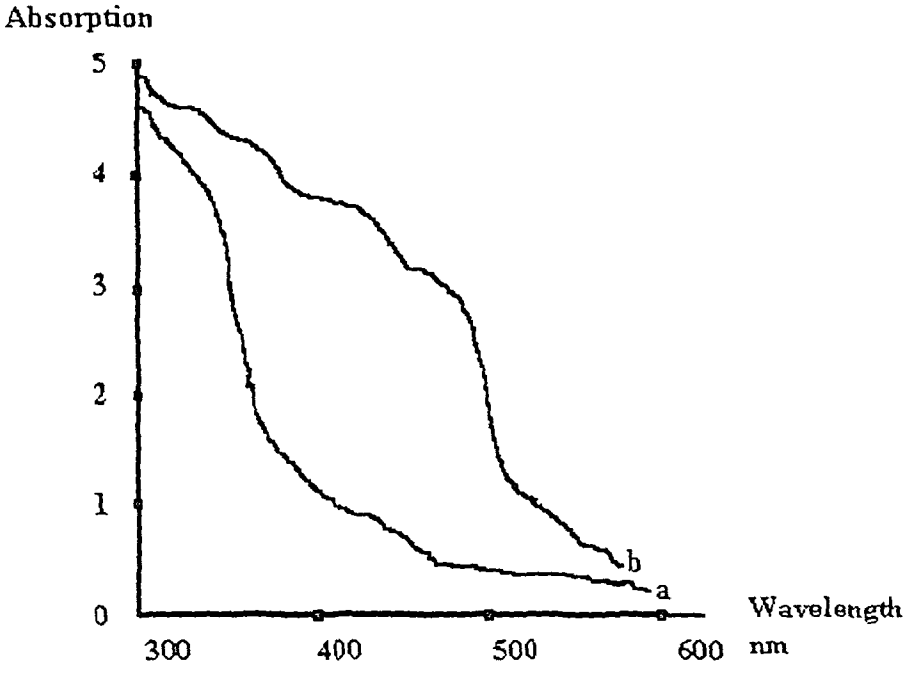


**Fig. 3.10: UV / VIS absorption spectra of CdS. a: quantum dot, b: bulk**

In the optical absorption spectra shown in fig 3.10 plot "a" stands for the spectrum of quantum dot while "b" stands for that of bulk specimen. These two spectra clearly show that absorption edge of quantum dot is strongly blue shifted at around 375 nm with respect to bulk specimen that possesses the edge at around 500 nm. From blue shift, the size has been estimated by adopting hyperbolic band model[13]. Table 3.5 gives band gap enhancement due to size quantization and the corresponding size, estimated from optical spectroscopy.

| Absorption edge in quantum dot | Band gap of CdS quantum dot | Absorption edge of bulk CdS | Energy gap of bulk CdS | Increase in band gap due to size quantization | Quantum dot size |
|---|---|---|---|---|---|
| 375 nm | 3 53 eV | 500 nm | 2.48 eV | 1.05eV | 7.6 nm |

*Table 3.5: Different data of CdS specimen revealed from optical spectroscopy*

### 3.5.4 Photoluminescence study

### I. Excitation source 200nm

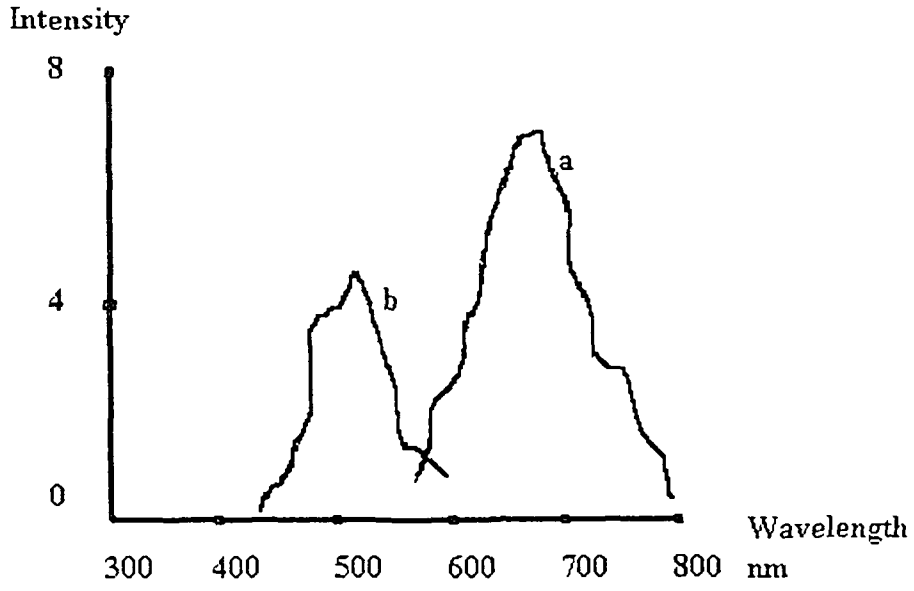


Fig. 3.11(A): PL spectra of CdS: Excitation source 220nm. (a) for CdS quantum dot and (b) for CdS bulk

Photoluminescence spectra of both CdS bulk and CdS quantum dot when excited with optical source of wavelength 200 nm well above band gap are shown in fig 3.11(A) and the corresponding data are put in the table 3.6

| Sample | Peak Position | Intensity |
|---|---|---|
| CdS Bulk | 500 nm | 4.2 |
| CdS quantum dot | 700 nm | 7.3 |

**Table 3.6: PL peak positions and intensities of CdS specimen with excitation source 220 nm**

These spectra clearly show that our prepared CdS quantum dot possesses luminescence peak at around 700 nm denoted by "a" with high intensity while pure CdS bulk specimen shows a comparatively weaker emission at around 500 nm denoted by "b". This is due to the fact that, during sample synthesis by chemical route, some excess $Cd^{++}$ were free to react with oxygen atoms in air, that produces a CdO phase in the sample. The presence of CdO phase is evident from the XRD peak at $40^0$ in the diffractogram[4], shown in fig 3.8. The created CdO produces an intermediate energy state that acts as donor level in the forbidden energy gap of CdS sample[12,13]. Due to this phenomenon, electron transition takes place between donor (CdO center) level and valence band of CdS producing intense luminescence[13] at 700 nm in the spectrum. Moreover pure CdS related luminescence at 500 nm lies in the excitation range of CdO related luminescence[8,13,14]. Hence, practically, in our sample, pure CdS related luminescence is completely quenched resulting in CdO phase related intense luminescence at 700 nm.

## II. Excitation source 630 nm

The PL spectrum of CdS quantum dot with excitation source of 630 nm does not differ from that of 200 nm excitation source as the mechanism is the same that is the presence of CdO phase but there is no luminescence in bulk CdS sample as the source is well below the band gap to cause emission. The spectrum is shown in fig 3.11(B).

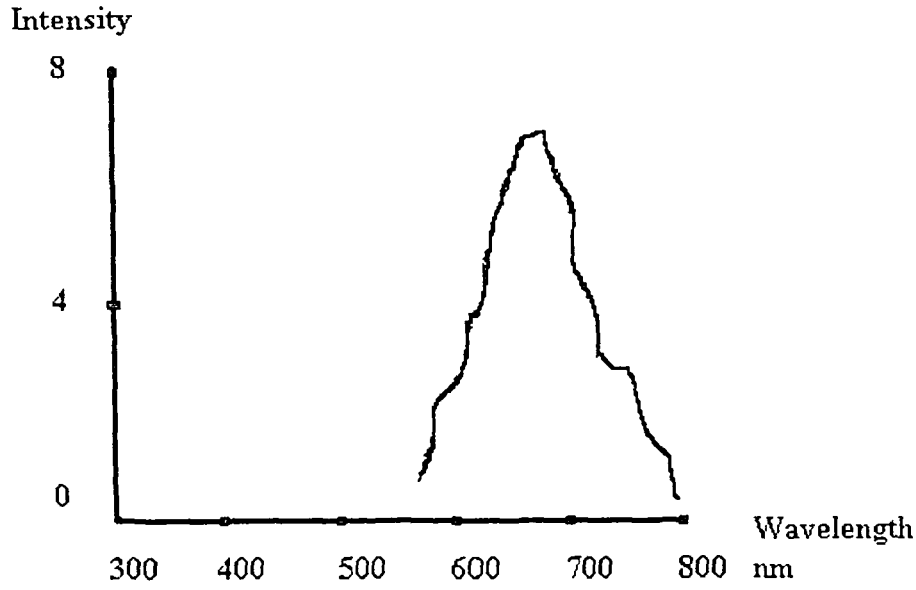


Fig 3.11 (B): PL spectrum of CdS quantum dot.

Excitation source 630 nm.

No emission has been observed in CdS sample with excitation source of wavelength more than 630 nm as this energy is not sufficient neither for band to band excitation nor CdO phase related excitation to cause luminescence.

## 3.6 Zinc Sulphide

| | | |
|---|---|---|
| Chemical formula | : | ZnS |
| Name of Matrix | : | Poly Vinyl Alcohol (PVA) |
| Sample code used | : | $S_2$ |
| Method of preparation | : | Chemical route |

### 3.6.1 X-ray diffraction study

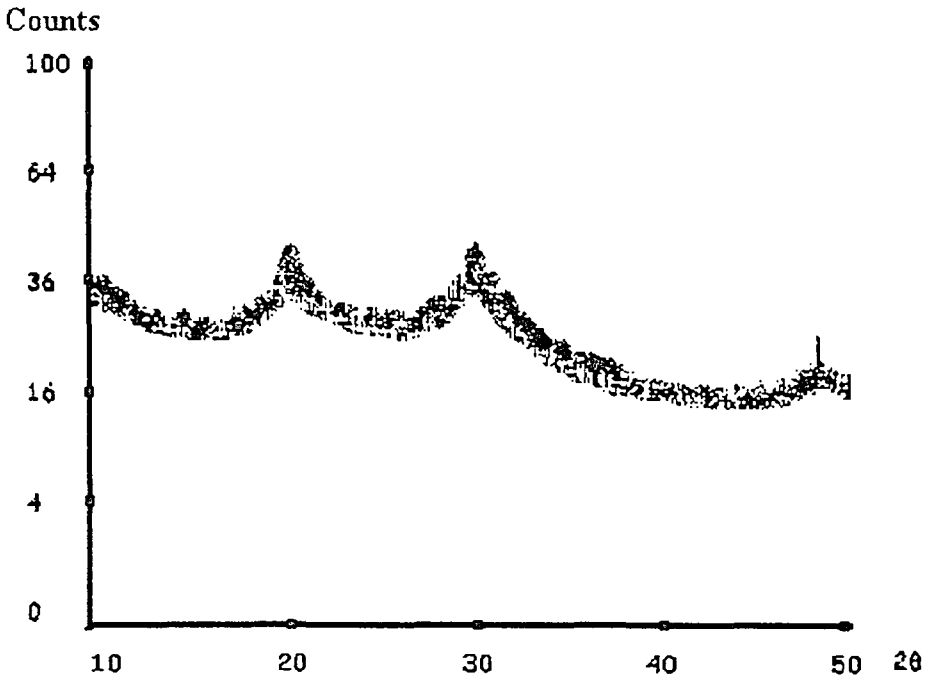


Fig. 3.12: X-ray diffractogram of ZnS quantum dot

Fig 3.12 shows the X-ray diffractogram and table 3.7 shows the experimentally ained diffraction angle along with the standard diffraction angles of ZnS specimen ile table 3.8 shows its average size, diffraction planes, etc.

| Experimental peak position (2θ in degrees) | Standard peak position (2θ in degrees) |
|---|---|
| 20 | 21 |
| 30 | 29 |
| 50 | 50 |

**Table 3.7: Experimental and standard diffraction angles of ZnS specimen**

| Peak position (degree) | FWHM (Radians) | d spacing (nm) | Diffraction planes | Size nm | Average size (nm) |
|---|---|---|---|---|---|
| 20 | 0.019 | 0.44 | 100 | 7.4 | 7.5 |
| 30 | 0.020 | 0.29 | 010 | 5.2 | |
| 50 | 0.016 | 0.18 | 011 | 9.7 | |

**Table 3.8: Various XRD data of ZnS quantum dot**

### 3.6.2 Transmission Electron Microscopy

TEM photograph of ZnS quantum dot is displayed in figure 3 13 while its size and the shape are put in the table 3 9.

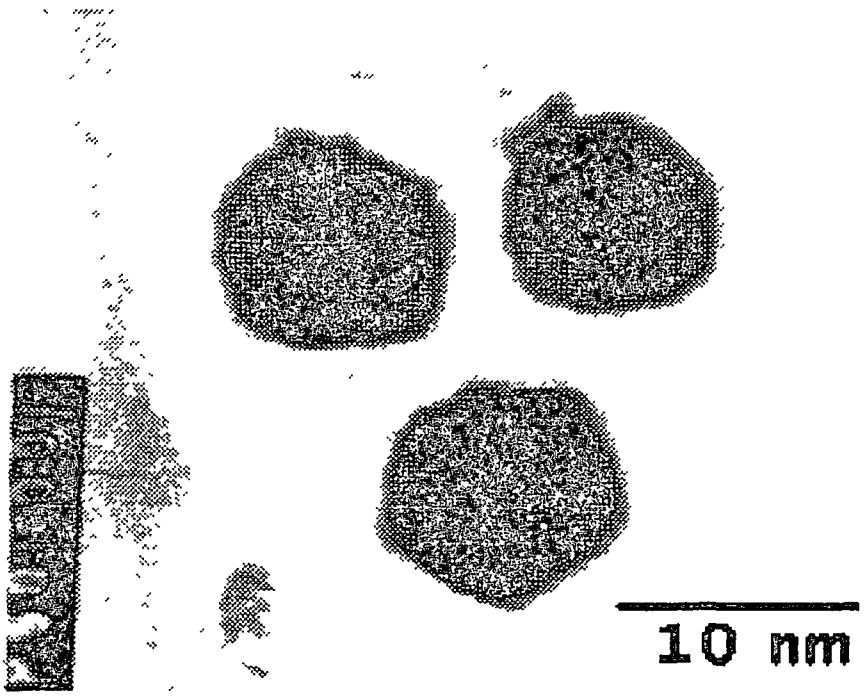


**Fig. 3.13: TEM Photograph of ZnS quantum dots**

| Average particle size | Particle shape |
|---|---|
| 7 nm | Spherical |

**Table 3.9: Various data of ZnS Sample obtained form TEM study**

### 3.6.3. Optical absorption spectroscopy

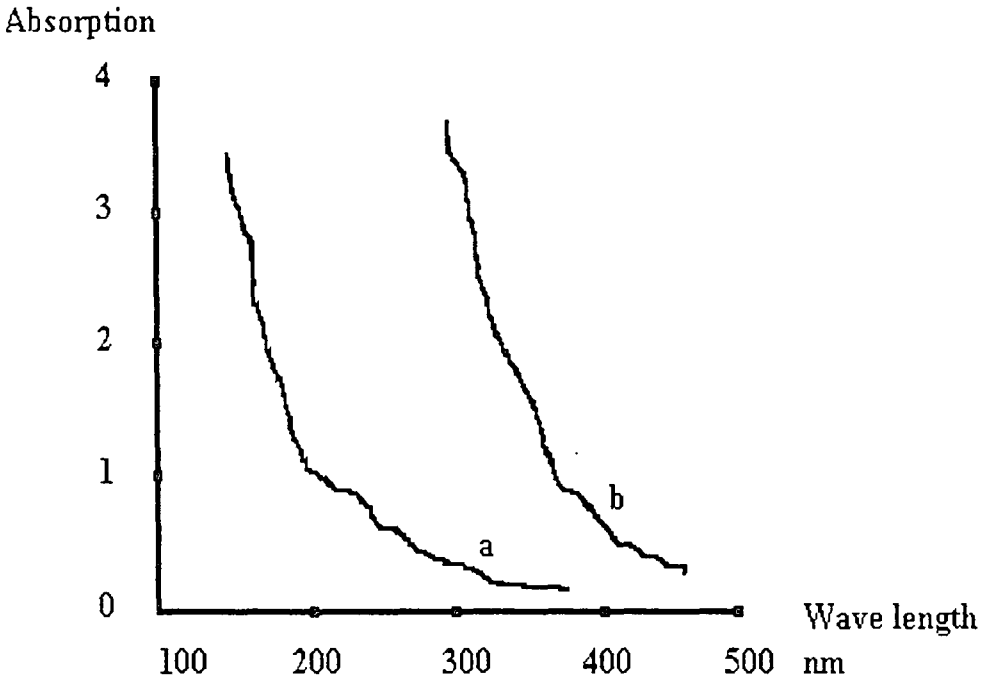


**Fig. 3.14: Optical absorption spectra of ZnS. a: quantum dot, b: bulk.**

In fig 3.14 optical absorption spectrum "a" stands for that of quantum dot sample while "b" for that of bulk specimen. The plots infer that the absorption edge of ZnS quantum dot is strongly blue shifted[14] at 200 nm with respect to bulk specimen that possesses the absorption edge at 350 nm. Table 3.10 shows the various data obtained from the study.

| Absorption edge in quantum dot | Band gap in In quantum dot | Absorption edge in bulk ZnS | Band gap in bulk ZnS | Increase in Energy gap due to size quantization | Particle size |
|---|---|---|---|---|---|
| 200 nm | 6.18 eV | 350 nm | 3.53 eV | 2.65 eV | 9 nm |

Table 3.10: Different data of ZnS specimen revealed from optical spectroscopy

### 3.6.4 Photoluminescence study

#### I. Excitation source 200nm.

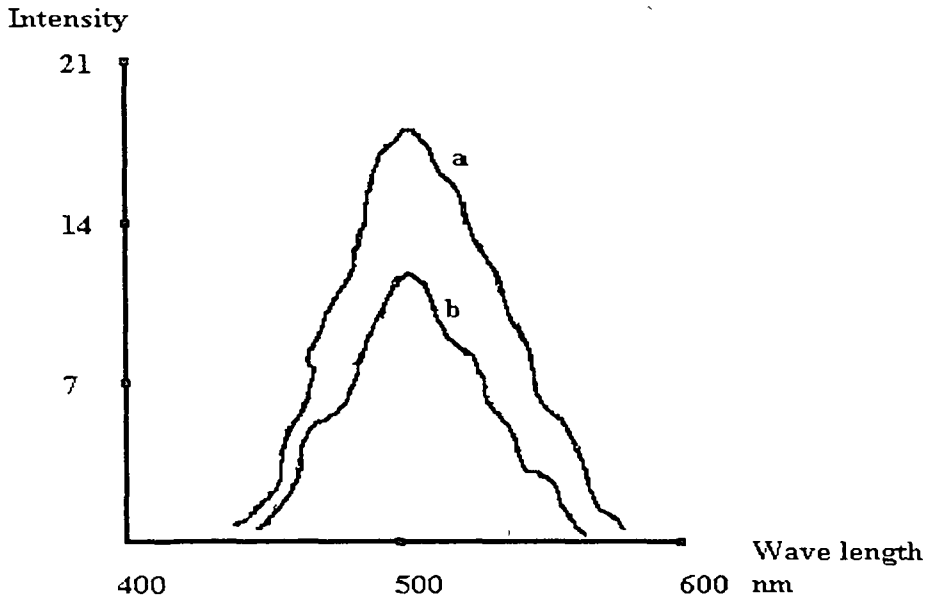


Fig. 3.15: PL spectra of ZnS specimen. a: ZnS quantum dot and b: ZnS bulk.

**II. Excitation source 460 nm**

Luminescence spectra of ZnS bulk and quantum dot excited with 460 nm below the band gap energy do not differ at all with that of 200 nm source because in ZnS specimens, luminescence is caused by surface states only that are excited with the source of 460 nm, well below the band gap energy.

No emission is observed in ZnS specimen above 460 nm of excitation source as neither band to band excitation nor surface state excitation can take place with exitation source having the wavelength above the said range.

## 3.7 Zinc Oxide

| | | |
|---|---|---|
| Chemical formula | : | ZnO |
| Name of matrix | : | Poly Vinyl Alcohol (PVA) and thiourea |
| Sample code | : | $S_3$ |
| Method of preparation | : | Quenching |

### 3.7.1 X-ray diffraction study

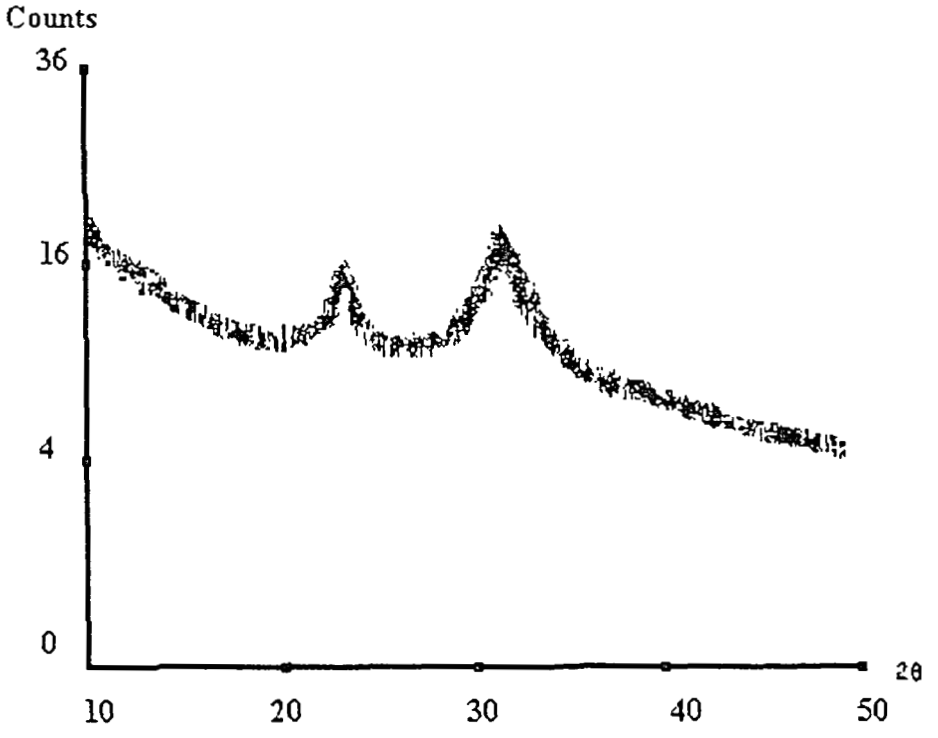


**Fig. 3.16: X-ray diffractoram of ZnO quantum dot**

X-ray diffractogram of ZnO quantum dot is displayed in fig 3 16 while the experimentally obtained diffraction angles and the standard diffraction angles of it are compared in the table 3.12. Next table 3.13 gives diffraction planes, average size etc of the sample.

| Experimental peak positions of ZnO quantum dot (2θ in degree) . | Standard peak positions of ZnO quantum dot (2θ in degree) |
|---|---|
| 23.5 | 25.8 |
| 31.6 | 32 |

**Table 3.12: Experimental and standard diffraction angles of ZnO specimen.**

| Peak position ( degree) | FWHM (radians) | d spacing (nm) | Diffraction planes | Size (nm) | Average size (nm) |
|---|---|---|---|---|---|
| 23.5 | 0.017 | 0.38 | 100 | 8.4 | 8 2 |
| 31.6 | 0.018 | 0.28 | 010 | 8 | |

**Table 3.13: Various XRD data of ZnO quantum dot**

### 3.7.2 Transmission Electron Microscopy (TEM)

TEM photograph of ZnO quantum dots is shown in figure 13.17 which provides the surface morphological view of the particles. The sample size and shapes are put in the table 3.14.

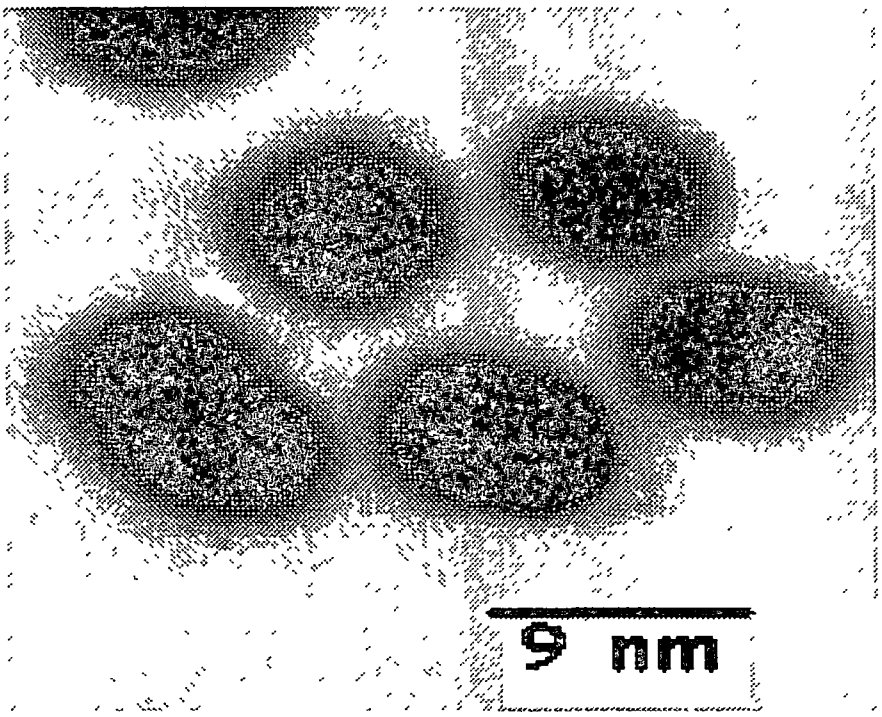


**Fig: 3.17 : TEM Photographs of ZnO**

| Average particle size | Particle Shape |
|---|---|
| 7 nm | Spherical |

**Table 3.14: Various data of ZnO sample obtained form TEM study**

### 3.7.3. Optical absorption spectroscopy

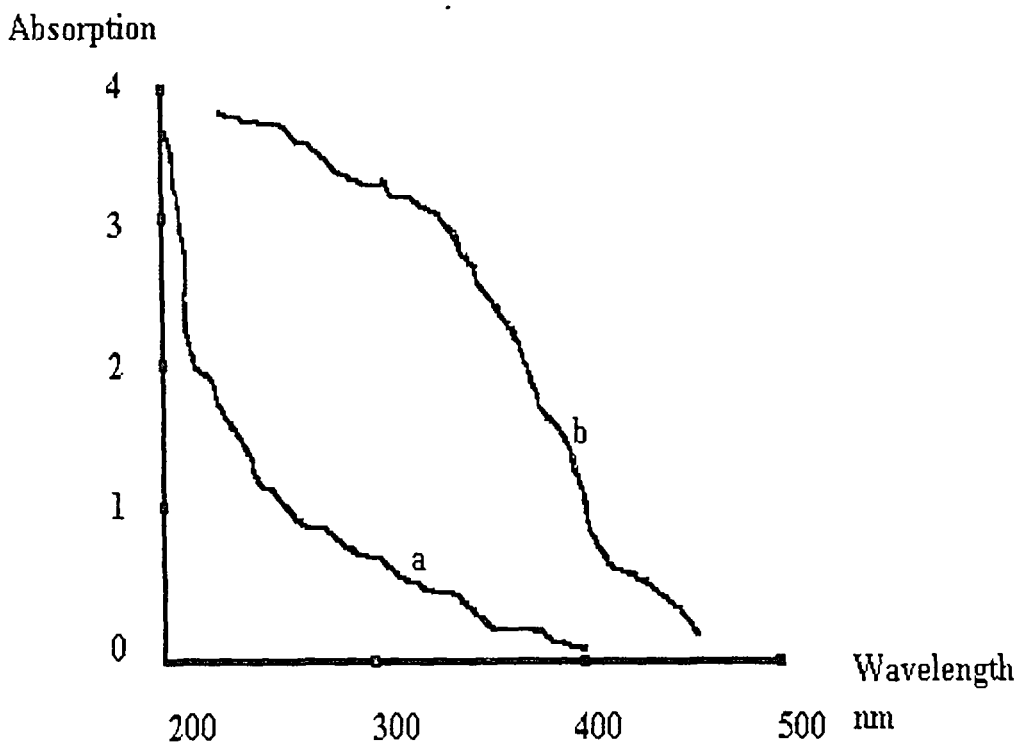


**Fig. 3.18: Optical spectra of ZnO. a: quantum dot, b: bulk**

In the optical absorption spectra shown in fig 3.18 "a" denotes the spectrum of ZnO quantum dot while "b" denotes that of bulk. It is seen that the band edge absorption in quantum dot is strongly blue shifted at 215 nm with respect to bulk specimen[15] which possesses the absorption edge at around 390 nm. The data obtained from the analysis are put in table 3.15.

| Absorption edge in quantum dot | Energy gap in quantum dot | Bulk absorption edge | Bulk band gap | Enhancement in band gap due to size quantization | Quantum dot size |
|---|---|---|---|---|---|
| 215 nm | 5.3 eV | 390 nm | 3.18 eV | 2.12 eV | 11 nm |

**Table 3.15: Different data of ZnO specimen revealed from optical spectroscopy**

### 3.7.4 Photoluminescence study

#### I. Excitation source 200 nm

For photoluminescence study of ZnO specimen, both bulk and quantum dot are first excited with 200 nm optical source corresponding to the energy above the band gap.

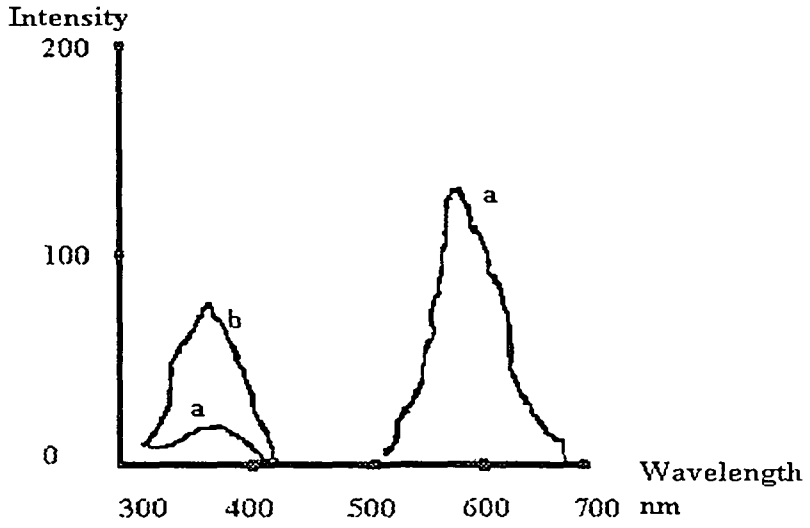


**Fig 3.19 (A): Photoluminescence spectra: Excitation source 200 nm,**

**a: ZnO quantum dot, b: ZnO bulk**

| Sample | 1st peak position | 2nd peak position | Intensity of 1st peak | Intensity of 2nd peak |
|---|---|---|---|---|
| ZnO bulk | 380 nm | NIL | 80 | 0 |
| ZnO quantum dot | 380 nm. | 600 nm. | 25 | 130 |

**Table 3.16: PL peak positions and intensities of ZnO specimen with excitation source 200 nm**

Fig 3.19(A) displays the PL spectra of ZnO specimen where spectrum "a" represents the luminescence plot of quantum dot and "b" represents that of bulk. The photoluminescence peak at 380 nm in bulk sample is caused by band edge emission[15]. On the other hand, The intense peak at 600 nm in ZnO quantum dot occurs due to the existence of oxygen vacancies[15,16] created by quenching process while preparing the sample. During ZnO powder sintering at around $800^0$ C there is a tendency in oxygen and Zn ions to dissociate that results in producing oxygen vacancies when the quenching process goes on. The reasons for band edge emission at 380 nm to be weaker in quantum dot is that, the emission of band edge luminescence lies in the absorption band of vacancy related luminescence[14]. Moreover, band edge emission cannot compete with faster radiative decay of vacancy related luminescence[15]. The PL data are put in the table 3.26.

## II. Excitation source 530 nm

Photoluminescence spectrum of ZnO quantum dot differs significantly from that with 200 nm excitation source when it is excited with optical source of 530 nm of energy well below the band gap. In this investigation, the luminescence at 600 nm remains the same with no emission at 380 nm. This is due to the fact that only the oxygen vacancies are excited with the energy corresponding to 530 nm while band edge emission cannot take place at all. Also, there is no emission of bulk ZnS specimen due to the same reason. The spectrum is displayed in fig 3.19 (B).

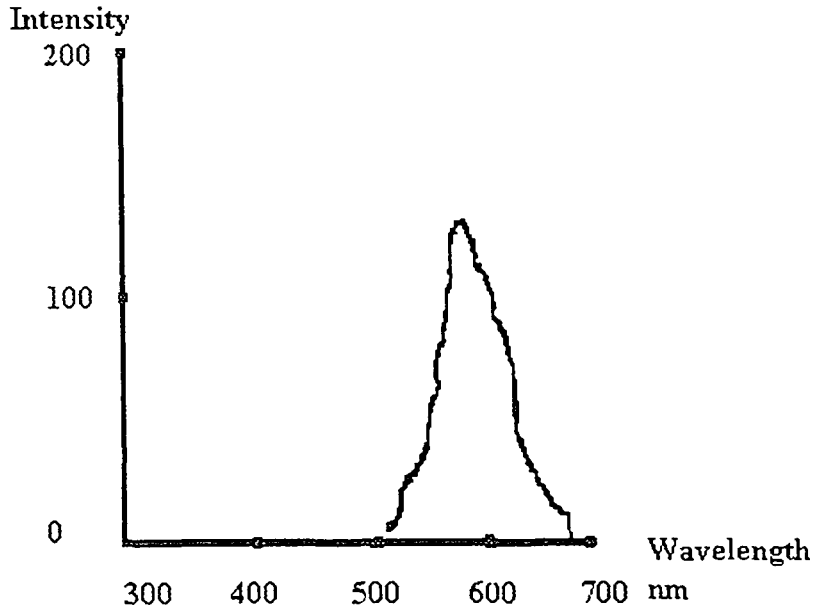


Fig 3.19 (B): PL spectra of ZnO quantum dot with excitation source 530 nm.

No emission in ZnO quantum dot has been observed with excitation source of wavelength above 530 nm as neither band to band nor vacancy can be excited with the source above the said wavelength.

## 3.8 Zinc Sulphide doped with Manganese

Chemical notation : ZnS : Mn

Name of Matrix used : Poly Vinyl Alcohol (PVA)

Sample code : $SM_1$

### 3.8.1 X-ray diffraction study

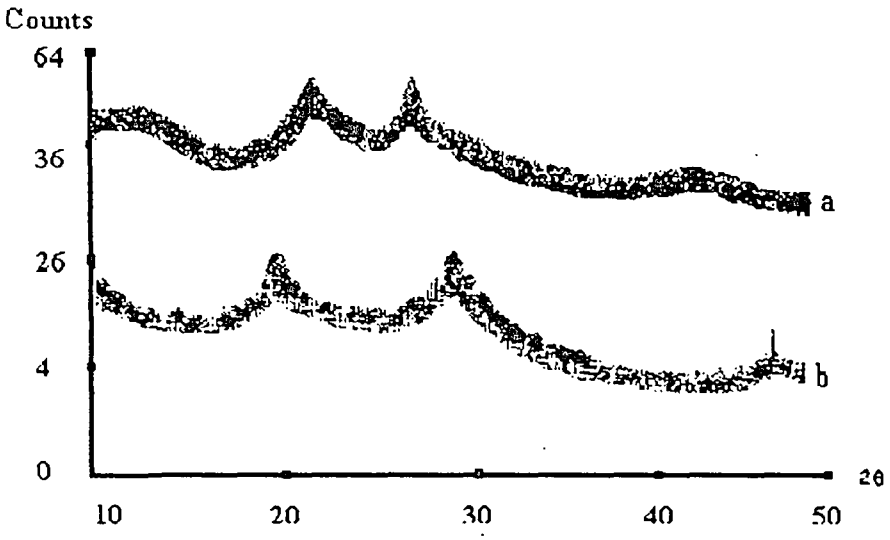


**Fig 3.20: X-ray diffractograms. a: ZnS : Mn quantum dot and b: ZnS quantum dot**

In the X-ray diffractograms shown in figure 3.20 "a" the diffractogram of ZnS:Mn quantum dot possesses two significant peaks while "b" the diffractogram

of undoped ZnS quantum dot contains three peaks within $50^0$ (in terms of 2θ) of diffraction angle. This deviation of diffraction angle of Mn doped ZnS quantum dot from that of undoped ZnS sample is due to doping of Mn in ZnS sample. Table 3.17 shows the diffraction angles of doped and undoped ZnS sample and table 3.18 gives the average particle size, and diffraction planes, etc. of ZnS.Mn quantum dot.

| Diffraction angle of ZnS:Mn specimen in degree | Diffraction angle of undoped ZnS specimen in degree |
|---|---|
| 23.5 | 20 |
| 28.5 | 30 |
| No peak | 50 |

**Table 3.17: Diffraction angles of ZnS:Mn and ZnS samples**

| Peak position ( degree) | FWHM (radians) | d spacing (nm) | Diffraction planes | Size (nm) | Average size (nm) |
|---|---|---|---|---|---|
| 23.5 | 0.015 | 0.38 | 100 | 8.8 | 8.86 |
| 28.5 | 0.014 | 0.31 | 010 | 10.2 | |

**Table 3.18: Various XRD data of ZnS:Mn quantum dot**

### 3.8.2 Transmission Electron Microscopy (TEM)

Transmission Electron Microscopy provides the pictorial view of ZnS Mn quantum dot as shown in fig 3 21 The corresponding data are listed in the table 3 19

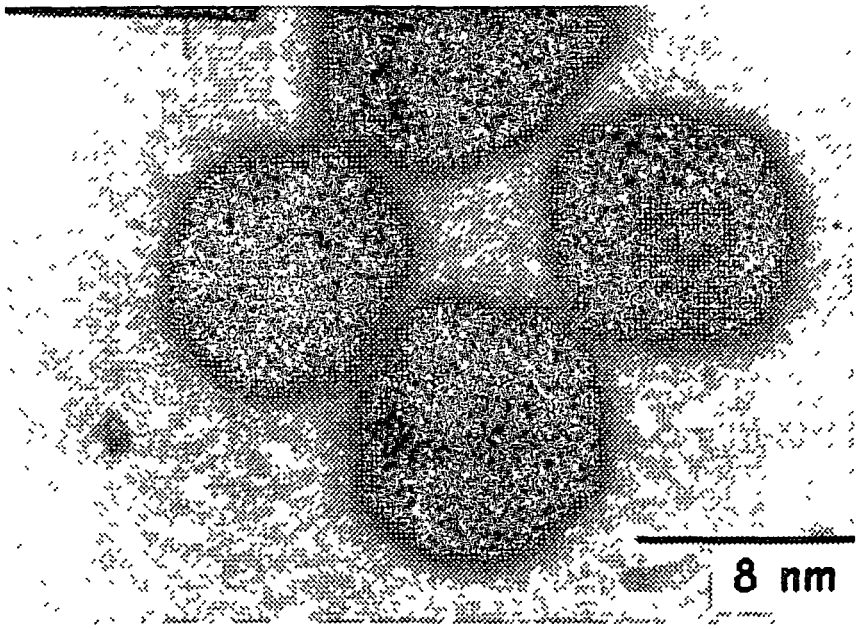


**Fig 3.21 : TEM photographs of ZnS:Mn quantum dots**

| Quantum dot size | Quantum dot shape |
|---|---|
| 11 nm | spherical |

**Table 3.19: Various data of ZnS:Mn Sample obtained form TEM study**

### 3.8.3 Optical absorption spectroscopy

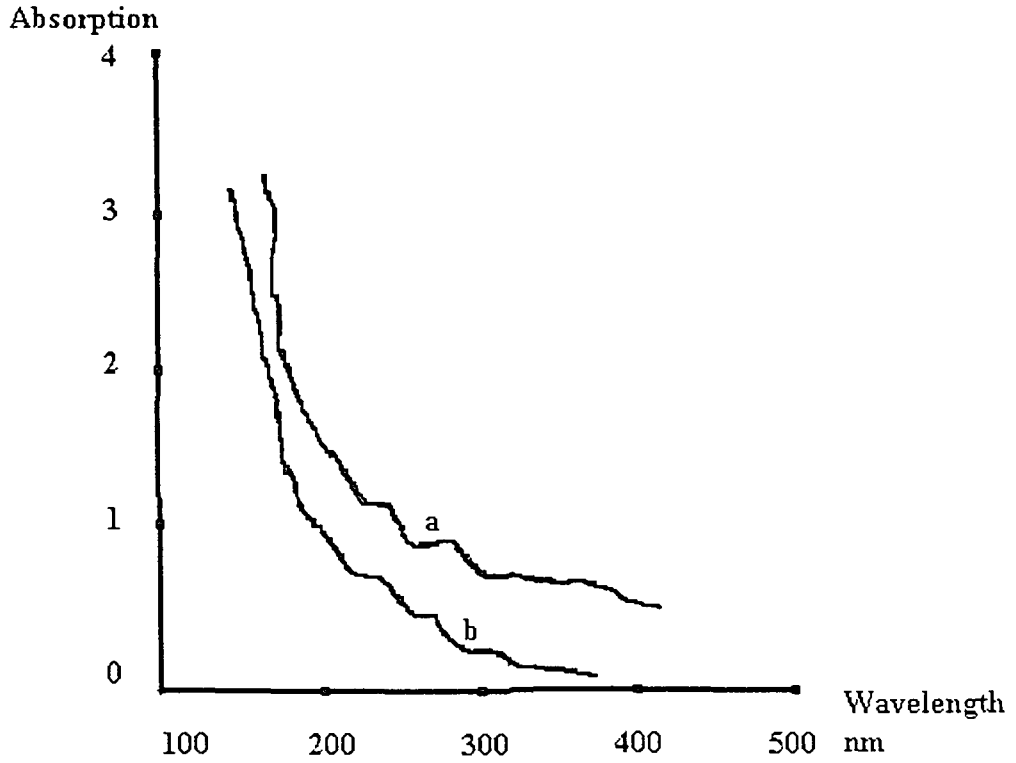


Fig. 3.22: Optical spectra of a: ZnS:Mn quamtum dot b: undoped ZnS quantum dot

| Absorption edge in ZnS:Mn | Band gap of ZnS:Mn | Undoped ZnS quantum dot absorption edge | Band gap of undoped ZnS quantum dot | Size of ZnS:Mn quantum dot |
|---|---|---|---|---|
| 215 nm | 6.10 eV | 200 nm | 6.18 eV | 10 nm |

Table 3.20: Different data of ZnS:Mn quantum dot revealed from optical spectroscopy

As shown in fig .22 the optical absorption spectrum of ZnS:Mn quantum dot does not differ much with that of ZnS (undoped) quantum dot in the blue region but the significant deviation occurs in the longer wavelength region of the spectra.

In the longer wavelength region, the absorption spectrum of ZnS:Mn denoted by "a" shows considerable tail absorption in comparison with "b" the spectrum of undoped ZnS quantum dot. This phenomenon takes place due to the fact that Mn doping produces an intermediate energy state in the forbidden gap of ZnS specimen[16-22]. This created energy state absorbs optical signal of lower energy. Data of optical spectroscopy are shown in the table 3.20.

### 3.8.4 Photoluminescence study

#### I. Excitation source 200 nm

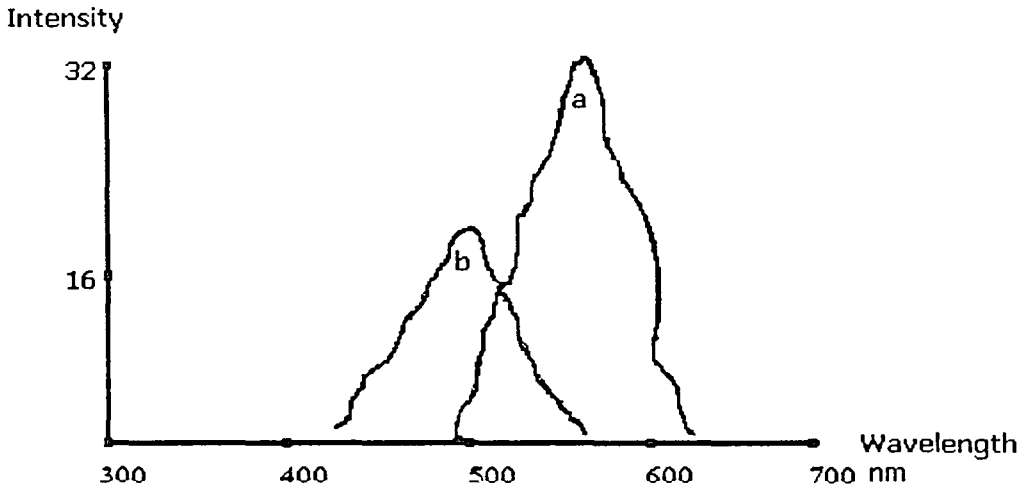


**Fig 3.23 (A) : Photoluminescence spectra: a: ZnS:Mn quantum dot, b: Undoped ZnS quantum dot. Excitation source 200nm**

| Sample | Peak .position | Intensity of 1st peak | Intensity of 2nd peak |
|---|---|---|---|
| ZnS quantum dot | 500 nm | 17 | 0 |
| ZnS:Mn quantum dot | 590 nm | 0 | 32 |

**Table 3. 21:Comparative PL data of ZnS:Mn and ZnS quantum dot**

Photoluminescence spectra of ZnS:Mn and undoped ZnS quantum dot, denoted by "a" and "b" respectively are displayed in the fig 3.23(A) when excited with 200 nm above the band gap energy . The spectrum "a" shows, a sharp broad peak at 590 nm which is attributed due the intermediate energy state produced by d- electrons[21,22] of Mn ions in the forbidden gap of ZnS specimen. The luminescence peak[14,16,21,22] at 500 nm in undoped ZnS quantum dot is completely quenched and cannot be observed in the sample when doped with Mn. This is due to the fact that, because of longer lifetime of surface state (defects) related emission at 500 nm, radiative decay can not compete with faster energy transfer to Mn to produce luminescence. Hence, Mn related luminescence, predominates over surface state emission in Mn doped ZnS sample[21]. PL data of this study are shown in table 3.21.

**II. Excitation source 530 nm.**

ZnS:Mn quantum dot shows the same emission phenomena as that of 200 nm source when excited with 530 nm optical source while undoped ZnS quantum dot does not luminescence at all. This is due to the reason that d-

electrons of Mn doped in ZnS quantum dot are excited with 530 nm source but it can excite no surface state electron to produce emission. The spectrum is shown in fig 3.23 (B)

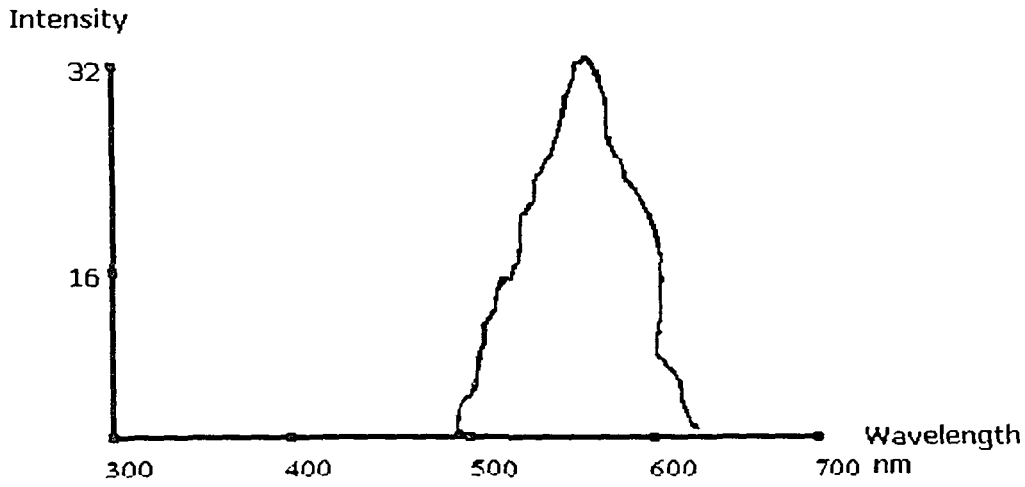


**Fig 3.23 (B): PL spectrum of ZnS:Mn quantum dot excited with 530 nm**

No luminescence has been observed in the sample with source possessing wavelength more than 530 nm as no d electron excitation takes place with the source of wavelength above the said range.

## 3.9 Conclusion

Sizes of the samples are estimated by three techniques XRD, TEM and optical absorption spectroscopy. For all the samples the sizes assessed from the three studies are well matching with each other. Also, the traps ( like surface states, vacancies etc) are detected by luminescence studies. It has been revealed that CdO phase in CdS, surface states in ZnS, oxygen vacancy in ZnO and d electrons in ZnS:Mn samples are the factors behind the luminescence phenomena.

## References


1. Woggon. U; *Optical Properties of Semiconductor Quantum dots*, Springer Tracts in Modern Physics, 136, Berlin,1996.
2 Boroditsky.M, Gontijo. I, Jackson. M, Vrijen. R, Yablonovitch. E, Krauss. T,Cheng- Chuan-Cheng, Scherer. A, Bhat. R, Krames. M; *J. Appl. Phys.* Vol. 87, No. 7, pp 3497, 2001.
3. Mugarza. A, Mascaraque. A, Pe'rez-Dieste. V, Repain. V, Rousset. S, Garci'a de, Abajo. F. J and Ortega. J .E; *Phys. Rev. Lett.* Vol. 87, No.10, pp 107601-1, 2001.
4.Ueda Naoyuki, Maeda Hirro, Hosono Hideo and Kawazoe Hiroshi; *J. Appl. Phys.* Vol. 84, No.11, pp 6174, 1998.
5. Nandakumar. P, Vijayan. C, Murty. Y.V.G.S, Dhanalakshmi. K and Sundararajan. G; *Ind. J. Pure & Appl.Phys.* Vol.37, pp 237,1999.
6. Bol. A .A , Meijerink. A; *Phys. Rev.* B 58, pp R 15997, 1998.
7. Agata M, Kurase. H, Hayashi. S and Yamamoto. K; *Solid State Commun.* Vol. 76, pp. 1061,1990.
8. Kouwenhoven Leo, Marcus Charles; *Physics World*, pp 35,June, 1998.
9. Zhang. P, Neftel. S. J, Sham. T. K; *J. Appl. Phys.* Vol. 90, No 6, pp 2755 2001.
10. Song. T. K, Kim. J and Kwun. S. I; *Solid state comm.* Vol. 97, pp 143,1996.

11. Kittel Charles; *Introduction to Solid State Physics*, John Wiley &Sons, New York, 1995.

12. Singhal. R. L; *Solid State Physics*, Kedar Nath Ram Nath & Co, Meerut,U.P, India, 1995.

13. Behera. S. N, Sahu, S. N, Nanda, K. K; *Ind. J. Phys*, 74 A (2),pp 81, 2000.

14. Chen Wei, Wang Zhanguo, Lin Zhaojun and Lin lanying; *J. Appl. Phys.* Vol.82, No. 6, pp 3111,1997.

15. Mahamuni. S, Bendre. B. S, Leppert. V .J, Smith. C. A, Cooke. D, Risbud. S. H and Lee. H .W .H ; *Nano. Struct. Mater.* Vol. 7, No. 6, pp 659, 1996.

16. Suyver. J. F, Wuister. S. F, Kelly. J.J and Meijerink. A: *Nano. Lett*, Vol. 1, No. 8, pp. 428, 2001.

17. Chen Wei, Malm Jan-Olle, Zwiller Valery, Wallenberg Reine and Bovin Jan-Olov; *J. Appl. Phys.* Vol. 89, No. 5, pp 2671,2001.

18. Mandal. S. K, Chaudhuri. S and Pal .A. K; *Ind. J. Phys. 74A(2)*,pp 143, 2000.

19. Jhon.L and Lo- D ; *J. Appl. Phys.* Vol. 89, No.11,pp 6145,2001.

20 Qadri. S. B and Skelton. E. F; *J. Appl. Phys.* Vol. 89, No. 1,pp. 115, 2001.

21. Mohanta. D, Nath. S. S, Mishara. N. C and Choudhury. A; *Bull. Mater.* Sci. Vol. 26, No. 3, pp 289, 2003.

22. Bhargava. R. N, Gallagher. D, Hong. X, Nurmikko. A; *Phy. Rev..Lett.* Vol. 72, pp 416, 1994.

**********

# CHAPTER 4

# EFFECTS OF SWIFT HEAVY ION ON QUANTUM DOTS

# CHAPTER 4

# Effects of swift heavy ion on quantum dots

## 4.1 Aims of ion irradiation

The changes in electronic, optoelectronic and optical properties of quantum dots after swift heavy ion (SHI) irradiation form the basic aims of this chapter.These changes in the said properties are caused by variations in sample size and occurrence of crystal defects[1-6]. In the present investigation, our prepared quantum dots namely, CdS, ZnS, ZnO and ZnS:Mn samples embedded on SBR latex and PVA matrices, are irradiated with 100 MeV chlorine ($Cl^{9+}$) beam. Ion irradiation may result in the following changes.

I. Change in the size of quantum dots

II. Occurrence of crystal defects.

III. Simple evaporation of particles.

IV. No effect.

In this chapter, we report sample characterization in an effort to explore which of these probable events have actually occurred. XRD and TEM studies show that the sample size does not change if the specimens are embedded on SBR latex but on PVA matrix, the particle size enhances with higher ion doses The optical absorption spectroscopy suggests that,

due to ion irradiation, some defects (vacancies, etc.) are created in the specimen and these defects cause optical absorption in longer wavelength region of optical signal. Lastly, the photoluminescence study indicates that, the luminescence intensity of irradiated samples increases remarkably due to the defects created by SHI. These form my contributions to quantum dot research. Following sections explain the effects of SHI on quantum dots.

**I.Change in the size of quantum dots**

When the heat, generated by ion beam in the samples, cannot be dissipated in a very short interval of time, the temperature of the specimen rises and it reaches very high (upto $1800^0$ C or more). If this temperature becomes equal to the melting point of quantum dots, the samples melt and if the dots are very close to each other, they agglomerate to form bigger particles.

**II. Appearance of crystal defects**

Swift heavy ion (SHI) creates point defects[7] in the specimens irradiated by ion. One such defect is Frenkel defect. These defects occur if an atom leaves its site and dissolves interstitially into the structure. Frenkel defect generation is controlled by temperature also. Higher the temperature, more are the defects.

**III. Evaporation**

If the heat supplied by ion beam, raises the sample temperature to a very high value which is equal to the boiling point of the specimen, then the substances evaporate, leaving nothing behind.

**IV. No effect**

If there is no sample evaporation and the diffusion length of the defects, produced by SHI is equal to crystal size, the defects diffuse into the grain boundaries of the specimen, resulting in no effect. Also,there is no affect if the particle density is very low in the host matrix.

To study the actual phenomena, occurred in our quantum dots due to SHI irradiation, the samples have been characterized by the following tests:

I. X-ray diffraction study (XRD).

II. Transmission Electron Microscopy (TEM).

III. Optical Absorption spectroscopy (in UV/VIS region).

IV. Photoluminescence Study (PL study)

## 4.2 Various parameters related to ion irradiation

**I. Electronic loss**

SHI hits the electrons that move round the nucleus with Bohr velocity that results in inelastic collision during which SHI delivers some of its energy to these electrons. This energy is called electronic loss and it is denoted by $S_e$ or ( dE/dx ) while its unit is eV/Å.

**II. Nuclear energy loss**

The energy absorbed by the nucleus of specimen from the irradiating ion beam, is called nuclear energy loss. It is denoted by $S_n$ or (dE/dX)n and its unit is eV/Å.

The above two parameters, have been calculated with the help of a software[8] called "SRIM" for each sample.

**III. Dose**

It is defined as the total number of irradiating ions, per square centimeter (Ions/ $cm^2$) of sample. It varies from sample to sample depending upon its sizes and material. This is also known as fluence and denoted by "ϕ".

## 4.3 Ion irradiation process and calculation of ion dose

For ion irradiation, the samples embedded on matrix are cut in 1cm x 1cm area and fixed on sample holder made of copper. The samples are put in a vacuum chamber. Finally, SHI beam irradiates the sample over the said area. The samples during ion irradiation are monitored on television screen.

Ion dose mainly depends on the size of specimen. For example, if the particle size (diameter) is 10 nm then the required dose, can be calculated in the way explained next page.

Total area of the particle

$$A = \pi R^2 = (3.14) \times (5 \times 10^{-9})^2 \text{ m}$$
$$= (3.14) \times (5 \times 10^{-7})^2 \text{ cm}$$
$$= 78.5 \times 10^{-14} \text{ cm}$$

$$\text{dose } \phi = \frac{1}{A} = \frac{1}{78.5 \times 10^{-14}} \text{ ions / cm}^2$$

$$= 1.27 \times 10^{12} \text{ ions / cm}^2$$

During ion irradiation process, doses are recorded by using a counter. Next relation relates the counts and the doses·

$$\text{Counts} = \frac{\phi q e}{S}$$

Where $\phi$ is the dose,

q is the charge state of ion beam,

e is the electronic charge ($1.6 \times 10^{-19}$ coulomb ),

S is the scale of counter,

## 4.4 Estimation of ion doses

In the present work, X-ray diffraction study, Transmission Electron Microscopy and Optical absorption spectroscopy infer that the sizes of our prepared quantum dot samples vary over the range from 4 nm to 20 nm and accordingly, we have selected four ion doses to irradiate the quantum dot samples. The doses are listed in table 4.1.

| Dose (Ions/ $cm^2$) | Dose in terms of counts | Dose notation used |
|---|---|---|
| $10^{11}$ | 4.8 | $\phi_1$ ($1^{st}$ dose) |
| $5 \times 10^{11}$ | 24 | $\phi_2$ ($2^{nd}$ dose) |
| $5 \times 10^{12}$ | 240 | $\phi_3$ ($3^{rd}$ dose) |
| $10^{13}$ | 480 | $\phi_4$ ($4^{th}$ dose) |

**Table 4.1: Ion doses and corresponding codes**

## 4.5 Characterization of ion Irradiated samples

### 4.5.1 Cadmium Sulphide

Chemical formula : CdS

Name of the matrix : SBR Latex

Sample code : $S_1$

| $S_e$ (eV) | $S_n$ (eV) | Projectile range (μm) |
|---|---|---|
| $1.003 \times 10^{1}$ | $1.070 \times 10^{-2}$ | 18.45 |

**Table 4.2: Electronic loss, nuclear loss and projectile range of Cl ion in CdS sample**

| Dose codes | Irradiated sample codes |
|---|---|
| $\phi_1$ | $S_1d_1$ |
| $\phi_2$ | $S_1d_2$ |
| $\phi_3$ | $S_1d_3$ |
| $\phi_4$ | $S_1d_4$ |

Table 4.3: Ion doses and corresponding sample codes

### 4.5.1.1 X-ray diffraction study (XRD study)

The X-ray diffractograms of virgin and irradiated CdS specimens are shown in fig 4 1 and the corresponding data are put in table 4.4.

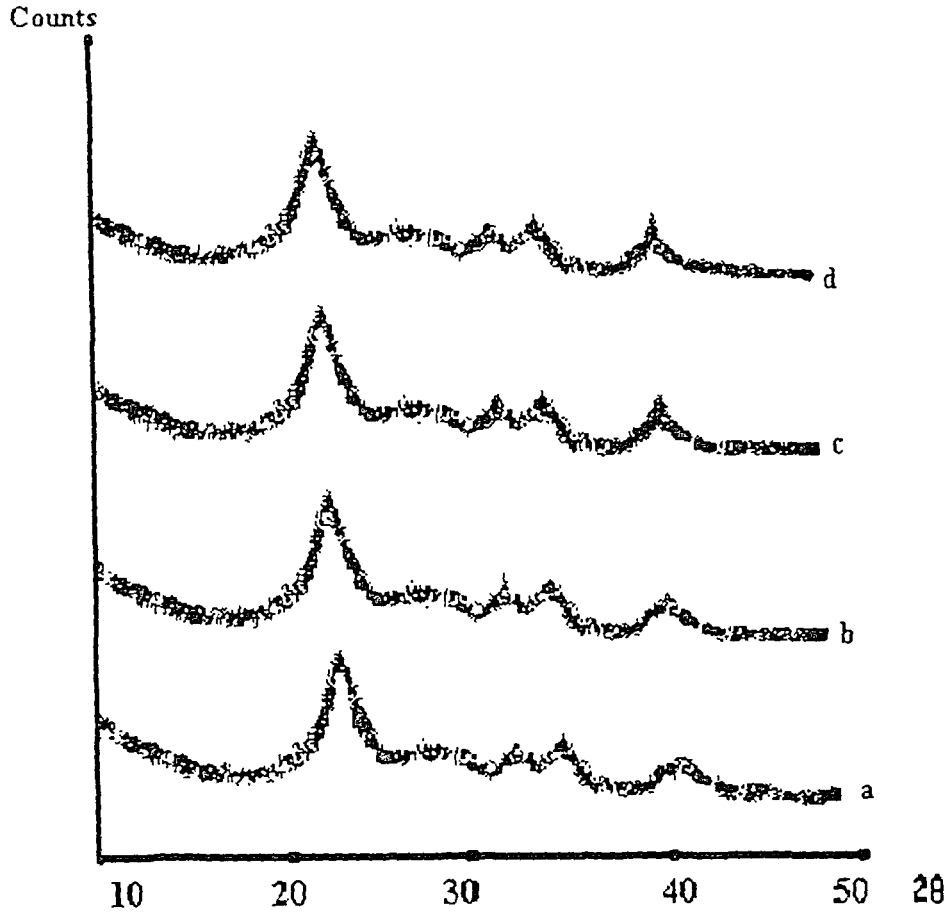


Fig 4.1 : X-ray diffractograms of CdS specimens: a, b, c and d correspond to the diffractograms of virgin sample and samples irradiated by 1st, 2nd and 3rd dose respectively.

| Sample | d spacing (nm) | Diffraction planes | Average size (nm) |
|---|---|---|---|
| $S_1$ | 0 36, 0.29, 0 28 | 100, 010, 001 | 8 41 |
| $S_1d_1$ | 0 36, 0.29, 0.28 | 100, 010, 001 | 8 6 |
| $S_1d_2$ | 0.36, 0 29, 0 28 | 100, 010, 001 | 8 9 |
| $S_1d_3$ | 0 36, 0.29, 0 28 | 100, 010, 001 | 8 5 |
| $S_1d_4$ | - | - | No sample |

**Table 4.4: XRD data of CdS specimens**

### 4.5.1.2 Transmission Electron Microscopy (TEM)

The TEM images of virgin (unirradiated) and ion irradiated samples of CdS quantum dots with four ion doses are displayed in fig 4 2 while the corresponding data are put in table 4 5

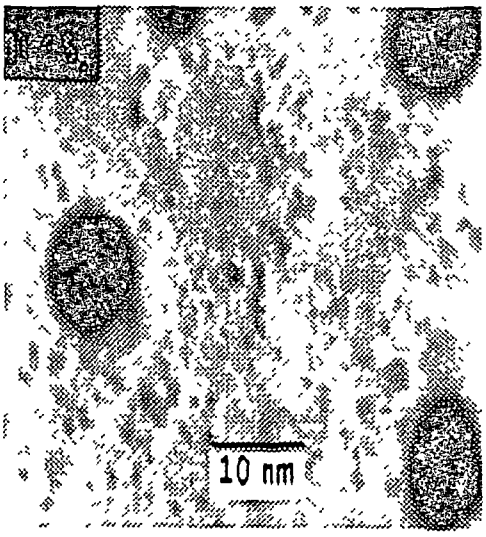


a

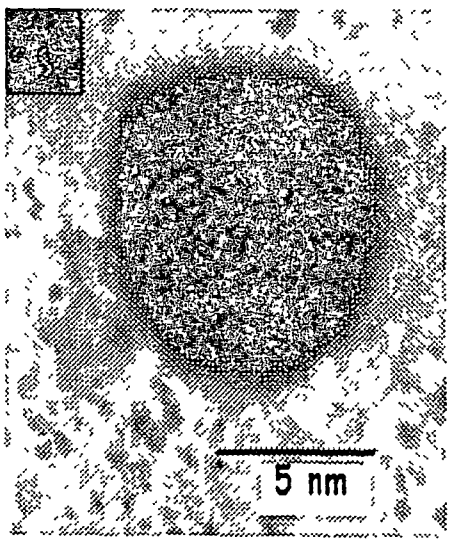


b

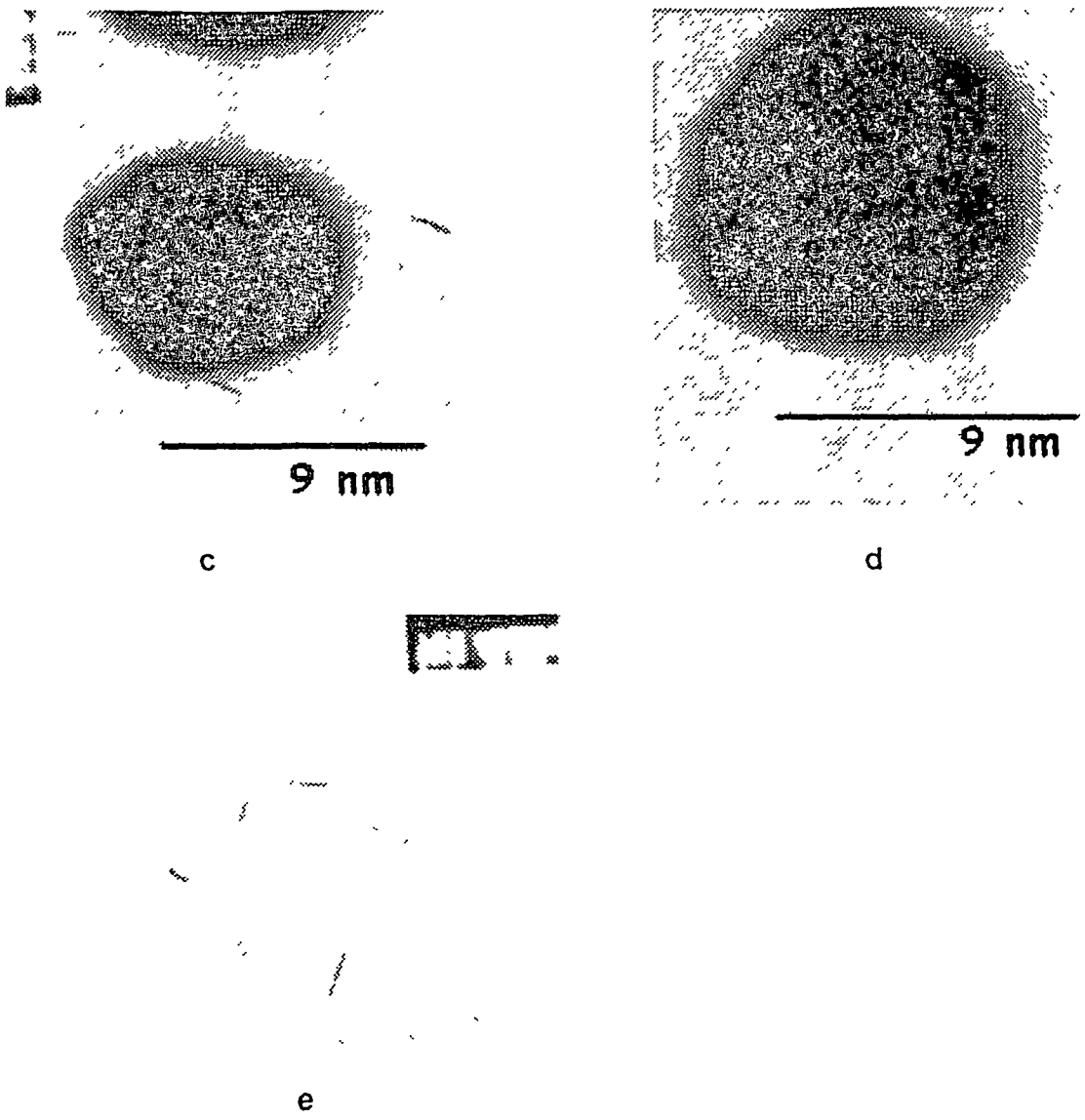


Fig 4.2: TEM images of CdS specimens: a, b, c, d and e correspond to virgin sample and samples irradiated by 1st, 2nd, 3rd and 4th dose respectively.

| Sample | Size | Shape |
|---|---|---|
| $S_1$ | 8.8 | Spherical |
| $S_1d_1$ | 8.6 | Spherical |
| $S_1d_2$ | 8.5 | Elliptical |
| $S_1d_3$ | 8.9 | Elliptical |
| $S_1d_4$ | No sample | No sample |

**Table 4.5: TEM data of CdS samples**

### 4.5.1.3 Results and discussions of XRD and TEM studies

Both the studies, XRD and TEM show that no considerable change in particle sizes and shapes occurs in CdS specimen up to 3$^{rd}$ ion dose. But it is very interesting to notice that, no CdS sample has been found to be present at all over the substrate that is irradiated to 4$^{th}$ dose of ion beam. These phenomena are attributed due to the fact that, in SBR latex, quantum dots are distributed in such a way that the interparticle distances are very large in comparison to sample dimensions which is shown in virgin TEM image displayed in fig 4.1 (a). When swift heavy ion (SHI) irradiates the samples, it delivers high energy to the dots causing steep rise in the sample temperature that reaches the melting point of the specimens and the samples melt. But as the interparticle distances are very large, they cannot agglomerate to form bigger clusters and ultimately no physical effect of ion irradiation occurs in the specimens. But, in 4$^{th}$ dose, ion generated heat is so

high that, all the samples evaporate completely leaving behind the empty substrate only.

#### 4.5.1.4 Optical absorption spectroscopy

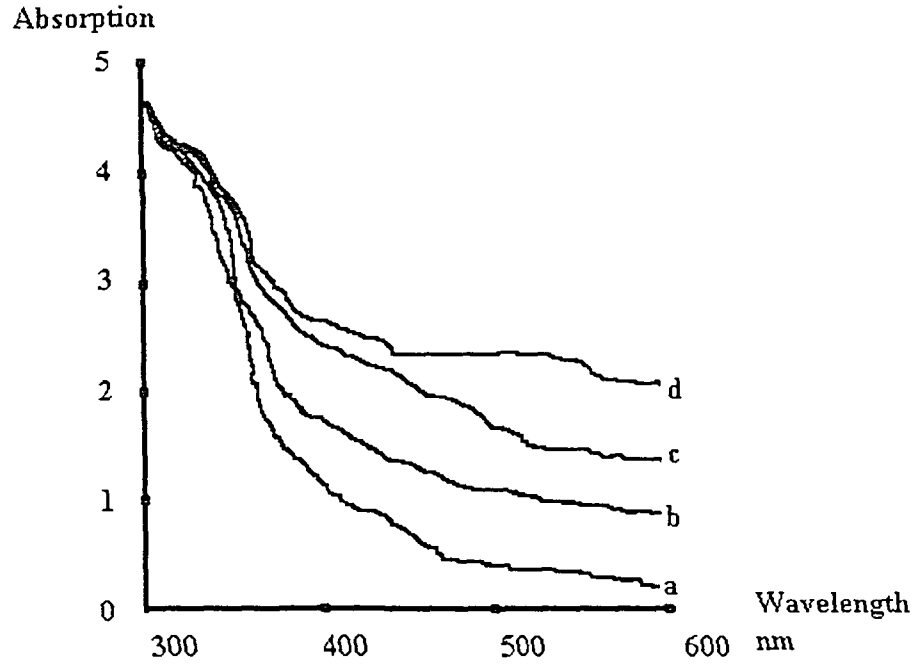


Fig 4.3: UV/VIS absorption spectra of CdS specimens. a, b, c, and d stand for virgin sample and samples irradiated by 1st, 2nd and 3rd dose respectively.

The optical absorption spectra of ion irradiated CdS samples possess two distinct parts. These are

I. Strong absorption edge and II. Tail absorption edge.

**I. Strong absorption**

Optical absorption spectroscopy of CdS samples shows no considerable shift of strong absorption edge up to 3rd ion dose ($\phi_3$). This

indicates no change in energy gap[9] which indicates that up to 3rd dose, no variation in particle size occurs. But In 4th dose ($\phi_4$), no absorption by the sample is observed, that indicates the absence of any sample on the substrate. Thus, this study also suggests the evaporation of quantum dots when exposed to 4th ion dose. Fig 4.3 displays the optical absorption spectra of virgin and irradiated samples while the corresponding data are put in table 4.6.

**II. Tail absorption**

The presence of tail absorptions in the optical spectra indicates the existence of some intermediate energy states in the forbidden gap of host material. In present investigation, it is the presence of CdO phase in CdS specimen. In virgin sample also, CdO phase is present but because of its very low density in the host specimen, it needs an effort to detect it by optical spectroscopy. On the other hand, in ion irradiated samples, it is well detected by the appearance of tail absorption. During SHI irradiation of CdS particles embedded in SBR latex deposited over glass substrate, some free oxygen atoms are produced which react with $Cd^{+2}$ ions in CdS specimens to form CdO phase. The intensity of tail absorption increases with higher doses as more CdO phase formation takes place, which is evident in the diffractograms (fig 4.1) of ion irradiated samples with a peak[10] at $40^0$, ( which indicates the presence of CdO phase) that goes on being stronger with higher ion doses.

| Sample | Absorption edge (nm) | Size (nm) |
|---|---|---|
| $S_1$ | 375 | 7.6 |
| $S_1d_1$ | 380 | 7.7 |
| $S_1d_2$ | 379 | 7.7 |
| $S_1d_3$ | 380 | 7.7 |
| $S_1d_4$ | No absorption | No sample |

Table 4.6: Optical spectroscopic data of CdS specimens

### 4.5.1.5 Photoluminescence study

### I. Excitation source 200 nm

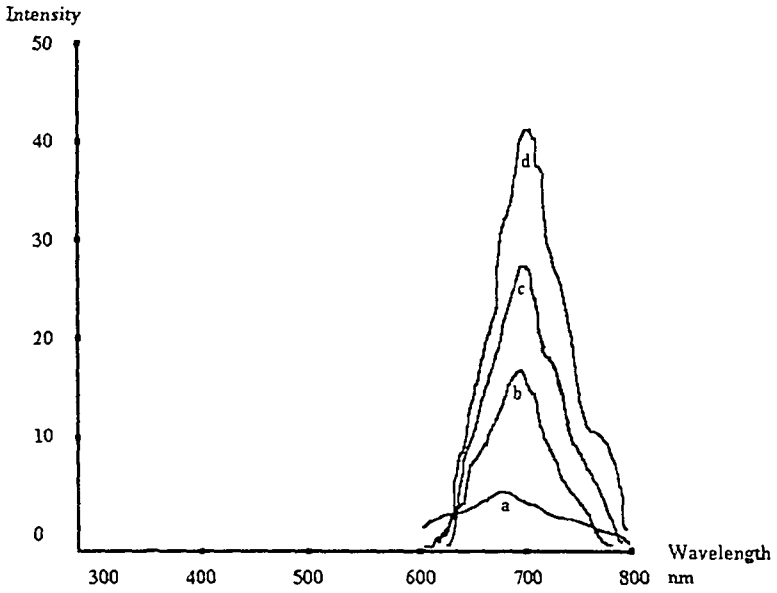


Fig 4.4: PL spectra of CdS samples a, b, c and d, stand for virgin sample and the samples irradiated by 1st, 2nd, and 3rd dose respectively.

The photoluminescence spectra of virgin and ion irradiated CdS samples, excited with 200 nm source, are shown in fig 4.4 and the corresponding data are put in table 4.7. The study[11] makes it clear that CdO phase related emission at 700 nm is dominant in ion irradiated specimens. Further, the emission intensity goes on increasing with higher ion dose as CdO phase increases with higher ion dose.

| Sample | Peak position (nm) | Peak intensity |
|---|---|---|
| $S_1$ | 700 | 7.3 |
| $S_1d_1$ | 700 | 18 |
| $S_1d_2$ | 700 | 28 |
| $S_1d_3$ | 700 | 41 |

**Table 4.7: PL data of CdS samples**

### II. Excitation source 630 nm

With 630 nm excitation source, CdS specimens show similar emission behaviour as that with 200 nm excitation source because in both the cases the CdO phase plays the role to cause the luminescence.

No luminescence phenomenon has been observed in the specimens with excitation above 630 nm.

### 4.5.2 Zinc Sulphide

Chemical formula : ZnS

Name of matrix : PVA

Sample code : $S_2$

| $S_e$ (eV) | $S_n$ (eV) | Projectile range (μm) |
|---|---|---|
| $1.201 \times 10^{1}$ | $1.266 \times 10^{-2}$ | 18.07 |

**Table 4.8: Electronic loss, nuclear loss and projectile range of Cl ion in ZnS sample**

| Doses notations | Irradiated sample codes |
|---|---|
| $\phi_1$ | $S_2d_1$ |
| $\phi_2$ | $S_2d_2$ |
| $\phi_3$ | $S_2d_3$ |
| $\phi_4$ | $S_2d_4$ |

**Table 4.9: Ion doses and corresponding sample codes**

#### 4.5.2.1 X-ray Diffraction Study (XRD)

The X-ray diffractograms of virgin and ion irradiated ZnS samples are displayed in figure 4.5 and the corresponding data are put in table 4.10.

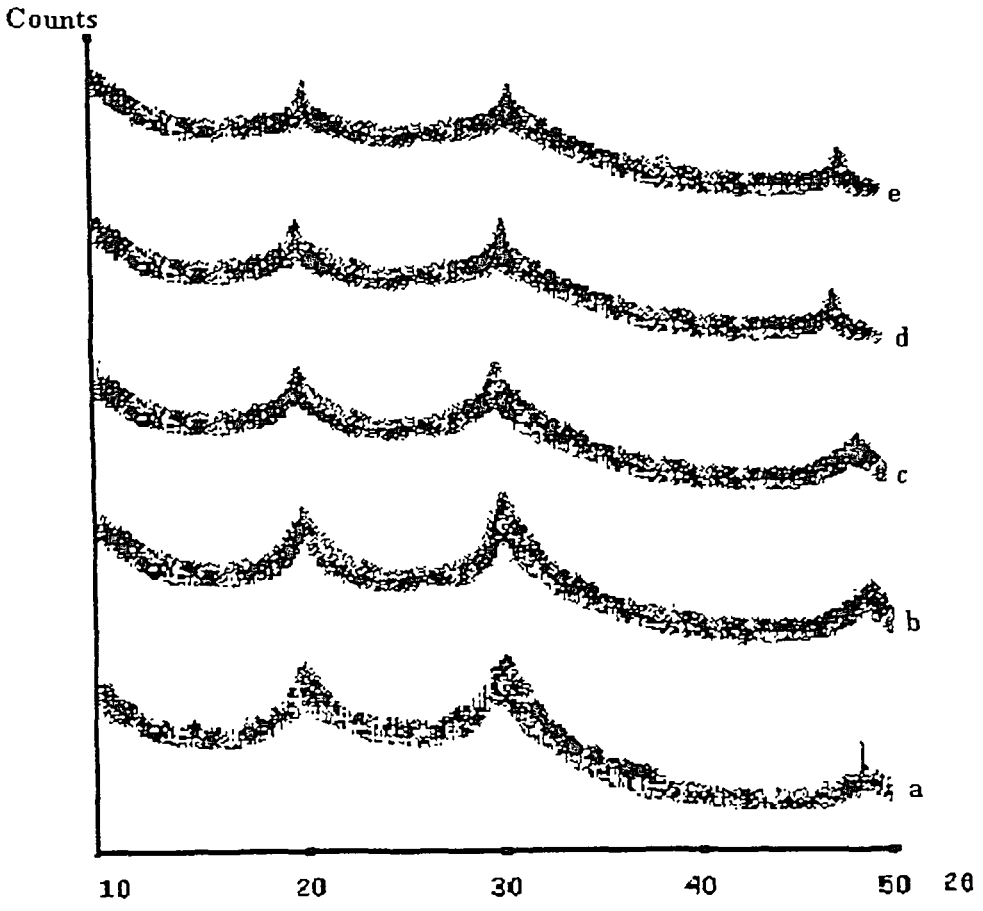


Fig 4.5 : X-ray diffractograms of ZnS specimens. a, b, c, d and e stand for the virgin sample and the samples irradiated by 1st, 2nd, 3rd and 4th dose respectively.

| Sample | d spacing (nm) | Diffraction planes | Average size (nm) |
|---|---|---|---|
| $S_2$ | 0.44, 0.29, 0.18 | 100, 010, 001 | 7.5 |
| $S_2d_1$ | 0.44, 0.29, 0.18 | 100, 010, 001 | 29 |
| $S_2d_2$ | 0.44, 0.29, 0.18 | 100, 010, 001 | 81 |
| $S_2d_3$ | 0.44, 0.29, 0.18 | 100, 010, 001 | 149 |
| $S_2d_4$ | 0.44, 0.29, 0.18 | 100, 010, 001 | 156 |

Table 4.10 : XRD data of ZnS specimens

### 4.5.2.2 Transmission Electron Microscopy

The TEM images of virgin and ion irradiated ZnS specimen are displayed in fig 4 6 and the corresponding data are put in table 4 11

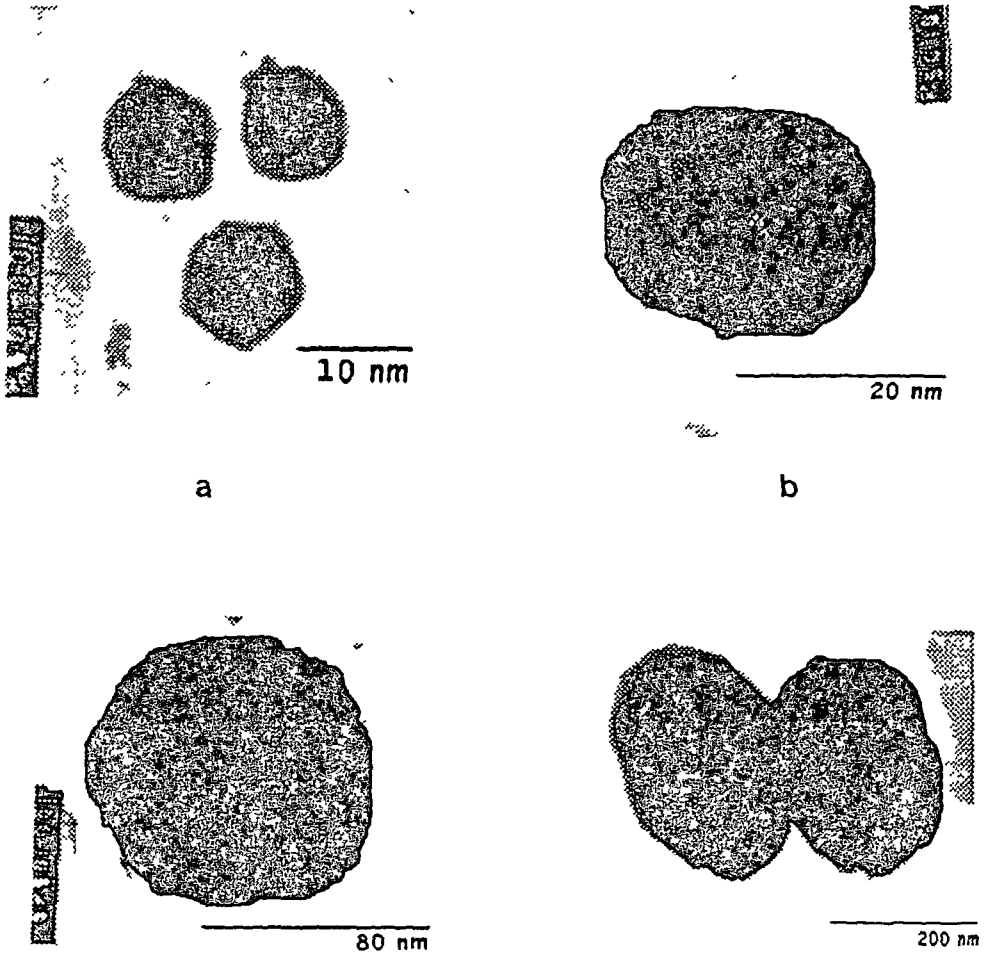

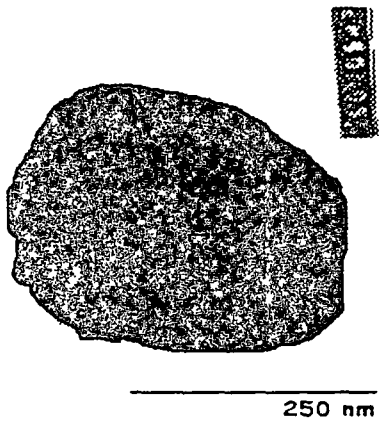


e

Fig 4.6: TEM images of ZnS specimens: a, b, c, d and e stand for the virgin sample and the samples irradiated by 1st, 2nd, 3rd and 4th dose respectively

| Sample | Size (nm) | Shape |
|---|---|---|
| $S_2$ | 7 | Spherical |
| $S_2d_1$ | 32 | Spherical |
| $S_2d_2$ | 80 | Spherical |
| $S_2d_3$ | 149 | Elliptical |
| $S_2d_4$ | 155 | Elliptical |

Table 4.11: TEM data of ZnS samples

### 4.5.2.3 Results and discussions of XRD and TEM studies

Both the studies XRD and TEM Studies show that with higher ion doses, the particle sizes become bigger while in 3rd and 4th doses the samples possess the dimension of bulk structure Next the reasons are explained

From transmission Electron microscopy it is inferred that unlike in SBR latex, in polyvinyl alcohol (PVA) matrix, the virgin quantum dot samples are more orderly distributed with very small inter particle distances separated by only a thin wall of polymer matrix as displayed in fig 4.6 (a). When SHI irradiates the sample, it gets heated up resulting in rise in sample temperature that reaches the melting point of the specimen. Due to this phenomenon, quantum dots melt and as they are very close to each other they start to agglomerate to form bigger particles. Practically, it has been found that higher the ion does, more is the generated heat, and hence bigger is the particle size.

### 4.5.2.4 Optical absorption spectroscopy

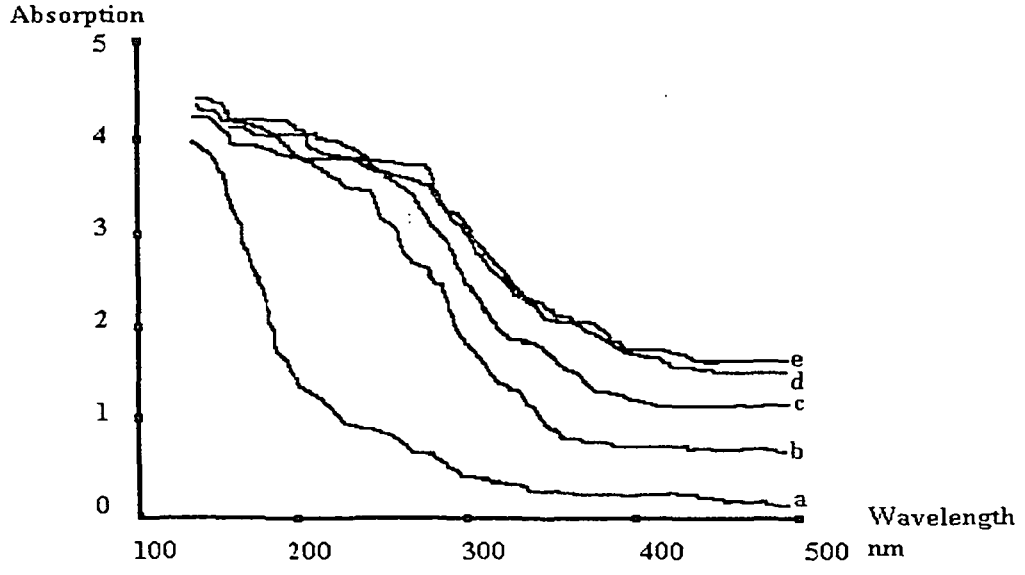


Fig 4.7: UV/VIS absorption spectra of ZnS specimen. a,b,c,d and e stand for virgin sample and samples irradiated by 1st, 2nd, 3rd and 4th dose respectively samples.

The optical absorption spectra in UV/Visible region of virgin and ion irradiated ZnS samples are shown in figure 4.7 and the data are put in table 4.12. It is clear that the spectra consist of two distinct parts.

I. Strong absorption and II. Tail absorption.

**I. Strong absorption**

The strong absorption in the spectra is caused by the band gap absorption of ZnS specimen. It is seen that with higher ion doses, the edges shift towards red, with respect to that of virgin sample, which is a clear signature of bigger particle formation[1,12], that has already been inferred from XRD and TEM studies.

**II. Tail absorption**

The appearance of tail absorption in the in the optical spectra is due to the presence of crystal defects in the sample. In virgin ZnS samples, though the surface states (crystal defects) are present[12] but due to their very low density, optical spectroscopy cannot detect them. On the other hand in ion irradiated samples, the surface states reduce with enhancement in particle sizes[12,13] but a large number of Zn vacancies are created in ZnS quantum dots by SHI beam. These vacancies absorb the optical signal of low energy below the band gap and cause the tail absorption[9,13-15]. It is seen that, higher the dose, more are the Zn vacancies and hence more intense is the tail absorption.

| Sample | Strong absorption edge (nm) | Size (nm) |
|---|---|---|
| $S_2$ | 200 | 9 |
| $S_2d_1$ | 330 | 40 |
| $S_2d_2$ | 345 | 80 |
| $S_2d_3$ | 350 | <=145 |
| $S_2d_4$ | 350 | <=145 |

Table 4.12 : Optical spectroscopic data of ZnS specimens

### 4.5.2.5 Photoluminescence study

### I. Excitation source 200 nm

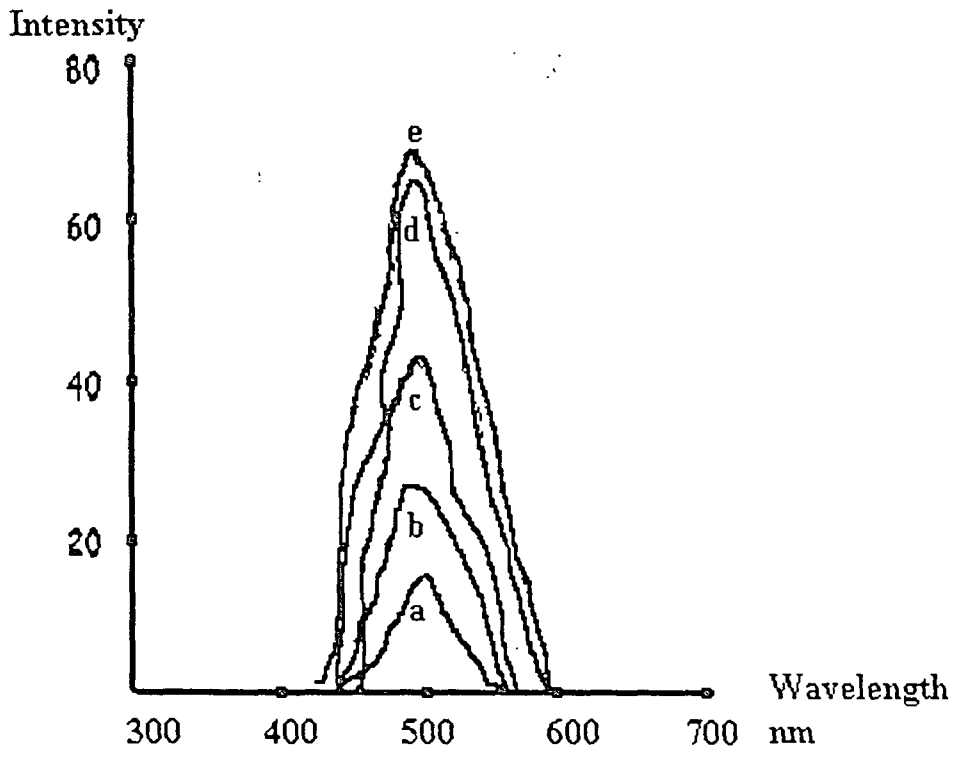


Fig 4.8: PL spectra of ZnS samples a, b, c, d and e stand for virgin sample and samples irradiated by 1st, 2nd, 3rd and 4th dose respectively

| Sample | Peak position (nm) | Peak intensity |
|---|---|---|
| $S_2$ | 500 | 17 |
| $S_2d_1$ | 500 | 24 |
| $S_2d_2$ | 500 | 41 |
| $S_2d_3$ | 500 | 68 |
| $S_2d_4$ | 500 | 70 |

**Table 4.13: PL data of ZnS samples**

Photoluminescence spectra of ZnS samples excited with 200 nm source, displayed in fig 4.8, show that, virgin ZnS quantum dots possess the surface state related luminescence with peak position at 500 nm as mentioned in Chapter 3. Due to ion irradiation, the crystal size increases and thereby reduce the surface states[12] that results in decrease in the corresponding luminescence. But, interestingly, though the surface states are reduced, but the newly created Zn vacancies[9] show intense emission that enhances with higher ion doses. It is experimentally found that the surface state related luminescence and the vacancy related luminescence are of same wavelength (around 500 nm) and practically they overlap[9,12-14].That is why, after ion irradiation, though the surface states are reduced, still we observe the

enhanced luminescence at 500 nm, which is actually due to Zn vacancies[14]. The data of this study are put in the table 4.13.

**II. Photoluminescence study with 460 nm excitation source**:

The luminescence study with 460 nm excitation source shows the same emission phenomenon as that when excited with 200 nm source.

No significant luminescence phenomenon has been observed in ZnS samples with excitation source above 460 nm.

### 4.5.3. Zinc Oxide

Chemical formula : ZnO

Matrix used : PVA

Sample Code : $S_3$

| Sample | $S_e$(eV) | $S_n$(eV) | Projectile Range |
|---|---|---|---|
| S3 | 5.530X102 | 5-828X10-1 | 18.07 μm |

**Table 4.14: Electronic loss, nuclear loss and projectile range of Cl ion in ZnO sample**

| Ion dose | Irradiated sample codes |
|---|---|
| $\phi_1$ | $S_3$ $d_1$ |
| $\phi_2$ | $S_3$ $d_2$ |
| $\phi_3$ | $S_3d_3$ |
| $\phi_4$ | $S_3d_4$ |

**Table 4.15: Ion doses and corresponding sample codes.**

### 4.5.3.1 X-ray diffraction study

The X-ray diffractograms of virgin and irradiated ZnO samples are displayed in figure 4 9 and the corresponding data are put in table 4 16

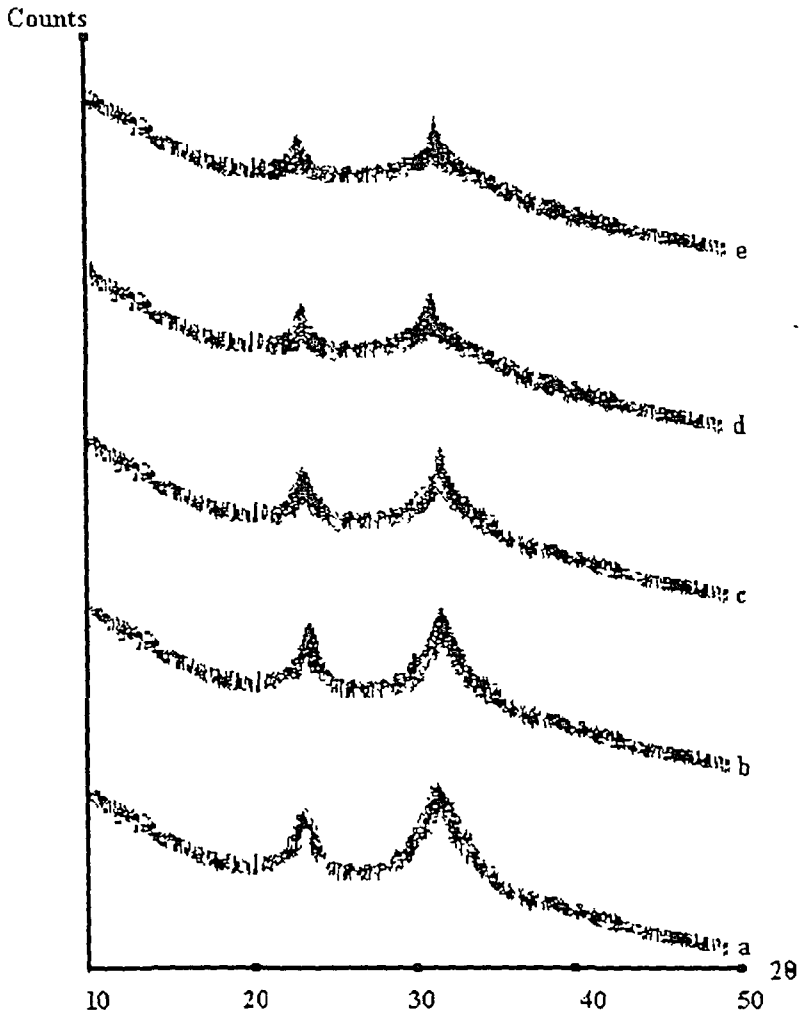


Fig 4.9: X-ray diffractograms of ZnO specimens: a,b,c,d and e correspond to the diffractograms of virgin sample and samples irradiated by 1st, 2nd, 3rd and 4th dose respectively.

| Sample | d spacing (nm) | Diffraction planes | Average size (nm) |
|---|---|---|---|
| $S_3$ | 0 38, 0 28 | 100, 010 | 8 2 |
| $S_{23}d_1$ | 0 38, 0 28 | 100, 010 | 41 |
| $S_3d_2$ | 0 38, 0 28 | 100, 010 | 99 |
| $S_3d_3$ | 0 38, 0 28 | 100, 010 | 118 |
| $S_3d_4$ | 0 38, 0 28 | 100, 010 | 150 |

**Table 4.16: XRD data of ZnO specimens**

### 4.5.3.2 Transmission Electron Microscopy (TEM)

The TEM images of ZnO samples are displayed in fig 4 10, while the corresponding data are put in table 4 17

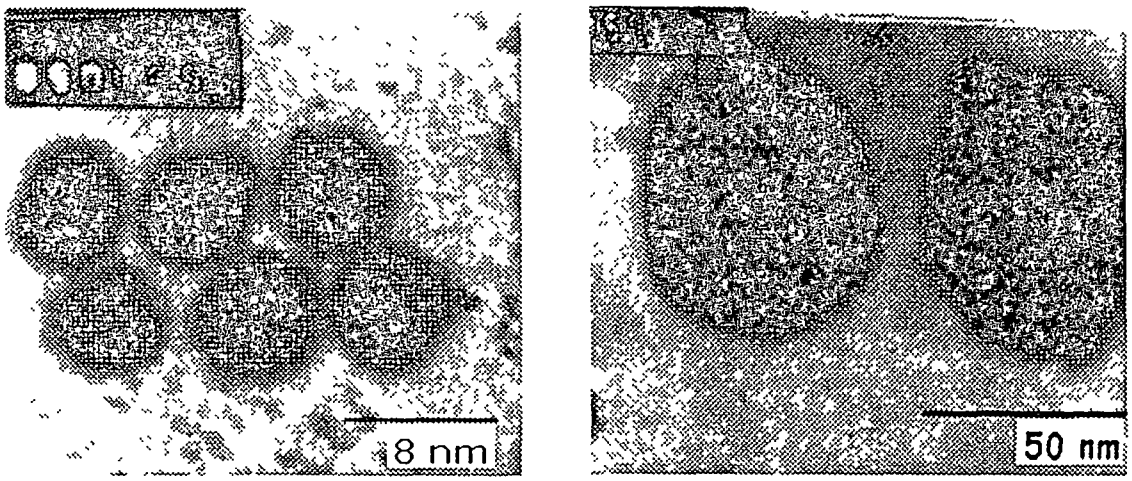


a b

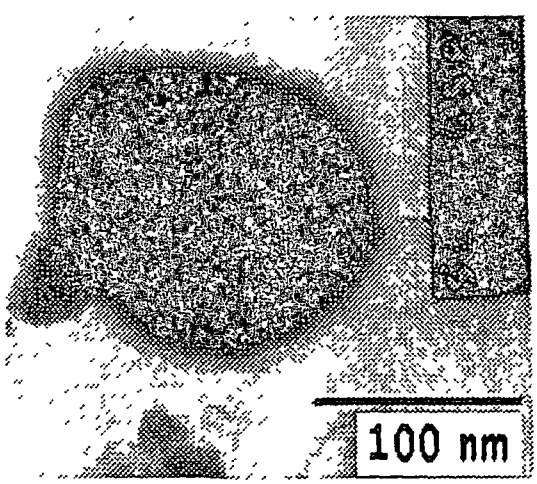


c

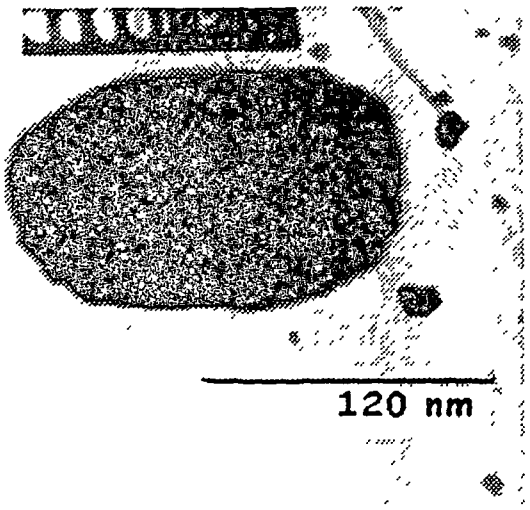


d

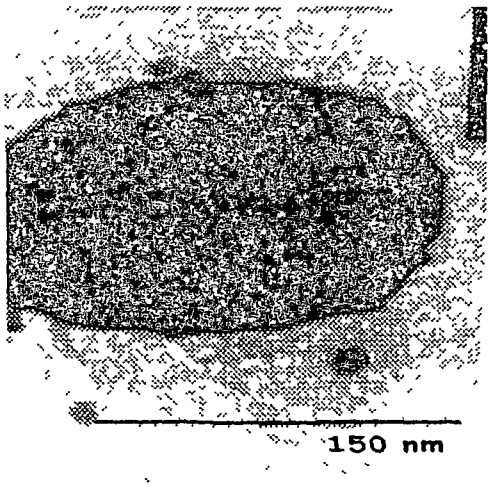


e

Fig 4.10: TEM images of ZnO specimens a, b, c, d and e correspond to virgin sample and samples irradiated by 1$^{st}$, 2$^{nd}$, 3$^{rd}$ and 4$^{th}$ dose respectively.

| Sample | Size (nm) | Shape |
|---|---|---|
| $S_3$ | 7 | Spherical |
| $S_3d_1$ | 40 | Spherical |
| $S_3d_2$ | 100 | Spherical |
| $S_3d_3$ | 120 | Elliptical |
| $S_3d_4$ | 151 | Elliptical |

**Table 4.17: TEM data of ZnO samples**

### 4.5.3.3 Results and discussions of XRD and TEM studies

Both XRD and TEM studies indicate the agglomeration of ZnO quantum dots after ion beam irradiation[16]. This phenomenon occurs due to unique property of PVA matrix, which has been explained while discussing the effect of ion beam on ZnS quantum dots embedded in PVA matrix in subsection 4.5.2.3.

### 4.5.3.4 Optical Absorption spectroscopy

The optical absorption spectra of virgin and ion irradiated samples are shown in fig 4.11 and the corresponding data are put in table 4.18. Like ZnS specimens, ion irradiated ZnO quantum dots also possess two distinct parts in optical absorption spectra. These are

I. Strong absorption

II. Tail absorption

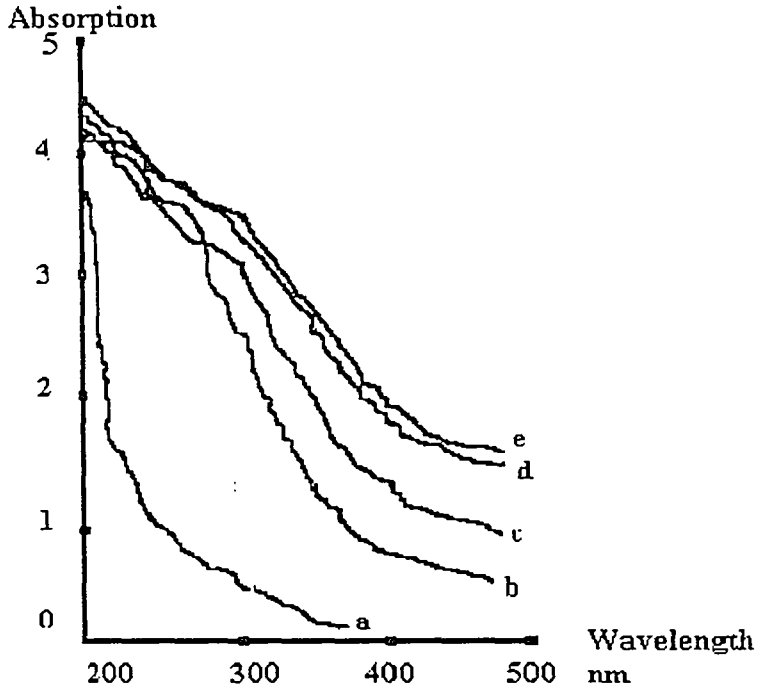


Fig 4.11: UV/VIS absorption spectra of ZnO specimens: a, b, c, d and e stand for virgin samples and samples irradiated by $1^{st}$, $2^{nd}$, $3^{rd}$ and $4^{th}$ dose respectively.

## I. Strong absorption

It is evident from the study that ion irradiated samples show red shift of strong absorption edge with respect to that of virgin sample. This is a clear signature of bigger particle formation[11,12,17]. The same result has already been indicated by XRD and TEM studies.

| Sample | Strong absorption edge (nm) | Size (nm) |
|---|---|---|
| $S_3$ | 215 | 11 |
| $S_3 d1$ | 360 | 42 |
| $S_3 d_2$ | 378 | 100 |
| $S_3 d_3$ | 385 | <=120 |
| $S_3 d_4$ | 385 | <=120 |

**Table 4.18: Optical spectroscopic data of ZnO specimens**

### II. Tail absorption

SHI, produces large number of oxygen vacancies[15] that have their own intermediate energy states in the forbidden gap of ZnO host lattice These intermediate energy states absorb the optical signal of lower energy below the band gap of host and produce the tail absorption. The density of oxygen vacancies enhances with higher ion doses, and so the tail absorption also increases. In virgin sample, due to the existence of few such vacancies only, optical absorption spectroscopy cannot detect them.

### 4.5.3.5. Photoluminescence study

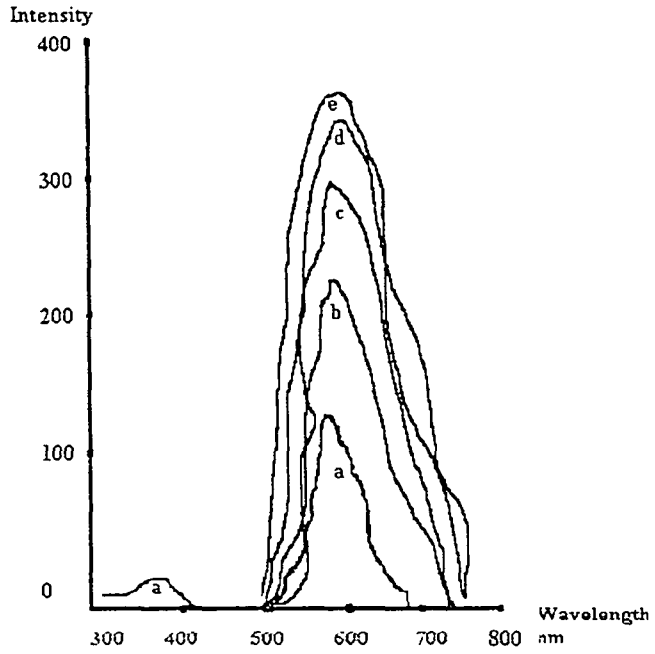


**Fig 4.12: PL spectra of ZnO samples: a, b, c, d and e stand for virgin sample and samples irradiated by 1st, 2nd, 3rd, and 4th ion dose respectively.**

#### I. Excitation source 200 nm

The virgin ZnO samples when excited with 220 nm source, produces two luminescence peaks[17] at 380 nm and 600 nm that are due to band edge emission and vacancy related emission respectively. In ion irradiated samples, it is clear that the luminescence at 600 nm is very intense while the emission at 380 nm is completely absent which indicates that the band edge emission is completely quenched at the cost of enhancement in oxygen vacancy related luminescence[17]. These phenomena occur due to following two reasons[12].

1. With higher ion doses the density of oxygen vacancies in ZnO samples increases. Trapping and detrapping in such vacancies are extremely fast (in the range of $10^{-13}$s - $10^{-14}$s) and strong in irradiated samples. So, comparatively slow band edge emission cannot compete with it and hence most of the energy supplied by the excitation source is transferred to the vacancies for excitation to produce luminescence.
2. The absorption edge of vacancies overlaps with the band edge emission[3] at 400 nm. So, the band edge emission is immediately absorbed by the vacancies to be excited. The PL spectra are shown in fig 4.12 and the data are put in table 4.19.

| Sample | PL intensity at 380 nm | PL intensity at 600 nm |
|---|---|---|
| $S_3$ | 25 | 130 |
| $S_3d_1$ | 0 | 230 |
| $S_3d_2$ | 0 | 300 |
| $S_3d_3$ | 0 | 345 |
| $S_3d_4$ | 0 | 350 |

**Table 4.19: PL data of ZnO samples**

**Excitation source 530 nm**

With 530 nm excitation source, the ZnO specimens show the similar luminescence behavior as that with 200 nm excitation source.

No significant emission has been observed in ZnO specimen with excitation source above 530 nm.

### 4.5.4 Mn doped Zinc sulphide

Chemical notation : ZnS:Mn

Matrix used : PVA

Sample Code : $SM_1$

| $S_e$ (eV) | $S_n$ (eV) | Projectile range (μm) |
|---|---|---|
| $1.226X10^{1}$ | $1.27X10^{-2}$ | 17.29 |

**Table 4.20: Electronic loss, nuclear loss and projectile range of Cl ion range in Zn:Mn sample**

| Doses notations | Irradiated sample notation |
|---|---|
| $\phi_1$ | $SM_1d_1$ |
| $\phi_2$ | $SM_1d_2$ |
| $\phi_3$ | $SM_1d_3$ |
| $\phi_4$ | $SM_1d_4$ |

**Table 4.21: Ion doses and corresponding sample codes**

### 4.5.4.1 X-ray diffraction study (XRD Study)

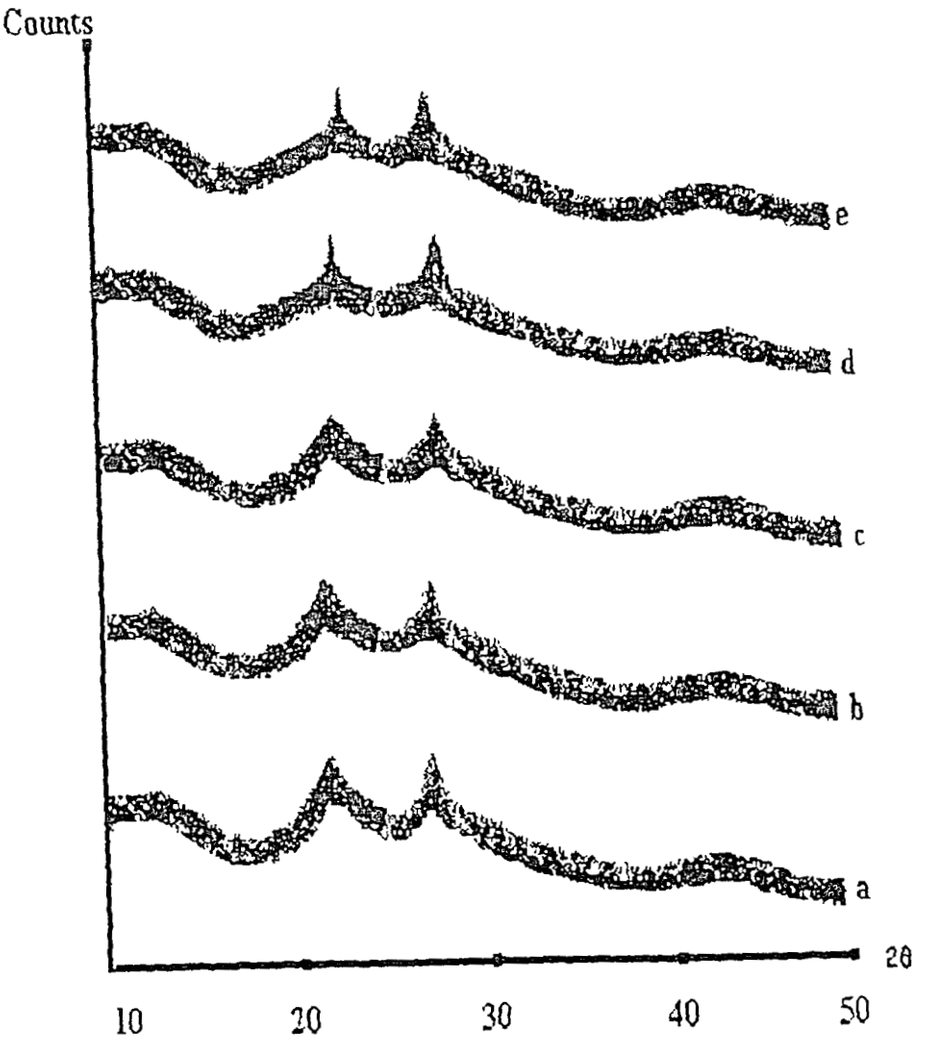


Fig 4.13: X-ray diffractograms of ion irradiated ZnS:Mn samples: a, b, c, d, and e correspond to the diffractograms of virgin samples and samples irradiated by 1st, 2nd, 3rd and 4th dose respectively.

The X-ray diffractograms of virgin as well irradiated ZnS Mn samples are shown fin fig 4 13, while the corresponding data are shown in table 4 22

| Sample | d spacing (nm) | Diffraction planes | Average size (nm) |
|---|---|---|---|
| $SM_1$ | 0 38, 0 31 | 100, 010 | 8 86 |
| $SM_1d_1$ | 0 38, 0 31 | 100, 010 | 32 |
| $SM_1d_2$ | 0 38, 0 31 | 100, 010 | 63 |
| $SM_1d_3$ | 0 38, 0 31 | 100, 010 | 198 |
| $SM_1d_4$ | 0 38, 0 31 | 100, 010 | 250 |

**Table 4.22: XRD data of ZnS:Mn specimens**

### 4.5.4.2 Transmission Electron Microscopy (TEM)

The TEM images of ZnS Mn samples are displayed in fig 4 14 and the corresponding data are listed in table 4 23

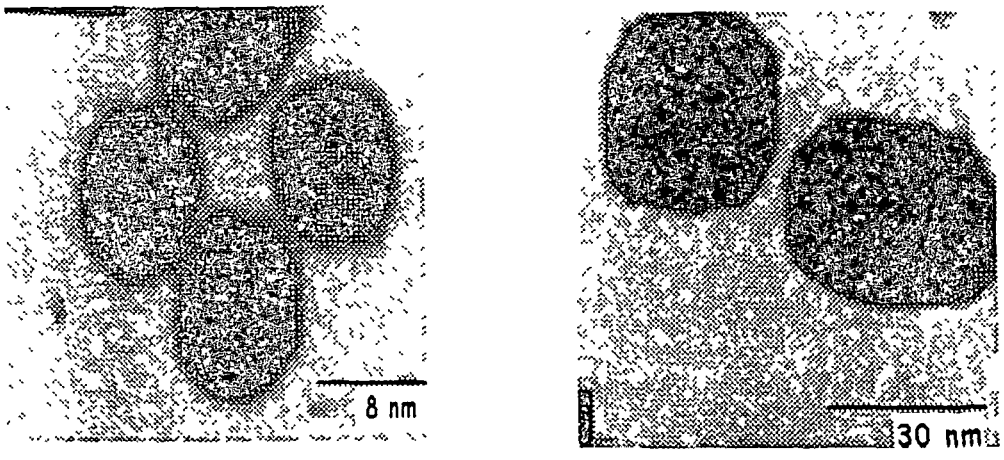


a b

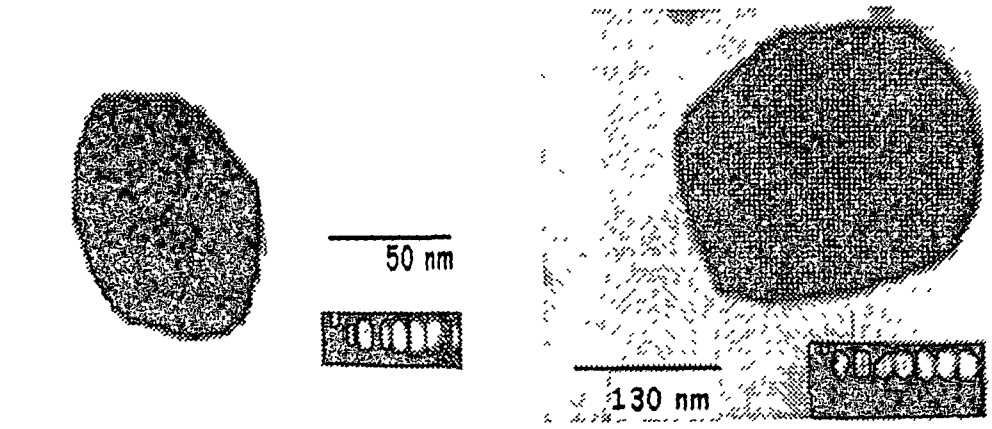


c d

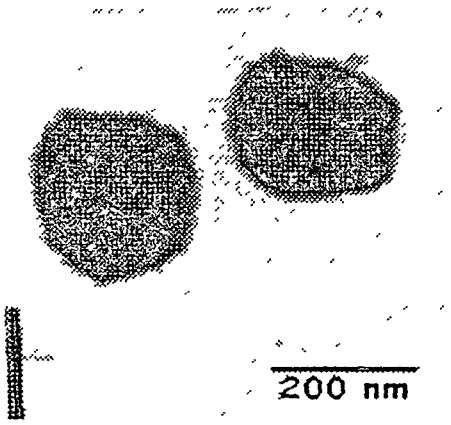


e

Fig 4.14: TEM images of ZnS:Mn specimens: a, b, c, d and e correspond to virgin sample and samples irradiated by 1st, 2nd, 3rd and 4th dose respectively.

| Sample | Size (nm) | Shape |
|---|---|---|
| $SM_1$ | 11 | Spherical |
| $SM_1d_1$ | 32 6 | Spherical |
| $SM_1d_2$ | 61 | Spherical |
| $SM_1d_3$ | 200 | Elliptical |
| $SM_1d_4$ | 250 | Elliptical |

Table 4.23: TEM data of ion irradiated ZnS:Mn samples

### 4.5.4.3 Results and discussions of XRD and TEM studies

The XRD as well as the TEM study show that when SHI beam irradiates ZnS:Mn, quantum dot, the particle agglomeration takes place. This phenomenon of bigger particle formation on PVA matrix has already been explained.

### 4.5.4.4 Optical Absorption Spectroscopy

Like ZnS and ZnO samples, the optical absorption spectra of ZnS:Mn samples in (UV/VIS region) possess two parts

I. Strong absorption and II. Tail absorption

**I. Strong absorption**

After SHI irradiation the strong absorption edges of ZnS:Mn sample shift towards red with respect to that of virgin sample. Red shift of absorption edge is a signature of decrease in band gap and hence the increase in particle size[13]. The same result has already indicated by XRD and TEM studies of these samples. The spectra are shown in fig 4.15 with the data in table 4.24.

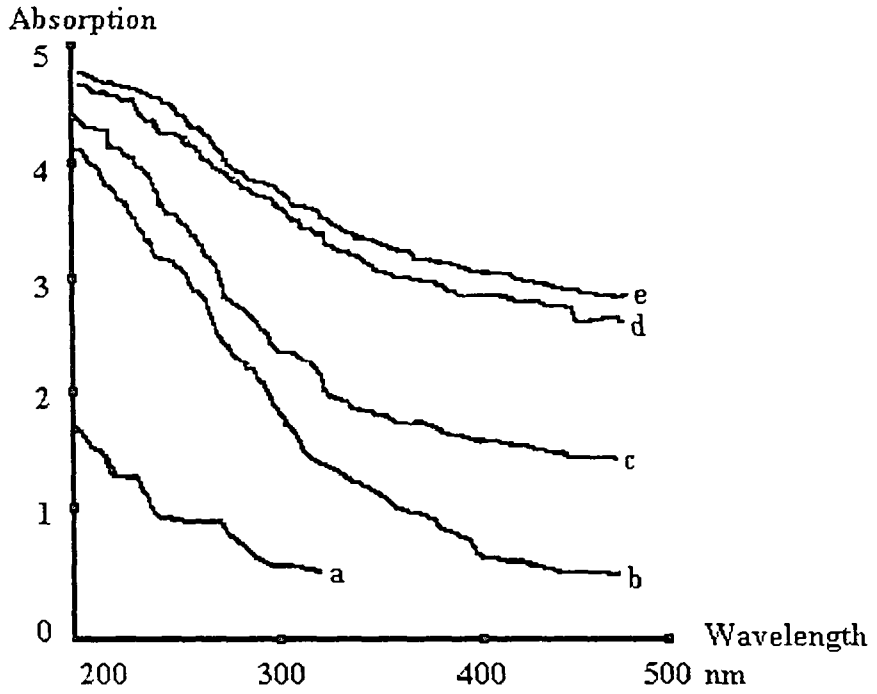


Fig 4.15 : UV/VIS absorption spectra of ZnS:Mn a, b, c, d and e stand for virgin sample and samples irradiated by 1st, 2nd, 3rd and 4th dose respectively

| Sample | Strong absorption edge (nm) | Size (nm) |
|---|---|---|
| $SM_1$ | 215 | 10 |
| $SM_1 d_1$ | 324 | 32 |
| $SM_1 d_2$ | 342 | 60 |
| $SM_1 d_3$ | 350 | <=145 |
| $SM_1 d_4$ | 350 | <=145 |

Table 4.24: Optical spectroscopic data of ZnS:Mn specimens

To carry out photoluminescence study of ZnS quantum dot as well as bulk specimen, the samples are excited first with 200 nm optical source well above the band gap energy. The spectra are displayed in fig 3.15 and the corresponding data are produced in the table 3.11.

| Sample | Peak position | Intensity |
|---|---|---|
| ZnS bulk | 500 nm | 10.5 |
| ZnS quantum dot | 500 nm | 17 |

**Table 3.11: PL peak positions and intensities of ZnS specimen with excitation source 200nm**

From fig. 3.15 and table 3.11 it is evident that though the luminescence intensity of ZnS increases significantly with reduction in size but the peak position does not shift with size variation. The similar investigations have been reported somewhere else[7]. Bulk ZnS possesses a luminescence peak at 500 nm that occurs due to surface states but as the surface states are very few in bulk sample, the emission is very weak[14]. On contrary, the quantum dot sample shows stronger emission at 500 nm which is also due to surface states but these are enhanced in number due to size quantization to produce intense luminescence.

**II. Tail absorption**

Mn has been doped in ZnS quantum dots by chemical method in the presence of no activator atom/element at a temperature of $80^0$C, discussed in chapter II. But for good Mn doping in ZnS specimen, either of the two conditions (1) an activator atom like 'Cl' at low temperature or (2) very high temperature in the presence of no activator atom[2,15,18] is to be fulfilled. SHI beam irradiation fulfills both the conditions by (1) providing Cl as an activator atom/element and (2) generating very high temperature. That is why, in higher ion doses, Mn doping enhances which is maximum and saturated in $3^{rd}$ dose. It is interesting to notice that the spectra of $3^{rd}$ and $4^{th}$ dose irradiated samples are almost overlapping. This is attributed due to that fact that the conditions (activator atom and the temperature) available in $3^{rd}$ ion dose are sufficient for complete doping of Mn and no further doping enhancement has been observed in the sample irradiated to $4^{th}$ ion dose. Doped Mn produces an intermediate energy states in the forbidden gap of ZnS specimen. This level produces the tail absorption edge by absorbing the optical signal of lower energy below the band gap.

### 4.5.4.5 Photoluminecence ( PL) Study

#### I. Excitation source 200 nm

The photoluminescence spectra of Mn doped ZnS quantum dot (virgin)possess the luminescence peak at 590 nm due to d electrons[13,14,19,20] of Mn that has been discussed in the PL analysis of virgin ZnS:Mn quantum dots in the previous chapter. Similarly, the spectra of ion irradiated samples also show the emission phenomenon[20] at 590 nm. But it goes on increasing up to 3rd ion dose and then it is saturated. This is due to the fact that Mn density (doping) in ZnS sample saturates at 3rd ion dose resulting in the saturation of corresponding luminescence intensity and no further enhancement has been observed in 4th dose.. The spectra are displayed in fig 4.16 and the data are put in table 4.25.

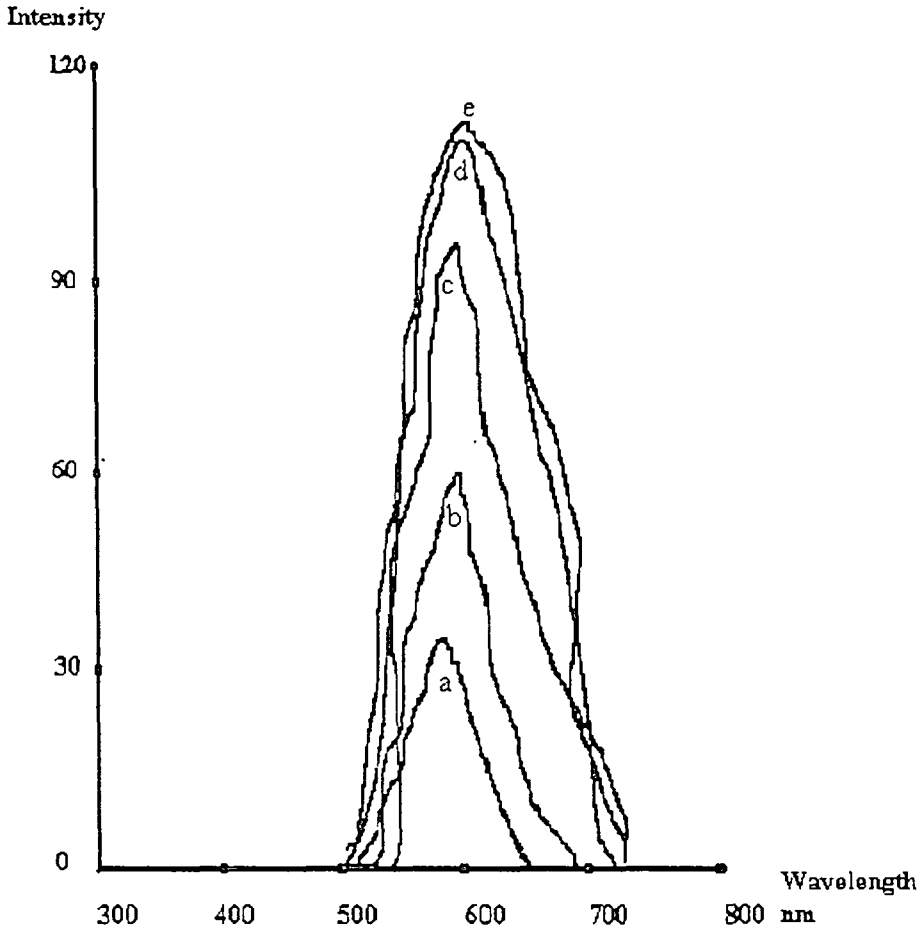


Fig 4.16: PL spectra of ZnS:Mn : a, b, c, d and e stand for virgin samples and samples irradiated by , 1st, 2nd, 3rd and 4th dose respectively

| Sample | PL intensity at 590 nm |
|---|---|
| $SM_1$ | 32 |
| $SM_1d_1$ | 60 |
| $SM_1d_2$ | 95 |
| $SM_1d_3$ | 105 |
| $SM_1d_4$ | 110 |

Table 4.25 : PL data of ZnS:Mn samples

### II. Photoluminescence with 530 nm excitation source

With 530 nm excitation source ZnS:Mn samples show the similar luminescence behavior as that with 200 nm source.

No emission has been observed in the samples with excitation source above 530 nm.

## 4.6 Conclusion

Studies of ion irradiated CdS samples on SBR show no enhancement in size and hence no shift of strong absorption edge. But the luminescence is enhanced due to increase in CdO phase in the sample. But ion irradiated ZnS specimen on PVA shows significant enhancement in size and hence it possesses considerable red shift of strong absorption edge. The luminescence is enhanced due to increase in Zn vacancies. Similarly ion irradiated ZnO samples on PVA increase in size and show the corresponding red shift. The luminence is increased due to increase in oxygen vacancies. Irradiated ZnS:Mn on PVA also show the similar kind of size enhancement and the red shift in absorption edge followed by the enhanced luminescence due to increase in Mn density in ZnS.

**Reference**


1. Turton Richard; *The Quatum Dot : Journey Into future Microelectronics*, Oxford University Press, New York, 1995.
2. Woggon. U; *Optical Properties of Semiconductor Quantum dots*; Springer Tracts in Modern Physics, Vol. 136, Berlin,1996.
3. Nanda. J and Sarma. D. D; *J. Appl. Phys.* Vol. 90, No. 5, pp 2504, 2001.
4. Tanaka Masanori, Masumoto Yasuaki; *Chem. Phys. Lett.* Vol. 324, pp. 249, 2000.
5. La Lee –Jene and Su Ching-Shen; *J. Appl. Phys.* Vol. 87, No. 1, pp 236. 2000.
6. Kim. Y. S, Lee. U. H, Lee D, Rhee.S. J, Leem.Y A, Ko. H.S, Kim. D.H and Woo. J. C; *J. Appl. Phys.* Vol. 87, No.1, pp 241, 2000.
7. Singh. J. P, Singh. R, Mishra. N. C, Ganesan. V, Kanjilal. D; *Nucl. Instr. And Meth. In. Phys. Res.* B 179, pp 37, 2001.
8. Zeigler. J. F; *SRIM-97 The stopping range of ions in matter* ( NY: IBM research), pp 1-28.
9. Suyver. J. F, Wuister. S. F, Kelly J. J and Meijerink A; *Nano Lett.* Vol. 1, pp 428, 2001.
10. Ueda Naoyuki, Maeda Hiroo, Hosono Hideo and Hiroshi Kawazoe; *J. Appl. Phys.* Vol. 84, No. 11, pp 6174,1998.

11. Behera. S. N, Sahu. S. N, Nanda K. K; *Ind. J. Phys.* 74 A (2), pp 81, 2000.

12. Chen Wei, Wang Zhanguo, Lin Zhaojun and Lin lanying; *J. Appl. Phys.* Vol. 82, No. 6, pp 3111,1997.

13. Arai. T, Yoshida. T and Ogawa. T; *Jpn. Appl. Phys.* Vol. 26, pp 396, 1987.

14 Agata. M, Kurase. H, Hayashi. S and Yamamoto. K; *Solid State Commun.* Vol. 76, pp. 1061, 1990.

15. Singhal. R.L; *Solid State Physics*, Keder Nath Ram Nath, Meerut, UP, India, 1995.

16. Mohanta. D, Nath. S. S, Bordoloi A, Choudhury A, Dolui. S .K and Mishra. N .C; *J. Appl. Phys.* Vol. 92, No. 12, pp 1, 2002.

17. Mahamuni. S, Bendre. B. S, Leppert. V .J, Smith. C. A, Cooke. D, Risbud. S. H and Lee H .W. H; *Nano. Struct. Mater.* Vol. 7, No. 6, pp 659,1996.

18 Madan. R .D; *Inorganic Chemistry*, S. Chand and Co, New Delhi, India, 1995.

19. Bhargava. R. N, Gallagher. D, Hong. X, Nurmikko. A; *Phy. Rev. Lett.* Vol. 72, pp 416, 1994.

20. Mohanta. D, Nath. S. S, Mishara. N. .C and Choudhury. A; *Bull. Mater.* Sci. Vol. 26, No. 3, pp 289, 2003.

**********

# CHAPTER 5

# APPLICATIONS

# CHAPTER 5

# Applications

## 5.1 Applications of quantum dots in different areas

Semiconductor quantum dots opened a new door to the world of nano physics and nano electronics. Recently, nano technology for developing electronic, optoelectronic and optic devices possessing very less and less response time delay[1-9], are replacing the conventional silicon technology. In the present work, an attempt has been made to apply our prepared quantum dots in area of (I) Electronics and Photonics and (II) nonlinear optics. In electronics and photonics, the samples have been tested for fast electronic and photonics switching while in non linear optics, the specimens are tested for fast optic switching. Although a number of other applications of quantum dots are possible in lasing communication and sensing technology, we have restricted our investigation to its possible application as electronic, photonic and optical switching.

In this chapter, we report the working of quantum dots as electronic and photonic switch and optic switch depending upon the input conditions. It is experimentally found that upto a critical bias potential, the specimens function as photonic switch while above the critical bias, the same sample acts as electronic switch. it has also been experimentally shown that the specimens act as optic

switch (optical wavelength converter) with optical input. The following sections define the three switches.

**I. Electronic switch:** Electronic switch is a device which converts electronic signal into another electronic signal that is fully different from input, by its pattern, shape etc. The conversion speed is very high.

**II. Photonic switch:** Photonic switch is a device which converts optical signal into electronic signal with very high conversion speed.

**III. Optic switch:** Optic switch is a device which converts optical signal of one wavelength into another optical signal of different wavelength in a ultra short interval of time.

## 5.2 Estimation of quantum efficiency and switching speed of quantum dot switches

### 5.2.1 Quantum efficiency

The efficiencies of different quantum dot devices are compared in terms of quantum efficiency. For photonic device, it is defined as the ratio of total number of electrons (charge carriers) excited by optical signal to the total number of photons incident on the specimen. In our quantum dot photonic switches, quantum efficiency is easily indicated by the intensity of photocurrent as the same optical source (of same strength) has been used to excite all the samples. For optic device, quantum efficiency is defined as the ratio of total number of electrons excited by optical source to cause luminescence, to total number of

photons incident on the sample. In this case also, it is indicated by the intensity of luminescence output because the optical source used to illuminate different samples is the same.

### 5.2.2 Estimation of switching speed

The response speed and the range of photosensitivity are explored from photoluminescence studies of the samples because it is the trapping and detrapping of electrons by the traps (e.g vacancies, surface states) that causes the switching phenomena[1,3,5-7,9-14]. From luminescence studies, the different traps (that is energy states like vacancies) are identified which gives the corresponding transition speed of electrons between any two traps. This transition speed is the response speed of the device. Response speed depends on the types of traps[9-11].

## 5.3. Application of quantum dots in Electronics and Photonics

Quantum dots can function as very efficient electronic and optoelectronic sensors that convert electronic and optical signal into electronic / electrical output with ultra fast switching speed in nano second or less. We have tested our virgin (unirradiated) quantum dots only for electronic and photonic switching because photoluminescence study already suggested that switching phenomena of virgin and irradiated samples are the same with the only difference that outputs of irradiated samples are of higher intensities, depending upon the ion doses

### 5.3.1 Basic Principle of quantum dot Electronic and Photonic switch

Current conduction in semiconductor occurs due to electronic transition between tow energy states in the specimen. These transitions and hence the current generations are of two types[4-6]. These are

I. Current generation takes place in semiconductor due to increase in electrical conductivity caused by bias voltage or photons of energy higher than or equal to band gap. Under this condition, free electron hole pairs are produced by applied bias or by absorption of incident photons while electron and holes serve as the charge carriers in conduction and valance band respectively producing current in external circuit.

II. In another type, current conduction is not of this intrinsic kind where impurities and imperfections play significant roles in producing output current with fast response speed, even with the bias voltage or photons having energy below the threshold (band gap energy) for production mobile electron / hole. In fact, in quantum dots, we cannot understand the experimental facts of conductivity, without invoking the presence of imperfections and impurities. Imperfections produce discrete energy level in the forbidden gap, which are called 'traps'. From this point of view, current conductivity is described as a process whereby, electrons are trapped and detrapped by crystal imperfections (traps), excited by bias voltage or photons and produce current in the external circuits.

Trapping and detrapping of charge carriers are very fast in the order of $10^{-9}$ sec to $10^{-14}$ sec (ns) depending upon the types of traps[7-13].

To investigate quantum dot as electronic and photonic switch with ultra fast switching speed, we experimentally show that it produces electronic (current) output excited by bias voltage or optical signal of proper energy. The response speed and optical operating range of the devices are revealed from photoluminescence studies, as the reason behind electronic and photonic switching is the same as that of photoluminescence phenomena that is, like luminescence process electronic and photonic switching are also caused by fast trapping and detrapping of charge carriers as explained in subsection 5.2.2.

### 5.3.2 Experimental setup to study Electronic and Photonic switching

Two ends of 99% pure fine silver wire of 0.01 mm diameter coated with gold are fixed very close to each other within micron range. By means of a syringe, a single tiny drop of quantum dot sample is gently put over the two free ends of silver wires to make the micro contact. The specimen is dried partially by natural process to avoid spilling and then in oven to stick it properly upon the substrate. After that, the free ends of probing wires are connected to a bias source (mV) with a micro ammeter in series. Precaution is taken to prevent error in measuring current due to improper insulation of wires or presence of other electro magnetic sources. The sample is ready for investigations. Nd:YAG laser in has been used to illuminate the sample. The setup is displayed diagrammatically in fig. 5.1(a).

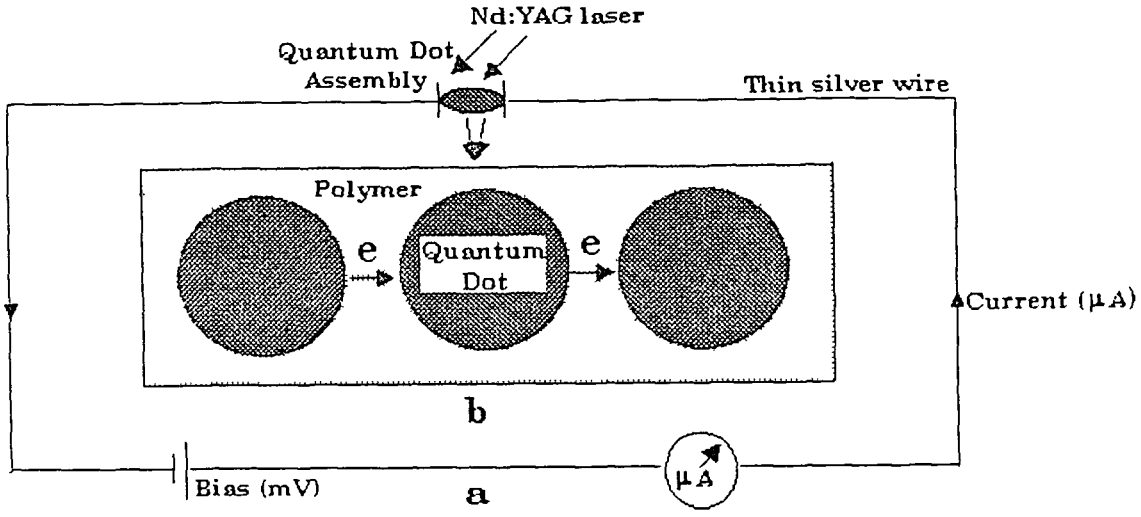


**Fig.5.1: a: Setup for electronic and photonic switching. b: Distribution of quantum dots on polymer matrix.**

### 5.3.3 General behaviour of quantum dot electronic and photonic switch

We have studied electronic and photonic switching behaviour of our prepared quantum dot samples and plotted the characteristic curves between current generated and bias voltage for various (here three) illumination intensities $\phi_1$, $\phi_2$ and $\phi_3$. The general pattern of such curve is shown in fig 5.2. First we consider the plot ABCDEFG for intensity $\phi_1$ This curve show that, in the presence of illumination with intensity $\phi_1$, photocurrent starts to flow at point A and produces a steep rise at point B and then saturates at point C. It falls at point D and again rises at point E with steep increase at point F and then saturated again at point G Next the reasons are explained.

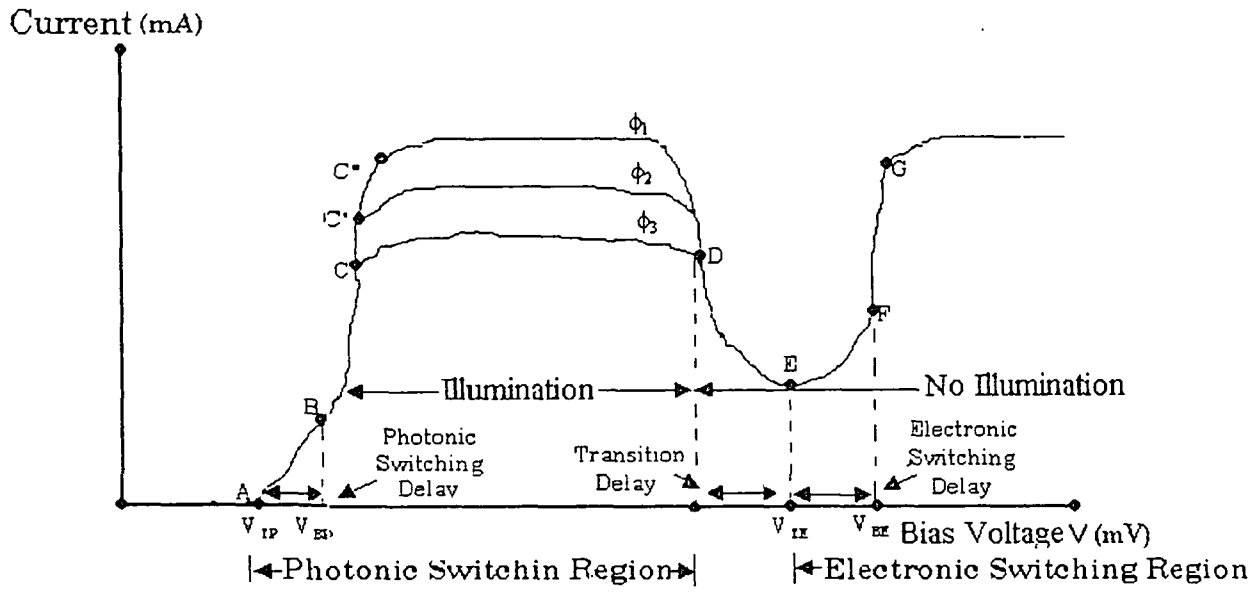


**Fig 5.2: Pattern of photonic and electronic switching characteristics of quantum dots**

**$\phi$ stands for illumination intensity where $\phi_1<\phi_2<\phi_3$.**

Optical signal excites charge carriers and produces corresponding traps (defect) related transitions in quantum dots. But to produce effective current, electron must tunnel from one dot to another through insulating polymer matrix wall as shown in fig 5.1(b). That is why, a minimum bias voltage is needed to cause electronic tunneling through the polymer. This voltage corresponds to the point A, and it is denoted by $V_{TP}$. Basically, it depends on property and thickness of matrix as well as electronic states of quantum dots. Further, at point B the bias voltage $V_{BP}$ produces breakdown phenomenon by causing all the charge carriers (generated in the samples) to tunnel through the polymer wall at a time and produce steep rise in photocurrent. This process may be compared with breakdown phenomenon of avalanche photodiode. Furthermore, at point C, photocurrent is saturated and no further change in it is observed from C to D

because the tunneling of charge carriers is saturated at point C. The similar behaviour of photocurrent is observed with higher illumination intensity with the only difference that photocurrent is saturated at higher intensity.

To observe the effect of bias in the absence of illumination, we switch off the optical source (Nd:YAG laser) at point D and photocurrent tend to fall but it does not reach zero, rather, it starts rising again at point E corresponding to the bias voltage $V_{TE}$ with a steep rise at point F corresponding to the bias $V_{BT}$ and then saturates at point G.

In the absence of illumination, photocurrent tends to cease, but at the critical point E, bias $V_{TE}$, itself can excite some of the charge carriers even in the absence of light while at point F the bias $V_{BE}$, causes the avalanche breakdown by detrapping all the charge carriers at a time, resulting in steep rise in output current. This phenomenon may be compared with zener breakdown of semiconductor diode or breakdown in FETs. Furthermore, at the point G the current is saturated as trapping and detrapping of charge carriers is saturated at this point.

The portion AB and EF indicate photonic switching speed and electronic switching speed respectively. Steeper[12-14] the proton higher is the response speed. Interestingly, in the actual plots, we find that, both the portions show similar kind of steep rise, which infer the same photonic and electronic switching speeds. This behaviour also suggest that, both the switching phenomena are caused by same mechanism that is, trap (defect) related charge carrier transition.

From this discussion, it is clear that, the characteristics can be divided in to two parts

I. Photonic switching region and

II. Electronic switching region.

It is experimentally found that, upto point E, corresponding to bias voltage $V_{TE}$, quantum dot act as photonic switch but beyond that, it act as electronic switch. It is also very interesting to notice that photonic region can be well compared with the characteristics of (common emitter) transistor if illumination intensity is compared with base current.

## 5.4. Electronic and photonics switching phenomena of our quantum dots

### 5.4.1 CdS quantum dot on SBR latex Matrix

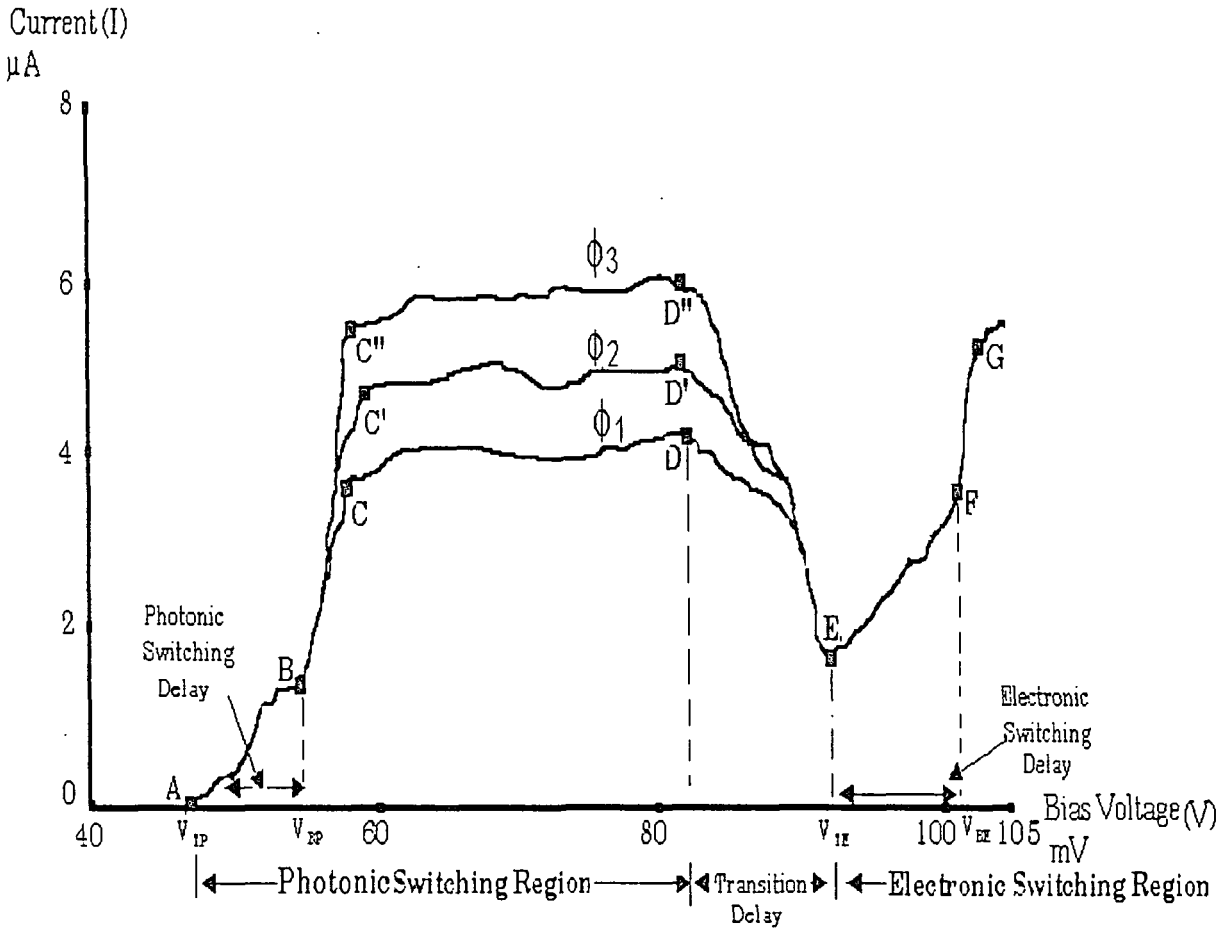


Fig 5.3: Photonic and electronic switching characteristics of CdS quantum dot assembly on SBR latex. $\phi$ stands for illumination intensity where $\phi_1<\phi_2<\phi_3$

Both photonic and electronic switching phenomena of CdS quantum dot assembly embedded on SBR latex are studied under the three illumination intensities $\phi_1$, $\phi_2$ and $\phi_3$

The reason behind the switching phenomena is the existence of CdO phase and hence the electronic transition between CdO center (donor level that acts as trap) and valence band of CdS quantum dots[10]. The behaviour of CdS samples on PVA matrix is similar to that of CdS samples on SBR latex with the exception that $V_{TP}$ is lower in the samples on PVA as the polymer wall between two dots is thinner and hence, lower bias can cause electron tunneling. The characteristic curves are displayed in fig 5.3 while the corresponding data are put in table 5.1and 5.2.

| Illumination | Saturation Current (μA) | $V_{TP}$ (mV) | $V_{BE}$ (mV) | Optical operating Range (nm) | Switching speed |
|---|---|---|---|---|---|
| $\phi_1$ | 4 | 47 | 55 | 200 to 630 | Of the order of $10^{-9}$ sec |
| $\phi_2$ | 5 | | | | |
| $\phi_3$ | 6 | | | | |

**Table 5.1: Photonic switching data of CdS quantum dot assembly on SBR latex**

| $V_{TE}$ (mV) | $V_{BE}$ (mV) | Saturation Current (μA) | Switching Speed |
|---|---|---|---|
| 90 | 101 | 5.6 | Of the order of $10^{-9}$ sec |

**Table 5.2: Electronic switching data of CdS quantum dot assembly on SBR latex**

## 5.4.2 ZnS quantum dots on PVA matrix

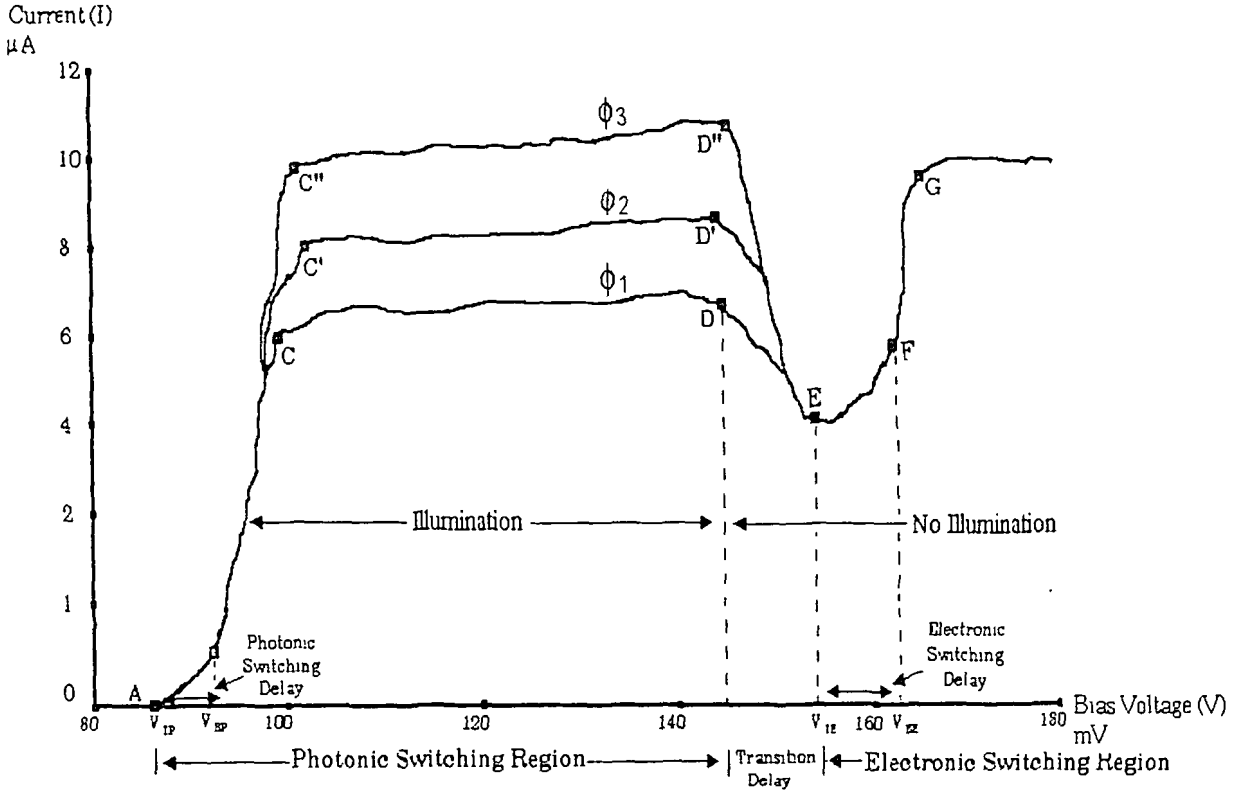


**Fig 5.4: Photonic and electronic switching characteristics of ZnS quantum dot assembly on PVA. $\phi$ stands for illumination intensity where $\phi_1<\phi_2<\phi_3$.**

Investigation of photonic and electronic switching phenomena of ZnS quantum dot assembly embedded on PVA matrix are carried out under three illumination intensities $\phi_1$, $\phi_2$ and $\phi_3$. The reason[11] behind both the switching phenomena is the presence of surface states and hence the trapping and

detrapping of electrons by them. The switching characteristics are displayed in fig 5.4 while the related data are put in the table 5.3 and 5.4.

| Illumination | Saturation Current (μA) | $V_{TP}$ (mV) | $V_{BE}$ (mV) | Optical operating range (nm) | Switching speed (nS) |
|---|---|---|---|---|---|
| $\phi_1$ | 6 | 88 | 92 | 200 to 460 | Of the order of $10^{-12}$ sec |
| $\phi_2$ | 8 | | | | |
| $\phi_3$ | 10 | | | | |

**Table 5.3: Photonic switching data of ZnS quantum dot assembly on PVA**

| $V_{TE}$ (mV) | $V_{BE}$ (mV) | Saturation Current (μA) | Switching Speed (nS) |
|---|---|---|---|
| 155 | 163 | 9.7 | Of the order of $10^{-12}$ sec |

**Table 5.4: Electronic switching data of ZnS quantum dot assembly on PVA**

### 5.4.3 ZnO Quantum dot with PVA

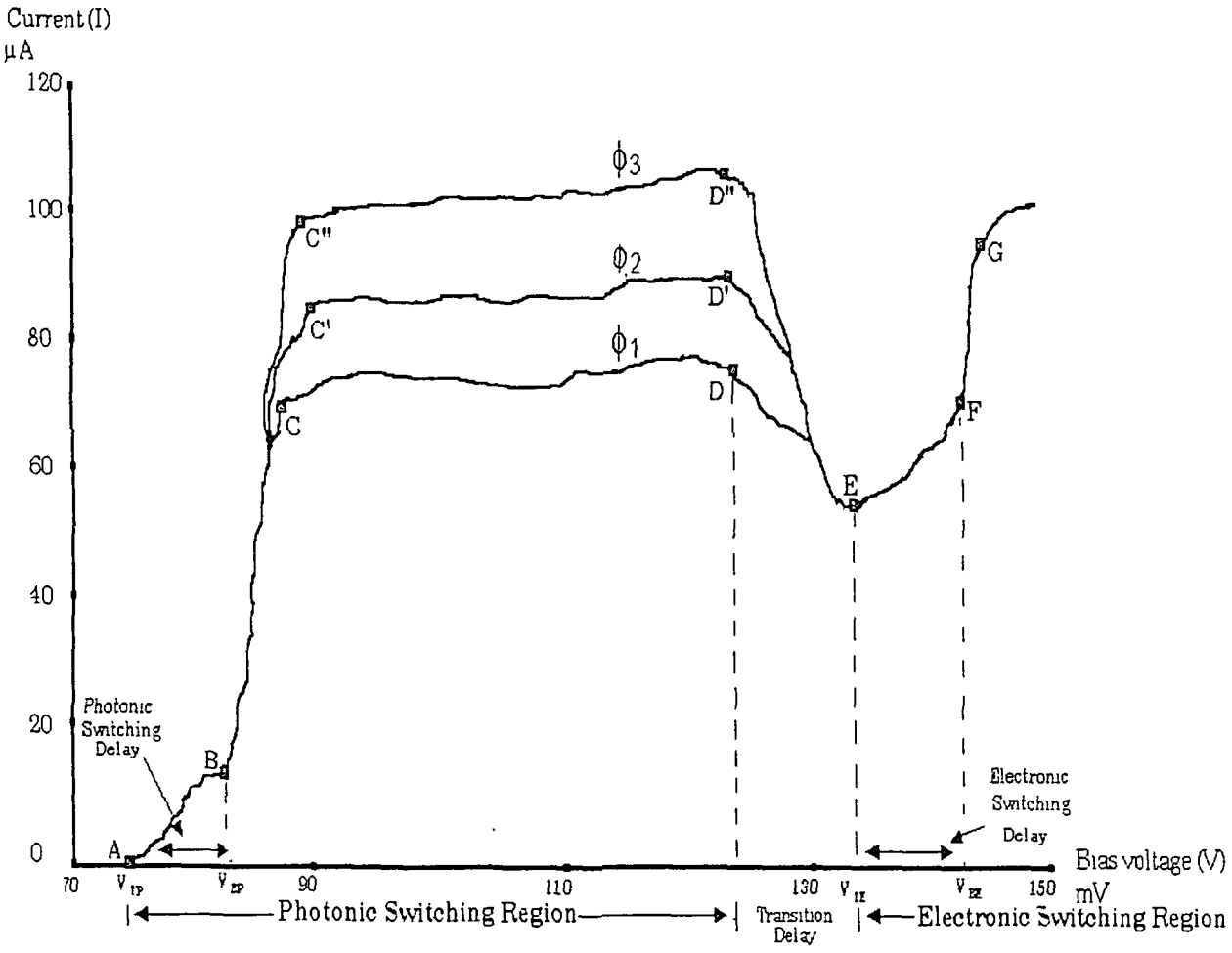


**Fig 5.5 : Photonic and electronic switching characteristics of ZnO quantum dot assembly on PVA. $\phi$ stands for illumination intensity where $\phi_1<\phi_2<\phi_3$.**

Studies of photonic and electronic switching phenomena of ZnO quantum dot assembly embedded on PVA matrix are carried out for illumination intensities $\phi_1$, $\phi_2$ and $\phi_3$ The mechanism[9] behind the switching technique is the existence of oxygen vacancies and hence the trapping and detrapping of electrons by them. The switching characteristics are displayed in fig 5.5 while the corresponding data are put in the table 5.5 and 5.6.

| Illumination | Saturation Current (μA) | $V_{TP}$ (mV) | $V_{BE}$ (mV) | Optical operating Range (nm) | Switching speed |
|---|---|---|---|---|---|
| $\phi_1$ | 70 | 76 | 84 | 200 to 530 | Of the order of $10^{-9}$ sec |
| $\phi_2$ | 82 | | | | |
| $\phi_3$ | 100 | | | | |

**Table 5.5: Photonic switching data of ZnO quantum dot assembly on PVA**

| $V_{TE}$ (mV) | $V_{BE}$ (mV) | Saturation Current (μA) | Switching Speed |
|---|---|---|---|
| 134 | 145 | 95 | Of the order of $10^{-9}$ sec |

**Table 5.6: Electronic switching data of ZnO quantum dot assembly on PVA**

### 5.4.4 Manganese doped ZnS quantum dot with PVA matrix

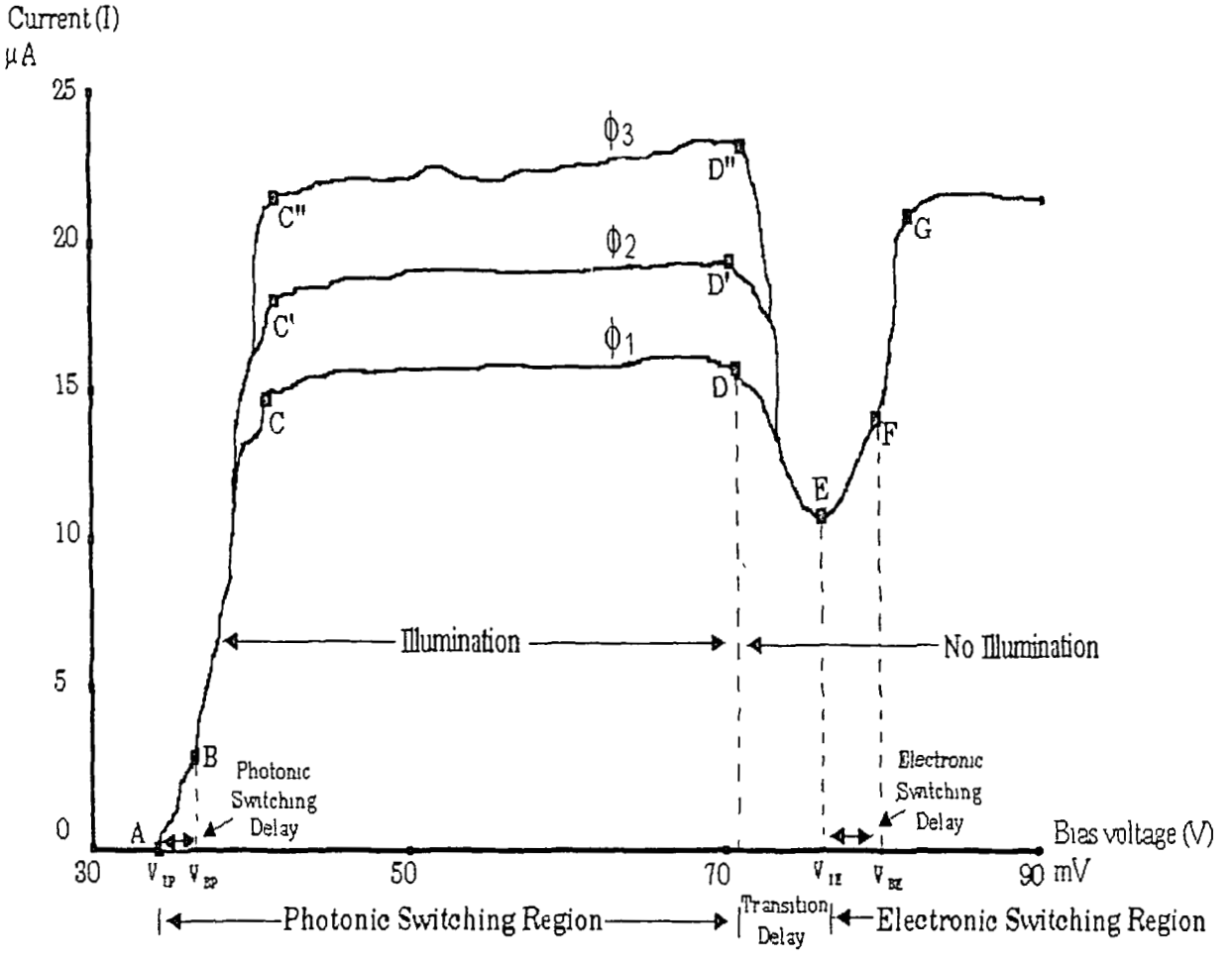


Fig 5.6: Photonic and electronic switching characteristics of ZnS:Mn quantum dot assembly on PVA. $\phi$ stands for illumination intensity where $\phi_1<\phi_2<\phi_3$.

ZnS:Mn quantum dots shows marvelous improvement in producing higher current with faster response speed over undoped samples. Both photonic and electronic switching phenomena of ZnS:Mn quantum dot assembly embedded in PVA matrix are investigated for three illumination intensities $\phi_1$, $\phi_2$ and $\phi_3$. The key reason[3] behind both the switching process is the presence of Mn energy state (trap) in the forbidden gap of ZnS host and its d electron related transitions. The switching characteristics are displayed in fig 5.6 while the related data are put in the table 5.7 and 5.8.

| Illumination | Saturation Current ($\mu$A) | $V_{TP}$ (mV) | $V_{BE}$ (mV) | Optical operating Range (nm) | Switching speed |
|---|---|---|---|---|---|
| $\phi_1$ | 15 | 36 | 38 | 200 to 530 | Of the order of $10^{-14}$ |
| $\phi_2$ | 18 | | | | |
| $\phi_3$ | 22. | | | | |

**Table 5.7: Photonic switching data of ZnS:Mn quantum dot assembly on PVA**

| $V_{TE}$ (mV) | $V_{BE}$ (mV) | Saturation Current ($\mu$A) | Switching Speed |
|---|---|---|---|
| 75 | 79 | 20 | Of the order of $10^{-14}$ sec |

**Table 5.8: Electronic switching data of ZnS:Mn quantum dot assembly on PVA**

## 5.5 Technological advantages of quantum dot switches over conventional semiconductor switching devices (diode and transistor)

I. Quantum dot switches are very small in dimension (nm) and the same device can function as photonic as well as electronic switch depending upon the bias while same diode or transistor can not be used for both the purposes.

II. Switching speed of quantum dots is faster than conventional devices.

III. Quantum dots are free from polarities. That is why, polarity of bias need not be considered while the conventional devices are very sensitive to polarities.

IV. In quantum dot switching phenomena are caused by trapping and detrapping by various traps. The avalanche phenomenon occurs when maximum trapping and detrapping (depending upon the number of traps), take place producing no damageable heat. Practically, quantum dots are self protecting devices. But, in conventional semiconductor devices, avalanche phenomena must be controlled by external resistance to avoid thermal runway that completely damages it.

V. Fabrication of quantum dot device is simpler and cheaper than that of conventional semiconductor device.

## 5.6 Application of quantum dot in non linear optics

Optic switching is an application of quantum dot in nonlinear optics that utilizes the properties of optical absorption (excitation) and photoluminescence of the specimen. Optical absorption in quantum dot is a nonlinear process[15]. That is why optic switch is a promising application of quantum dot in the area of nonlinear optics.

### 5.6.1 Principle of optic switching

Optic switching is the phenomenon where the optical signal of one wavelength is converted into a signal of different wavelength in nano seconds or less. For example, the optical signal of 200 nm wavelength may be converted in to a signal of wavelength 500 nm in nano second or less. Photoluminescence[3,9-12] studies of both virgin and irradiated quantum dots show that they can act as very efficient optical wavelength converter with very high conversion speed of the order of $10^{-9}$ sec to $10^{-14}$ sec or more. The mechanism behind the wavelength conversion is the existence of intermediate energy states (crystal defects) known as traps, in the forbidden gap of host atoms that has already been discussed in chapter3 and chapter4. In this part, we shall put the photoluminescence data of the samples from chapter 3 and 4 because luminescence study is the base of optic switching. Functioning of optic switch may be compared with the action of convex lens or optical filter. Fig 5.7 shows the optic switching technique of

quantum dots. The speed of response is explored from luminescence behaviour as explained in subsection 5.2.2.

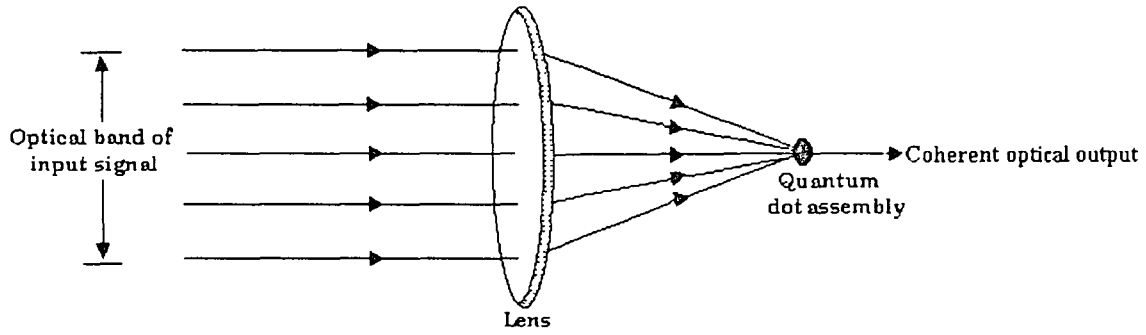


**Fig 5.7 : Schematic diagram for quantum dot optic switching**

## 5.7 Optic switching phenomena of our prepared quantum dots

### 5.7.1 CdS quantum dot on SBR latex

To study optic switching phenomenon of CdS quantum dots, we excite the samples with optical signal of wavelength ranges from 200 nm to 630 nm and record the emission at 700 nm as discussed in chapter 3 and 4. It means that, optical signal lying in the said wavelength band is converted in to a signal of wavelength of 700 nm. The key reason[10] for optic switching is the presence of CdO phase as explained already. Table 5.9 shows the data of optic switching.

| Sample | Optical operating range (nm) | Optical output wavelength (nm) | Output intensity | Switching speed |
|---|---|---|---|---|
| $S_1$ | 200 to 630 | 700 | 7.3 | Of the order of $10^{-9}$ sec |
| $S_1d_1$ | 200 to 630 | 700 | 18 | |
| $S_1d_2$ | 200 to 630 | 700 | 28 | |
| $S_1d_3$ | 200 to 630 | 700 | 41 | |

**Table 5.9: Optic switching data of CdS samples**

Similar optic switching phenomena are observed with CdS sample on PVA.

### 5.7.2 ZnS quantum dot in PVA matrix

To observe optic switching phenomena of ZnS quantum dots, the samples have been excited with optical signal of wavelength band from 200 nm to 460 nm and the corresponding optical emissions at 500 nm are recorded. This means that, optical signal lying within the said band is converted in to an optical signal of wavelength of 500 nm. Reason[11] behind the switching is the existence of surface states in virgin samples and Zn vacancies in ion irradiated samples as discussed already. The data are put in table 5.10.

| Sample | Optical operating range (nm) | Optical output wavelength (nm) | Output intensity | Switching speed |
|---|---|---|---|---|
| $S_2$ | 200 to 460 | 500 | 17 | Of the order of $10^{-12}$sec |
| $S_2d_1$ | 200 to 460 | 500 | 24 | |
| $S_2d_2$ | 200 to 460 | 500 | 41 | |
| $S_2d_3$ | 200 to 460 | 500 | 68 | |
| $S_2d_4$ | 200 to 460 | 500 | 70 | |

**Table 5.10: Optic switching data of ZnS samples**

### 5.7.3 ZnO quantum dot on PVA

For observing optic switching process of ZnO quantum, the samples have been excited with optical signal of wavelength band from 200 nm to 530 nm to produce output at 600 nm. This shows that, optical signals within the band of 200 nm to 530 nm are converted in to an optical signal of wavelength 600 nm. The key reason[9] for switching is the presence of oxygen vacancies in both virgin as well as irradiated specimens. The data are put in table 5.11.

| Sample | Optical operating range (nm) | Optical output wavelength (nm) | Optical intensity | Switching speed |
|---|---|---|---|---|
| $S_3$ | 200 to 530 | 600 | 130 | Of the order of $10^{-9}$sec |
| $S_3d_1$ | 200 to 530 | 600 | 230 | |
| $S_3d_2$ | 200 to 530 | 600 | 300 | |
| $S_3d_3$ | 200 to 530 | 600 | 345 | |
| $S_3d_4$ | 200 to 530 | 600 | 350 | |

**Table 5.11: Optic switching data of ZnO samples**

### 5.7.4 ZnS:Mn quantum dot on PVA

To investigate optic switching phenomena of ZnS:Mn quantum dots, the samples have been excited with optical signal of wavelength band of 200 nm to 530 nm while the optical output at 590 nm has been observed. This shows that, optical signal lying in the wavelength band of 200 nm to 530 nm is converted by ZnS:Mn quantum dot into a signal of wavelength of 590 nm. Reason[3] behind the

switching is the presence of Mn energy states that provides d electrons in both virgin and irradiated samples. The data are put in table 5.12.

| Sample | Optical operating range (nm) | Optical output wavelength (nm) | Optical intensity | Switching speed |
|---|---|---|---|---|
| $SM_1$ | 200 to 530 | 590 | 32 | Of the order $10^{-14}$sec |
| $SM_1d_1$ | 200 to 530 | 590 | 60 | |
| $SM_1d_2$ | 200 to 530 | 590 | 95 | |
| $SM_1d_3$ | 200 to 530 | 590 | 105 | |
| $SM_1d_4$ | 200 to 530 | 590 | 110 | |

**Table 5.12: Optic switching data of ZnS:Mn samples**

## 5.8 Comparative studies

### 5.8.1 Comparison among CdS, ZnS and ZnO quantum dots switching devices

| CdS quantum dot switch | ZnS quantum dot switch | ZnO quantum dot switch |
|---|---|---|
| 1. The key of CdS switching is the presence of CdO phase in the specimen | 1. The key of ZnS switching is the presence of surface states and Zn vacancies in the specimen | 1. The key of ZnO switching is the existence of oxygen vacancies in the specimen |
| 2. CdS quantum dot needs very low threshold energy (threshold voltage and wavelength) for its switching functioning | 2 .ZnS quantum dot needs higher threshold energy than CdS and ZnO quantum dots. | 2 .ZnO quantum dot needs higher threshold energy than CdS dot but lower than ZnS quantum dot. |
| 3. CdS quantum dot device has lowest quantum efficiency. | 3. ZnS quantum dot device has moderate quantum efficiency. | 3. ZnO quantum dot device has the highest quantum efficiency. |
| 4. Switching speed of CdS quantum dot device is moderately high and it is of the order $10^{-9}$ sec. | 4. Switching speed of ZnS quantum dot device is very high and it is of the order $10^{-12}$ sec. | 4. Switching speed of ZnO quantum dot device is moderately high and it is of the $10^{-9}$ sec. |
| 5. Optical sensing range of CdS photonic and optic switch is the largest | 5. Optical operating range of ZnS photonic and optic switch is the | 5. Optical operating range of ZnO photonic and optic switch is |

| | | |
|---|---|---|
| one and it ranges from 200 nm to 630 nm of optical wavelength.<br><br>**6.** CdS optic switch produces optical output at 700 nm. | smallest one that ranges from 200 nm to 460 nm of optical wavelength.<br><br>**6.** ZnS optic switch produces optical output at 500 nm. | moderately large and ranges from 200 nm to 530 nm.<br><br>**6.** ZnO optic switch produces optical output at 600 nm. |

### 5.8.2 Comparison between ZnS and ZnS:Mn quantum dot switch

| ZnS quantum dot switch | ZnS: Mn quantum dot switch |
|---|---|
| **1.** The key behind ZnS switching is the presence of surface states and Zn vacancies<br>**2.** ZnS switching device needs comparatively higher threshold energy for its operation.<br>**3.** ZnS quantum dot has low quantum efficiency<br>**4.** Switching speed of ZnS quantum dot device is of the order $10^{-12}$ sec.<br><br>**5.** Optical sensing range of ZnS device is from 200 nm to 460 nm.<br><br>**6.** ZnS optic switch produces optical output at 500 nm. | **1.** The key behind ZnS:Mn switching is the presence of Mn energy state and its d electrons<br>**2.** ZnS:Mn device needs very less threshold energy for its switching operation.<br>**3.** ZnS:Mn quantum dot has very high quantum efficiency<br>**4.** Switching speed of ZnS:Mn quantum dot device is more than $10^{-14}$ sec.<br><br>**5.** Optical sensing range of ZnS:Mn device is from 200 nm to 530 nm.<br><br>**6.** ZnS:Mn optic switch produces optical out put at 590 nm. |

### 5.8.3 Comparison between optic switch and convex lens

| Optic switch | Convex lens |
|---|---|
| **1.** Optic switch converts the whole optical band or any signal lying in the band into another signal of different wavelength. | **1.** Convex lens only focuses the whole optical band at a point in space. There is no change in wavelength. |
| **2.** The key of optic switching is the existence of traps. | **2.** The key of focusing is the curvature as well as the refractive index of lens. |
| **3.** Output signal of optic switch possess only single specific wavelength, which means that, output signal is coherent. | **3.** Output of lens possesses all the wavelengths that are present in the input, which means that output is incoherent. |

### 5.8.4 Comparison between optic switch and optical filter

| Optic switch | Optical filter |
|---|---|
| **1.** Optic switch converts the whole optical band or any signal lying in the band into another signal of different wavelength. | **1.** Optical filter passes the signal of any specific wavelength and blocks the others. |

| | |
|---|---|
| **2.** The key of optic switching technique is the existence of traps. | **2.** The key of optical filtering is the lattice and phonon vibrations in the specimen. |
| **3.** The influence of whole wavelength band (or the signals in the band) is evident in output. | **3.** There is no influence of blocked input signals in the output. |

### 5.9 Conclusion

It has been shown that our prepared quantum dots act as fast electronic, photonic and optic switch depending on the bias and the input conditions. The optical operating range, quantum efficiencies and the response speed vary from material to material. Largest range of optical sensitivity is found in CdS sample while the quantum efficiency is found to be maximum in ZnO specimen and the response speed is found to be highest in ZnS:Mn specimen.

## References


1. Sengupta. A, Mandal. K. C and Zhang. J. Z; *J. Phys.. Chem.B,* Vol. 104, pp 1396. 2000
2. Sengupta. A, Jiang. B, Mandal. K. C and Zhang. J. Z; *J. Phys. Chem.B,* Vol. 103, 1999.
3. Dinsmore. A .D, Hsu. D. S, Qadri. S .B, Cross. J. O, Kennedy. T. A, Gray. H. F and Ratna. B. R; *J. Appl. Phys.* Vol. 88, No. 9, 2000.
4. Singhal. R L; *Semiconductor Physics,* Keder Nath Ram Nath, Meerut, (U.P), India, 1999.
5. Boroditsky. M, Gontijo. I, Jackson. M, Vrijen. R, Yablonovitch. E, Krauss. T, Cheng- Chuan -Cheng, Scherer A, Bhat R and Krames M; *J. Appl. Phys.,* Vol. 87, No 7, pp 3497, 2000.
6. Benerjee. S, Pal. R, Maity. A. B, Chaudhuri. S, and Pal .A .K; *Nano Struct. Mater.* Vol. 8, No. 3, 1997.
7. Brus. L. E; *IEEE J. Quantum Electron*, 22, 416, 1986.
8. Coe Seth, Woe, Wing–Keung, Bawendi Moungi and Bulovic Vladimir; *Letter To Nature ,* Vol. 420, pp 800, 2002
9. Mahamuni. S, Bendre. B. S, Leppert. V. J, Smith. C. A, Cooke. D, Risbud S. H and Lee. H.W.H; *Nano. Struct. Mater.* Vol. 7, No. .6, pp 659, 1996.
10. Behera. S. N, Sahu .S. N, Nanda. K. K; *Ind. J. Phys.* 74 A (2), pp 81, 2000.
11. Chen Wei, Wang Zhanguo, Lin Zhaojun and Lin Lanying; *J. Appl. Phys*, Vol. 82, No. 6, pp 3111.1997.

12. Sahu. S .N, Patel. B, Behera. S .N and Nanda. K. K; *Indian. J. Phys.* 74A(2), pp 93, 2000.

13. Kamat. P. V and Patrick. B; *J. Phys. Chem.* Vol. 96, pp 6829, 1992.

14. Wang. Y and Herron. N; *J. Phys. Chem.* Vol. 195, pp 525,1991.

15. Woggon. U; *Optical Properties of Semiconductor Quantum Dots*, Springer Tracts in Modern Physics, Vol.136, Berlin, 1996.

**********

# CHAPTER 6

# THESIS CONCLUSION AND FEATURE DIRECTIONS OF RESEARCH

# CHAPTER 6

## Thesis conclusion and future directions of research

### 6.1 Thesis conclusion

We have successfully synthesized quantum dots of average size within 10 nm range by chemical and quenching method on two matrices SBR latex and PVA matrix. Sizes of the samples are estimated by three techniques XRD, TEM and optical absorption spectroscopy. The different energy states in quantum dots are detected by optical absorption spectroscopy and luminescence studies. It has been revealed that CdO phase in CdS, surface states in ZnS, oxygen vacancy in ZnO and d electrons in ZnS:Mn samples are the key behind the luminescence phenomena.

We have also found that ion irradiated CdS sample on SBR shows no enhancement in size and hence no shift of strong absorption edge with respect to virgin samples. But the luminescence is enhanced due to increase in CdO phase density. On contrary, ion irradiated ZnS specimen on PVA shows significant enhancement in size and hence the considerable red shift of strong absorption edge. The luminescence is increased due to the enhancement in Zn vacancies. Similarly ion irradiated ZnO samples on PVA increase in size and show the corresponding red shift. The luminescence is enhanced due to increase in

oxygen vacancies. Irradiated ZnS:Mn sample on PVA also shows the similar kind of size enhancement and the red shift. It also shows enhanced luminescence phenomenon due to increase in Mn density in ZnS host.

Lastly, we have been successful to show that our quantum dots act as fast electronic, photonic and optic switch depending on the bias and the input conditions. The quantum efficiencies, the response speed and range of optical sensitivity vary from material to material. The optical operating range in largest in CdS quantum dot and the quantum efficiency is found to be maximum in ZnO specimen while the response speed is found to be highest in ZnS:Mn specimen.

## 6.2 Future research direction

We expect rich dividends if further research is carried out on quantum dots in the following directions.

### 6.2.1 Possible modifications in synthesis procedure

We have synthesized quantum dots by controlling three parameters (i) stirring rate period (ii) temperature and (iii) amount of reagents. In future another parameter like pH of chemical solutions may be also varied to achieve more precise and uniform growth of samples[1]. The reaction should be carried out in a dark vacuum chamber to increase the purity of specimen.

### 6.2.2 Synthesis of quantum dots on conducting matrix

To enhance the electrical conductivity of quantum dot assembly, conducting matrix[2] like Nafion 117 and polyaniline may be used for quantum dot preparation. In that case, the electron will not tunnel but drift from one dot to another through the conducting matrix more easily to produce higher electronic or optical output with higher quantum efficiency.

### 6.2.3 Quantum dot synthesis without matrix

Without using matrix but by controlling different control parameters[3] at a time (like reaction temperature, reaction time and pH etc.) of chemical solutions, controlled growth of sample can be achieved. Care should be taken to control the parameter very preciously. On the other hand, synthesis of quantum dots may be tried using electro-deposition technique where by controlling input electrical signal to the electrochemical workstation, preparation of quantum dot may be tried. But this method is costly.

### 6.2.4 New materials to synthesize quantum dot

The samples prepared in the present work possess optical sensitivity over the range from UV to VIS region only but do not have considerable sensitivity in infrared range. It is possible to detect infrared region also by quantum dot provided it is prepared with material that possess very low band gap ( less than 1 eV). PbS is one such candidate. So this work may be extended to cover these areas.

### 6.2.5 Quantum dot doping with some new metals

Apart from Mn doping in ZnS sample, doping with silver and gold promises to offer new characteristics for device fabrication[4]. In fact, a comparative study among the samples doped with manganese, silver and gold may turn out to be very useful in device fabrication.

### 6.2.6 Lower energy ( KeV ) ion beam irradiation

Doping of quantum dot of higher band gap (<=3 eV) with the material of comparatively lower band gap (<=1 eV) may be excellently used to develop optoelectronic and optical transducer over wide optical range with uniform sensitivity. The device will be of heterostructure type. In lower wavelength region (say UV/VIS) the host specimen functions as detector while in longer wavelength region (say infrared). Technologically this is advantageous because only one device can work over a large range of optical signal.

This can be achieved by irradiating the samples to lower energy (KeV) ion beam so that, lower energy ion beam cannot pass through the sample and hence the quantum dots be uniformly ion implanted by the beam.

### 6.2.7 Stability

The samples prepared by present method, are found to be stable for a year or so. But after that, the specimens agglomerate irregularly and their properties detoriate. For better stability[5], the samples have been coated with some protecting material like silica. But further research is necessary in this field

for extensive use of stable quantum dot devices in electronics, photonic and nonlinear switching. We have mainly confined our studies to these specific areas amongst the vast possibilities and the current use of quantum dots in the area of electronics, photonics and nonlinear optics.

## References


1. Behra S. N., Sahu S. N., Nanda K. K. ; *Indian J. Phys*, 74. A (2) 2000.
2. Sahu. S .N, Patel. B, Behera. S .N and Nanda. K. K; *Indian. J. Phys.* 74A(2), pp 93, 2000.
3. Chen Wei, Wang Zhamguo, Lin Jhaojum and layıng ; *J. of Appd. Phys,* Vol 82, No 2, 1997.
4. Dinsmore A. D, Hsu D.S., Qauadri S. B., Cross J. O.; *J. of Appd. Phys.*, Vol 88, No 9, 2000.
5. Caruso Rachel A and Antoniett Markusi ; *Chem. Mater*, Vol. 13, 2001


**********

# APPENDIX

## PHOTOGRAPHS AND SPECIFICATIONS OF THE INSTRUMENTS USED

**Fig. 1.a : Set up for X-ray Diffraction study.**

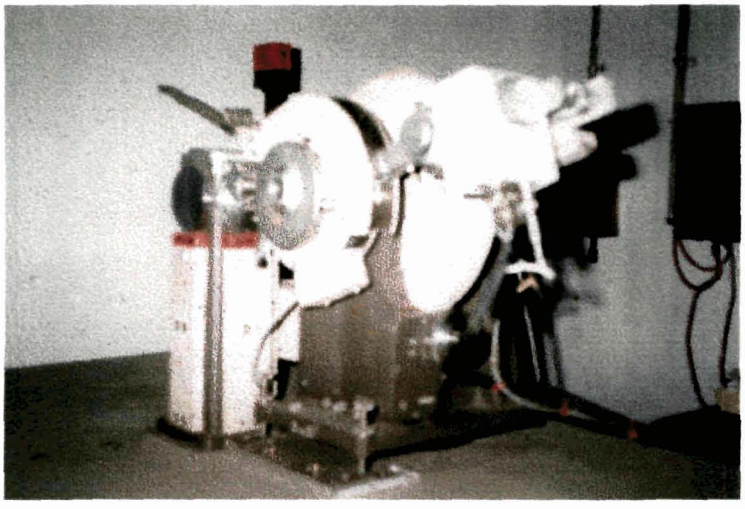

**Fig.1.b:X-ray generation, detection and Sample holder section of X-ray diffractometer.**

## Specifications X-ray diffractometer

| | | |
|---|---|---|
| Model | : | APD - 1700, PHILIPS. |
| Average X-ray wavelength | : | 0.1541 nm |

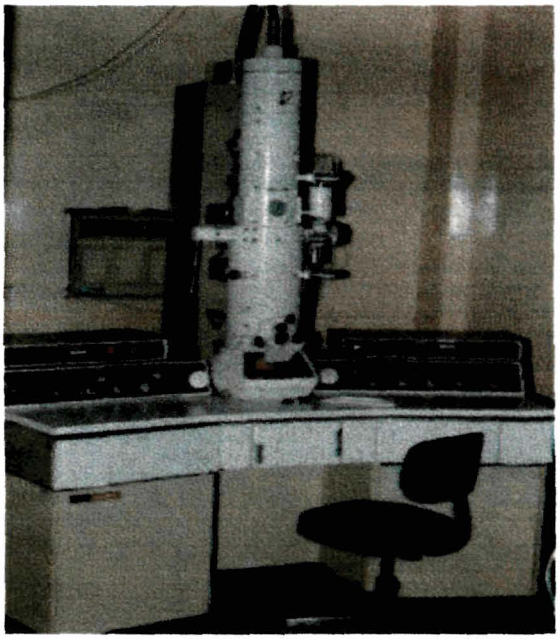

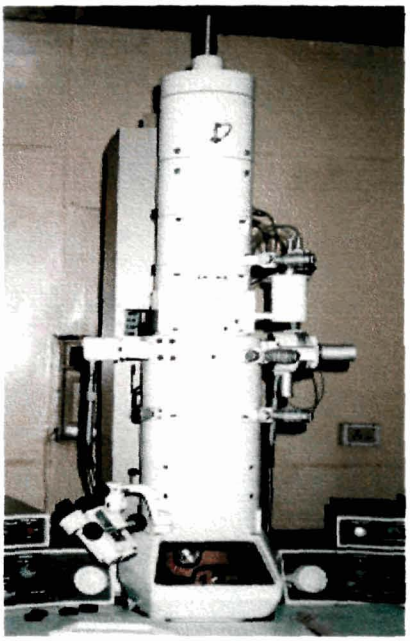

**Fig: 2**

**a**

**Transmission Electrom Microscope (TEM)**

**b**

**Electron generation and image viewing section of TEM**

## Specifications of TEM

| | | |
|---|---|---|
| Model | : | JEM 1000C X II |
| Resolution | : | 0.3 nm to 14 nm |
| Accelerating voltage | : | 200 kV to 100 kV |
| Specimen stage | : | Air-lock mechanism |

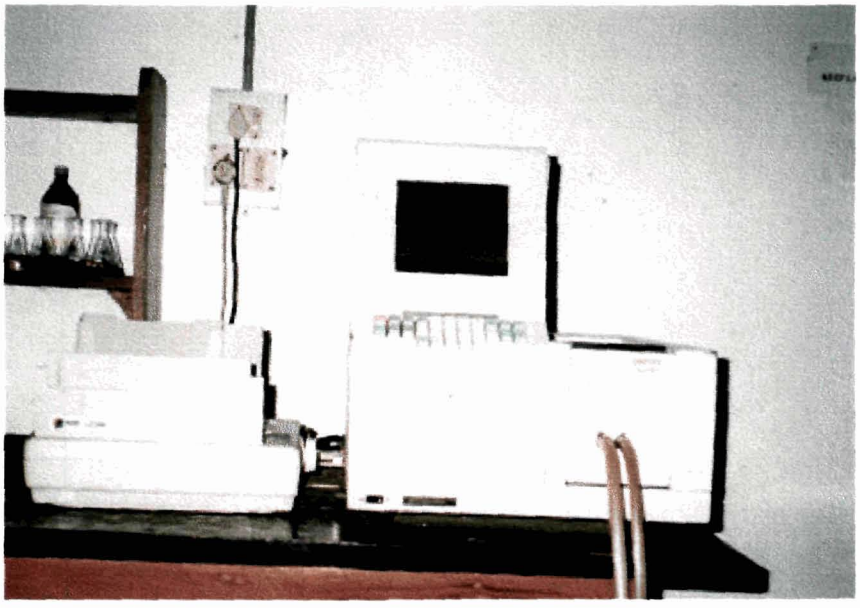

**Fig. 3: Experimental setup for UV/VIS absorption spectroscopy**

## Specifications of spectrophotometer

| | | |
|---|---|---|
| Model | : | HITACHI-U-2001. |
| Optical emission and detection range: | | 200 nm to 800 nm. |

**Fig. 4: Experimental setup for photoluminescence study**

## Specifications of spectrophotometer

| | |
|---|---|
| Model | : HITACHI-F- 2500 |
| Excitation source | : Xenon lamp of 150 w. |
| Excitation and detection range | : 200 nm to 800 nm. |

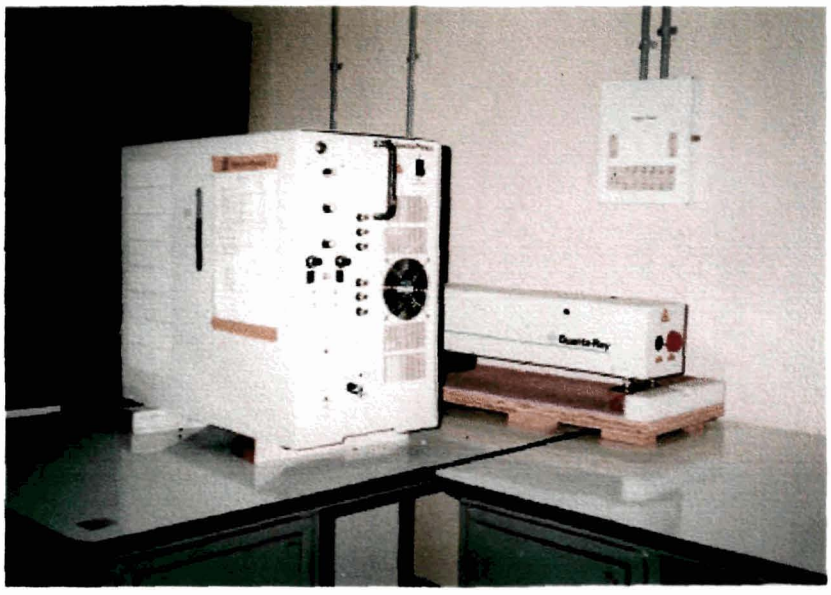

**Fig 5: Nd:YAG laser**

**Specifications**

Model : INDI- 50 , Spectra physic, Calformia Made.

| *Emission wavelength* | *Range* | *Power* |
|---|---|---|
| 1064 nm | IR | 500 mJ |
| 532 nm | VIS (GREEN) | 225 mJ |
| 261 nm | UV | 25 mJ. |

Long pulse width form 8 ns to 10 ns with repetition rate of 10 Hz to 20Hz.

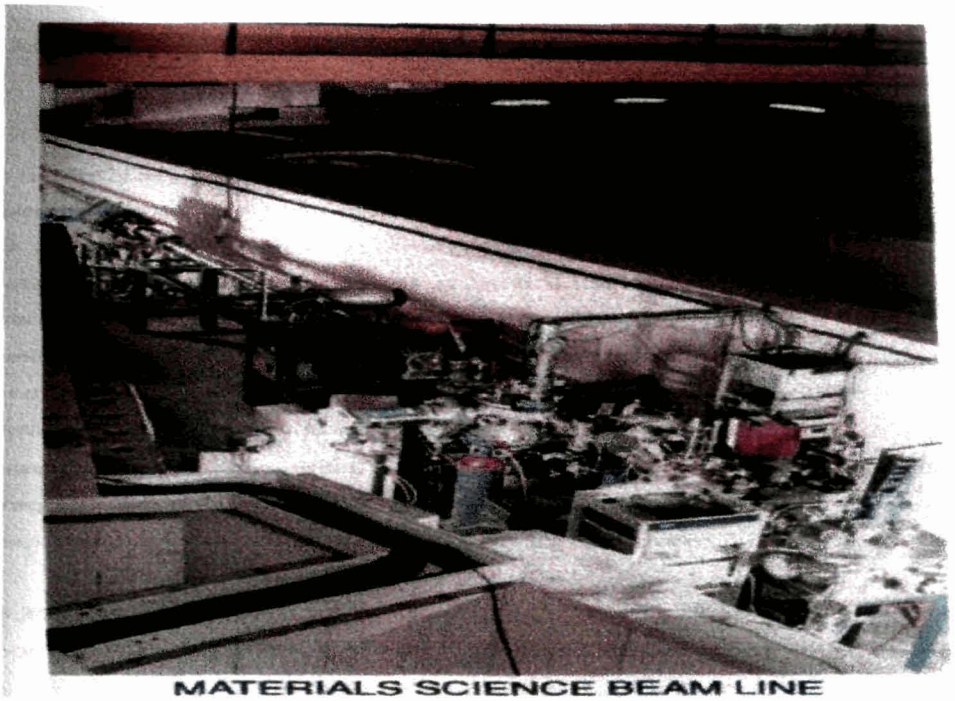

MATERIALS SCIENCE BEAM LINE

**Fig 6**

# List of Publications

# LIST OF PUBLICATIONS

## Journals

1. Optical absorption study of 100-MeV chlorine ion irradiated hydroxyl free ZnO semiconductor quantum dots, J. Appl. Phys., Vol. 92, No. 12, pp.1, 2002.
2. Ion irradiation response of semiconductor nanoparticles emnedded in polymer matrix, Annu . Report 2001-2002, Nuclear Science Centre, p-116.
3. Size estimation and luminescence enhancement of II-VI seminconductor quantum dots , *Asian J. Physics,* 12, No. 1, pp. 57, 2003.
4. Irradiation induced grain growth and surface emission enhancement of ZnS:Mn / PVOH semiconductor nanoparticles by $Cl^{+9}$ ion impact, *Bull. Mat. Sci.,* Vol. 26, No.3, pp. 289, 2003.
5. SHI induced grain growth and grain fragmentation effect of polymer embedded CdS quantum dot system, J. Chem. Phys., ( Communicated).
6. Spectroscopic study of chemically synthesized Mn doped ZnS quantum dot. *Asian J. Physics.* (communicated).
7. Synthesis of ZnO Quantum Dot by Quenching Method and its spectroscopic study, *Indian J Pure and Appl. Phys.* (communicated).
8. Effect of swift heavy ion on ZnS: Mn quantum dot, J. Appl. Phys. (Communicated)

## Proceedings

1. Defect modified suppression of recombination emission in CdS quantum dots stimulated by thermal means, *Proceedings of the 2nd Regional conference on physics research, PANE,* Cotton College, Guwahati, Assam, India,October 28, pp. 21. 2001.
2. Preparation of ZnO quanrum dot and its characterization, *Proceedings of the 4th Annual Technical Session*, Assam Science Society, Dibrugarh, Assam, India, February, pp. 128, 2002.
3. Preparation of Mn doped ZnS quantum dot on pol. Matrix and study of its thermostimelated behaviour, National conference on laser and spectroscopy,. Dibrugarh, Assam, India, November,pp 82, 2001.